LBL-11011 c.2

Lawrence Berkeley Laboratory
UNIVERSITY OF CALIFORNIA

Accelerator & Fusion Research Division

COMMERCIALIZATION OF A HIGH ENERGY NEUTRAL BEAM ION SOURCE

FINAL REPORT

McDonnell Douglas Astronautics Company
St. Louis, Missouri

RECEIVED
LAWRENCE
BERKELEY LABORATORY

JUN 20 1980

LIBRARY AND
DOCUMENTS SECTION

December 1979

TWO-WEEK LOAN COPY

This is a Library Circulating Copy
which may be borrowed for two weeks.
For a personal retention copy, call
Tech. Info. Division, Ext. 6782.

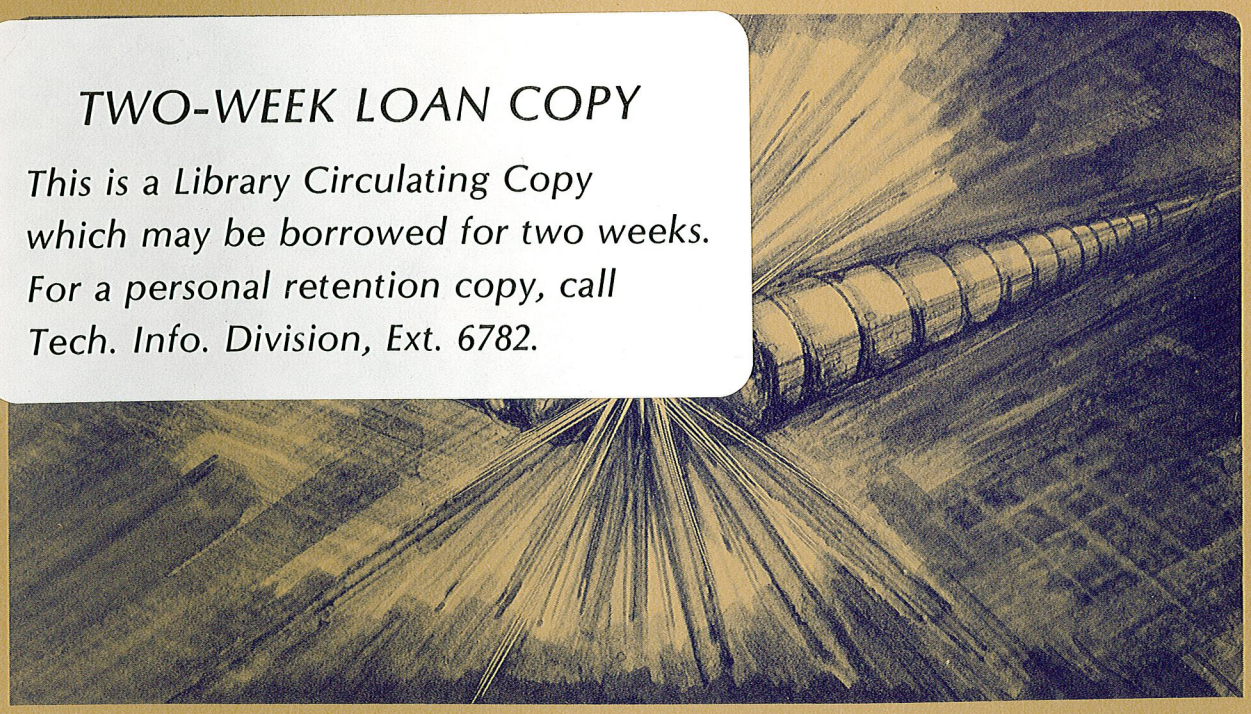

LBL-11011 c.2

COPY NO. 5

DISCLAIMER

REPORT MDC E2189 ● 21 DECEMBER 1979

Commercialization of a High Energy Neutral Beam Ion Source

FINAL REPORT

FUSION ENGINEERING

SUBMITTED TO LAWRENCE BERKELEY LABORATORY,
UNIVERSITY OF CALIFORNIA, BERKELEY, CALIFORNIA 94720
UNDER PURCHASE ORDER 3152102

MCDONNELL DOUGLAS ASTRONAUTICS COMPANY - ST. LOUIS

Box 516, Saint Louis, Missouri 63166 (314) 232-0232

MCDONNELL DOUGLAS CORPORATION

DISTRIBUTION OF THIS DOCUMENT IS UNLIMITED

TABLE OF CONTENTS

SECTION	TITLE	PAGE
	INTRODUCTION AND SUMMARY	1-4
1.0	ENGINEERING	1-1
1.1	PRODUCTION DRAWINGS	1-1
1.2	DEVELOPMENT TESTING	1-4
1.2.1	ACCELERATOR CERAMIC HIGH VOLTAGE INSULATOR	1-4
1.2.2	HARD VACUUM DIELECTRIC SEAL INSULATORS	1-10
1.2.3	DEEP DRAWN MOLYBDENUM SHIELDS	1-14
1.3	DESIGN CHANGES	1-14
1.3.1	PLASMA GENERATOR CHANGES	1-17
1.3.2	ACCELERATOR	1-19
1.4	STRUCTURAL ANALYSIS	1-19
1.4.1	CERAMIC/NIOBIUM TEST SPECIMENS	1-25
2.0	MANUFACTURING	2-1
2.1	MANUFACTURING PROCESS	2-1
2.1.1	PLASMA SOURCE ASSEMBLY	2-1
2.1.2	ACCELERATOR GRID ASSEMBLIES	2-3/2-4
2.1.3	ACCELERATOR INSULATOR ASSEMBLY	2-25
2.1.4	FINAL ASSEMBLY	2-26
2.2	MANUFACTURING PROBLEMS AND SOLUTIONS	2-32
2.2.1	HARD VACUUM DIELECTRIC SEAL INSULATORS	2-32
2.2.2	HARD "C" SEALS	2-37
2.2.3	INCREASED PLASMA SOURCE FASTENERS	2-38
2.2.4	ACCELERATOR GRID RAIL BLUSHING	2-38
2.2.5	REPAIR OF BROKEN SUPPRESSOR GRID	2-38
2.2.6	BRAZED ACCELERATOR HIGH VOLTAGE INSULATOR LEAKS	2-39

LIST OF FIGURES

FIGURE NO.	TITLE	PAGE
1-1	TFTR NEUTRAL BEAM SOURCE	2
1.2.1-1	ACCELERATOR INSULATOR ASSEMBLY	1-5
1.2.1-2	TENSILE TEST BRAZE SPECIMEN	1-7
1.2.1-3	THERMOCOUPLE LOCATIONS FOR SIMULATED FULL SCALE RINGS	1-7
1.2.1-4	TIME - TEMPERATURE CHART FOR BRAZING FULL SCALE RING TEST SPECIMEN	1-8
1.2.1-5	TEST PART AFTER PRESSURE TESTING	1-9
1.2.2-1	THERMAL EXPANSION COMPARISON OF COPPER AND ENAMEL	1-12
1.2.2-2	TIME TO PART THICKNESS FIRING CYCLE	1-13
1.2.2-3 (A)&(B)	STAINLESS STEEL PLATE .032" THICK	1-15/1-16
1.2.3-1	DEEP DRAW MOLYBDENUM SHIELD TFTR ACCELERATOR GRADIENT GRID	1-17
1.2.3-2	TFTR ACCELERATOR DEEP DRAWN MOLYBDENUM SUPRESSOR GRID (INSTALLED)	1-18
1.3.1-1	PLASMA SOURCE FASTENER REDESIGN	1-20
1.4-1	AXIAL THERMAL STRESSES IN THE CERAMIC AND BRAZE SHEAR STRESS FOR VARIOUS MATERIAL COMBINATIONS	1-21
1.4-2	BENDING STRESSES IN THE CERAMIC DECREASE AS THICKNESS INCREASES	1-23
1.4-3	NASTRAN FINITE ELEMENT MODEL OF ACCELERATOR SUBASSEMBLY CORNER AT BELLOWS END	1-24
1.4-4	RADIAL RUNNING SHEAR FORCE AND TIPPING MOMENT AS A FUNCTION OF LOCATION AROUND CORNER AT BELLOWS END	1-25
1.4-5	COMBINED STRESSES IN CERAMIC END FRAME AT CENTER OF CORNER	1-26
1.4-6	FULL SCALE ALUMINA/NIOBIUM/ALUMINA BRAZE ASSEMBLY	1-27
1.4-7	STRESSES IN THE TWO CYLINDRICAL TEST SPECIMENS	1-28
1.4-8	FULL SCALE TEST ARTICLE PRESSURE HISTORY	1-30
1.4-9	STRAIN GAGE DATA AT INSIDE CENTER OF LONGSIDE INDICATES CRACKING OCCURRED AT AN AUTOCLAVE PRESSURE OF 152 psig	1-31
2.1.1-1	PLASMA SOURCE ASSEMBLY MANUFACTURING FLOW	2-4/2-5 through 2-6/2-7
2.1.2-1	SOURCE GRID ASSEMBLY MANUFACTURING FLOW	2-9/2-10
2.1.2-2 (A)&(B)	GRADIENT GRID BRAZING ASSEMBLY	2-11/2-12 through 2-13/2-14

LIST OF FIGURES - (Continued)

FIGURE NO.	TITLE	PAGE
2.1.2-3 (A)&(B)	SUPPRESSOR GRID ASSEMBLY MANUFACTURING FLOW	2-15/2-16 through 2-17/2-18
2.1.2-4 (A)&(B)	EXIT GRID ASSEMBLY MANUFACTURING FLOW	2-19/2-20 through 2-21/2-22
2.1.2-5	TFTR ACCELERATOR SUPPRESSOR GRID.	2-24
2.1.3-1	INSULATOR ASSEMBLY MANUFACTURING FLOW	2-27/2-28
2.1.4-1	RAIL ALIGNMENT USING TOOLING HOLES.	2-29
2.1.4-2	ASSEMBLY DRILL JIG - FOR RAIL ALIGNMENT USING INDEXING PINS.	2-30
2.1.4-3	CENTER DEFLECTION OF GRID RAILS DUE TO MEASURING INSTRUMENT'S STYLUS FORCE.	2-31
2.1.4-4	FINAL ASSEMBLY MANUFACTURING FLOW	2-33/2-34 through 2-35/2-36
2.2.6-1	CERAMIC INSULATOR VACUUM LEAKS.	2-40

LIST OF TABLES

TABLE NO.	TITLE	PAGE
1.1-1	TFTR ION SOURCE DRAWING LIST.	1-1/1-3

LIST OF PAGES

Title Page

ii through v

1 through 4

1-1 through 1-31

2-1 through 2-41

INTRODUCTION AND SUMMARY

In a reactor that produces useful energy by fusion, energy has to be supplied initially in order to establish the proper conditions (plasma temperature and density) for the thermonuclear reactions to take place at a significant rate. One of the most promising methods for producing and heating plasma is the injection of intense beams of energetic neutral deuterium. Neutral beams of very high energy are produced by first adding energy to deuterium ions in an accelerator and then neutralizing the ions by passing them through a chamber containing deuterium gas. Neutral atoms are needed since ionized particles cannot penetrate the intense magnetic field surrounding the plasma.

Development of a neutral beam injection system is a major effort in support of the Department of Energy (DOE) primary objective of developing fusion power by magnetic confinement. One of the major subcomponents of a neutral beam injector is the neutral beam ion source (Figure 1-1). The source is a high technology, precision assembly containing refractory metals and manufactured to close tolerance.

A 120 KeV, 65 ampere, 0.5 sec neutral beam ion source has been developed and tested by the University of California Lawrence Berkeley Laboratory (LBL). An industrial partner is required to fabricate the relatively large number of these ion sources, approximately 106, required over the next 5 to 10 years. These sources are needed for near term tokamak and mirror machines and are essential for attainment of their operating goals.

The job for industry was to help improve the design and manufacturing procedures to make the ion source more economical to produce, more reliable, and of longer life. The experience and broad manufacturing capabilities of industry were to be used in accomplishing these objectives. Maximum reliability and life becomes increasingly important as duty factor and reactor cost increase and as deuterium and tritium fuels are used, complicating repair and maintenance with the resultant induced radioactivity. The first reactor that imposes all of these factors is the TFTR. It is for this reason, the TFTR requirements were used as the design baseline for the first industry produced ion source.

This final report summarizes the effort and presents the results of a Phase II fabrication effort to build an industrial prototype of the LBL developed

TFTR NEUTRAL BEAM SOURCE

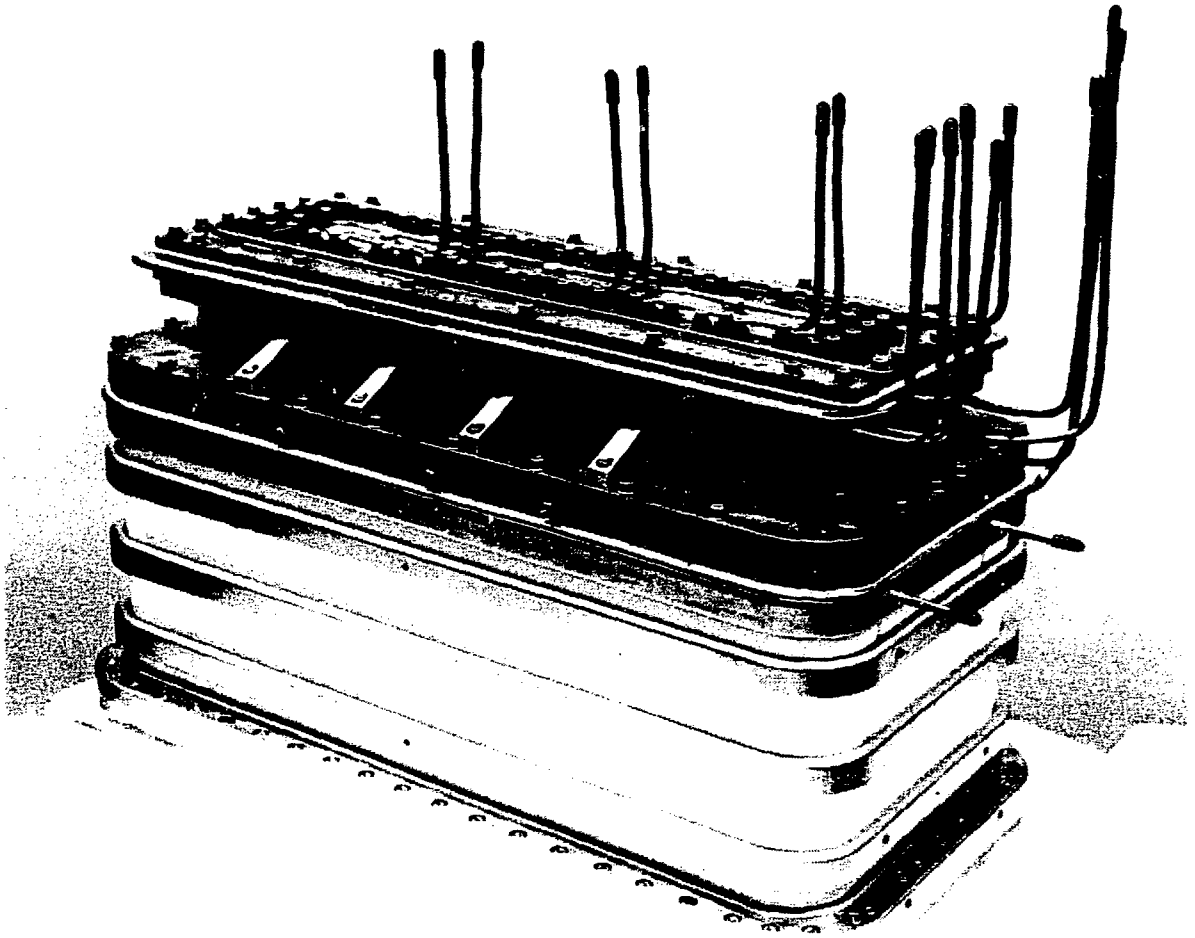

13–2700

FIGURE 1-1

high energy neutral beam source. The effort was primarily concentrated on incorporating hard vacuum dielectric seals and a ceramic high voltage accelerator insulator. Several other design changes were incorporated for cost, reliability or life improvements to include: (1) accelerator grid locating dowel pins to aid final alignment, (2) plasma source to accelerator captive fasteners to aid filament replacement during source maintenance, (3) molybdenum cooling tubes on all accelerator grids, (4) additional fasteners in the plasma generator to facilitate hard seals, (5) modified suppressor grid rails and holders to simplify final grid alignment, (6) adjusting screws on exit grid rail holders to simplify final grid alignment, (7) addition of adjusting screws to the grid end pieces to simplify

alignment, and (8) addition of accelerator hat shims to allow two different grid positioning locations.

The potential requirements for the TFTR Neutral Beam Sources dictated that the industrialization program be established at the outset as a full production program within the engineering and manufacturing departments of MDAC-St. Louis. Production engineering drawings and manufacturing operation work orders, tooling orders and quality assurance inspection orders were prepared to facilitate a full production program. A highly projectized organization was assembled and co-located in a separate facility to maximize efficiency. The unique requirements of high precision and refractory metals fabrication dictated assigning personnel with extensive related hardware experience that could be dedicated to ion source fabrication. As a result and in keeping with the industrialization concept, a team of highly trained production personnel are now available with extensive experience in ion source part fabrication, assembly and accelerator grid alignment.

Facilities and equipment were purchased specifically for TFTR Neutral Beam Source fabrication. A vacuum-hydrogen brazing furnace was procured for vacuum brazing the accelerator ceramic high voltage insulators, for hydrogen brazing the molybdenum accelerator grids and for hydrogen firing of the grid shields. A 3-axis coordinate measuring machine was purchased for inspection of precision machined parts and final alignment of the accelerator grids.

During the manufacturing process, major problems occurred in three (3) areas: ceramic insulator brazing, molybdenum shield welding, and hard vacuum dielectric seal fabrication.

Although the full scale accelerator ceramic insulator braze specimen was tested to five (5) times the operating pressure (2 atmosphere data pressure), failure of the first production unit occurred during final machining. Leaks developed at one corner of the two end flanges. Ultrasonic testing of the assembly showed braze separation and cracks in the ceramic at the leaking corners. All braze joints at the other flange corners and center feedthrough rings were good with no voids or separations. Results of failure analysis indicated radial shear and tipping moments occurred during brazing between the end flanges and the ceramic rings at the corners. A ceramic back-up ring was added for the second

unit to reverse the direction of the bending moment across the braze and reduce it by approximately a factor of two. Shear stresses were reduced by approximately 20%. The second unit was successfully brazed with back-up ceramic rings added on both flanges.

Initial design of the gradient and suppressor grid molybdenum shields required welding at the four corners. Several attempts to weld the shields resulted in cracking at the corners during installation. The shields must fit tightly to the grids after installation and as such must withstand some stresses at the welded corners during installation. Welding of the thin (.010 inch) metal resulted in a brittle zone at each corner. The imbrittled area could not withstand the installation loads and would crack during installation on the grids. Rewelding only increased the brittle zone. To facilitate a more reliable, lower cost shield for future production TFTR ion sources, the shields were redesigned and a deep draw forming process was used. Production shields were successfully formed and installed on the suppressor and gradient grids.

The original hard vacuum dielectric seal approach involved the application of porcelain enamel directly to the plasma source copper electrodes with a hard "C" seal installed in the opposing electrode to provide the vacuum seal. Problems developed when the porcelain enamel was applied to the thicker production cathode plate. The 34% difference in the expansion coefficient between the enamel and copper resulted in poor adherence of porcelain to the copper. The thick copper cathode plate would not yield thereby exceeding the enamel's compression strength. Adjustment of the enamel formulation to increase its expansion coefficient was too time consuming so an alternate design approach was selected. The alternate approach, which proved successful, was to apply porcelain enamel to a thin stainless steel substrate which was used as an insulator between two hard "C" seals. This concept maintained the interchangeability between "C" seals and "O" rings and also allowed replacement of a damaged insulator without replacing an electrode. The only drawback with this approach was that the number of hard "C" seals required was doubled over the original concept.

The TFTR ion source has been delivered to LBL for beam line testing.

1.0 ENGINEERING

Production engineering drawings incorporating LBL approved design changes and the required material and process specifications were prepared. The ion source was subjected to mechanical checks, vacuum leak checks and voltage holding demonstration tests and delivered to LBL for further evaluation.

1.1 Production Drawings - Experienced and capable people in the areas of electrical and mechanical design and manufacturing processes were assigned to finalize the ion source design and produce production engineering drawings. A total of one hundred twelve (112) production drawings were made. Each drawing was reviewed with LBL personnel for concurrence prior to manufacturing go-ahead authorization. Table 1.1-1 is a complete listing of the TFTR Neutral Beam Source engineering drawings.

TABLE 1.1-1

TFTR ION SOURCE DRAWING LIST

00E057000 GENERAL ASSY (SOURCE/EXTRACTOR)

01 SOURCE ASSY
02 ACCELERATOR ASSY
03 INSULATOR ASSY
04 SOURCE GRID ASSY
05 GRADIENT GRID ASSY
06 SUPPRESSOR GRID ASSY
07 EXIT GRID ASSY
11 POSITIVE FILAMENT ELECTRODE
12 NEGATIVE FILAMENT ELECTRODE
13 WALL ELECTRODE ASSY
14 CATHODE PLATE
15 ANODE PLATES
16 TUNGSTEN FILAMENTS
17 FILAMENT CHUCK
18 GAS DIVERTER
19 ANODE SUPPORT
20 RAIL AND HOLDER GRID SOURCE

TABLE 1.1-1

TFTR ION SOURCE DRAWING LIST

00E057000 GENERAL ASSY (SOURCE/EXTRACTOR, (Continued)

21 SOURCE GRID BRAZING ASSY
22 SOURCE GRID END-PIECE
23 SOURCE GRID RAIL HOLDER MOLY SHIELD

25 PLATE-MOUNTING SOURCE GRID
26 RAIL AND HOLDER GRADIENT GRID
27 GRADIENT GRID BRAZING ASSEMBLY
28 GRADIENT GRID COOLING TUBE
29 GRADIENT GRID RETAINING STRIP
30 GRADIENT GRID END-PIECE
31 GRADIENT GRID RAIL HOLDER MOLY SHIELD
32 GRADIENT GRID ASSY MOLY SHIELD
33 GRADIENT GRID HAT
34 GRADIENT GRID MOLY SHIELD
35 RAIL AND RAIL HOLDER SUPPRESSOR GRID
36 SUPPRESSOR GRID BRAZING ASSY
37 SUPPRESSOR GRID, HAT SHIELD
38 SUPPRESSOR GRID MOLY SHIELD
39 SUPPRESSOR GRID COOLING TUBE
40 SUPPRESSOR GRID HAT
41 SUPPRESSOR GRID END-PIECE
42 FAIL AND RAIL HOLDER EXIT GRID
43 EXIT GRID BRAZING ASSY
44 EXIT GRID HAT
45 EXIT GRID END PIECE
46 EXIT GRID MOLY SHIELD
47 EXIT GRID RETAINING STRIP
48 SEALS - SOURCE HARD VACUUM
49 CERAMIC INSULATORS
50 POTENTIAL DIVIDER RING
51 VOLTAGE FEED THRU RING
52 INSUL. FLANGE (BELLOWS END)

TABLE 1.1-1

TFTR ION SOURCE DRAWING LIST

00E057000 GENERAL ASSY (SOURCE/EXTRACTOR) (Continued)

53 INSUL. FLANGE (SOURCE END)
54 COVER FLANGE, VOLT. FEED THRU RING
55 EXIT GRID COOLING TUBE
58 SOURCE GRID COOLING TUBE
59 GRADIENT GRID SHIM
63 GUSSET-ELECTRODE WALL TANK
83 SOURCE GRID PLATE WATER FITTING
84 SUPPRESSOR GRID WATER FITTING
86 EXIT GRID WATER FITTING
87 SUPPRESSOR GRID, SHIM
88 PLASMA SOURCE INSULATOR BUSHINGS

91 SUPPRESS OR GRID RAIL RETAINER
93 EXIT GRID SHIMS
94 GRID TOOLING PINS
95 GRID WATER COOLING SEALS
96 "O" RING VACUUM SEALS
97 ACCELERATOR - PROBE PLATE ASSY
98 SELF RETAINING SOURCE TO PROBE PLATE BOLT

100 HAT ADJUSTMENT SHIMS
101 TOP MOLY SOURCE GRID SHIELD
102 MOLY SOURCE GRID STRAP
104 PLATE-SHIPPING BOX
105 RING-CERAMIC, SOURCE AND BELLOWS END
107 RING-BELLOWS END
108 INSULATOR HARD DIELECTRIC VACUUM SEAL
110 SHIELDS-PROBE PLATE
111 SHIELD-EXIT GRID END PIECE

1.2 Development Testing - Development testing was performed on the hard vacuum dielectric seals, the accelerator high voltage ceramic to metal brazed insulator and deep draw forming of the suppressor and gradient grid molybdenum shields. The development tests were performed early in the program to aid in final design selection. Additional development testing was conducted during the manufacturing phase to evaluate and select changes to eliminate problems occurring during manufacturing.

1.2.1 Accelerator Ceramic High Voltage Insulator - One of the major changes to the LBL developed neutral beam ion source was the replacement of the epoxy accelerator insulator with a ceramic insulator. The ceramic insulator assembly must structurally support the entire ion source, provide a vacuum tight enclosure meeting leakage rates of 10^{-10} scc/sec of helium as well as provide high voltage electrical insulation between the insulator grid feedthrough rings. The insulator assembly is shown in Figure 1.2.1-1.

The two major concerns in fabricating a brazed ceramic insulator assembly are: fabricating a rectangular ceramic ring to the specified size and tolerances and structurally joining the ceramic to metal to provide support for the entire ion source while also providing a vacuum tight assembly. Three ceramic materials were selected for study; 85% aluminum oxide, MACOR and electrical porcelain. Development contracts were issued to the Lapp Insulator Company and the Coors Porcelain Company to develop the rectangular rings from electrical porcelain and alumina respectively. Development efforts on MACOR were not instituted since LBL had a program well underway on fabricating a MACOR insulator.

In conjunction with selection of a ceramic insulator, an investigation into selection of a compatible metal for the feedthrough rings was undertaken. It was essential to select a material combination that would minimize the difference between the thermal expansion coefficients, thereby minimizing the thermal stresses in the braze joint built up during cool down from the brazing temperature.

Following the trade study, the 85% Al_2O_3 and Niobium (Nb) materials were selected which have a thermal expansion coefficient of 7.1×10^{-6} in./ in./^{o}C and 8.14×10^{-6} in./in./^{o}C respectively. This expansion difference was

ACCELERATOR INSULATOR ASSEMBLY

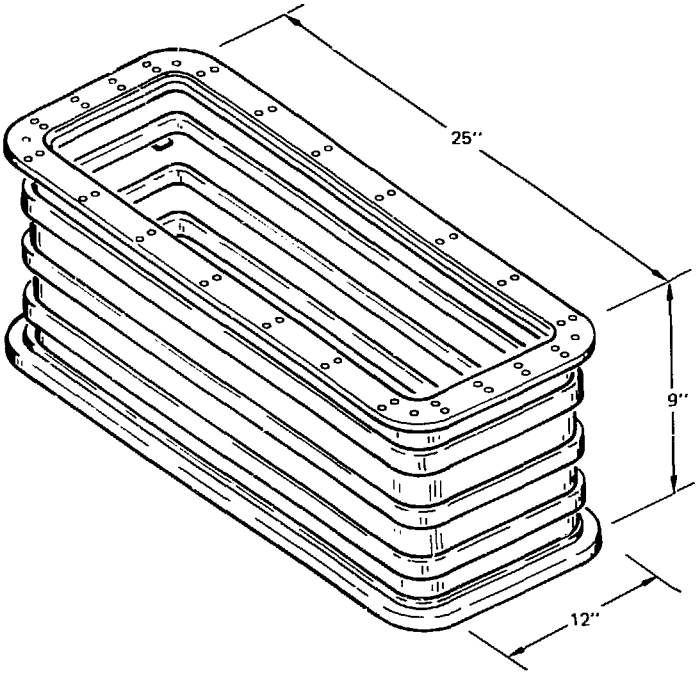

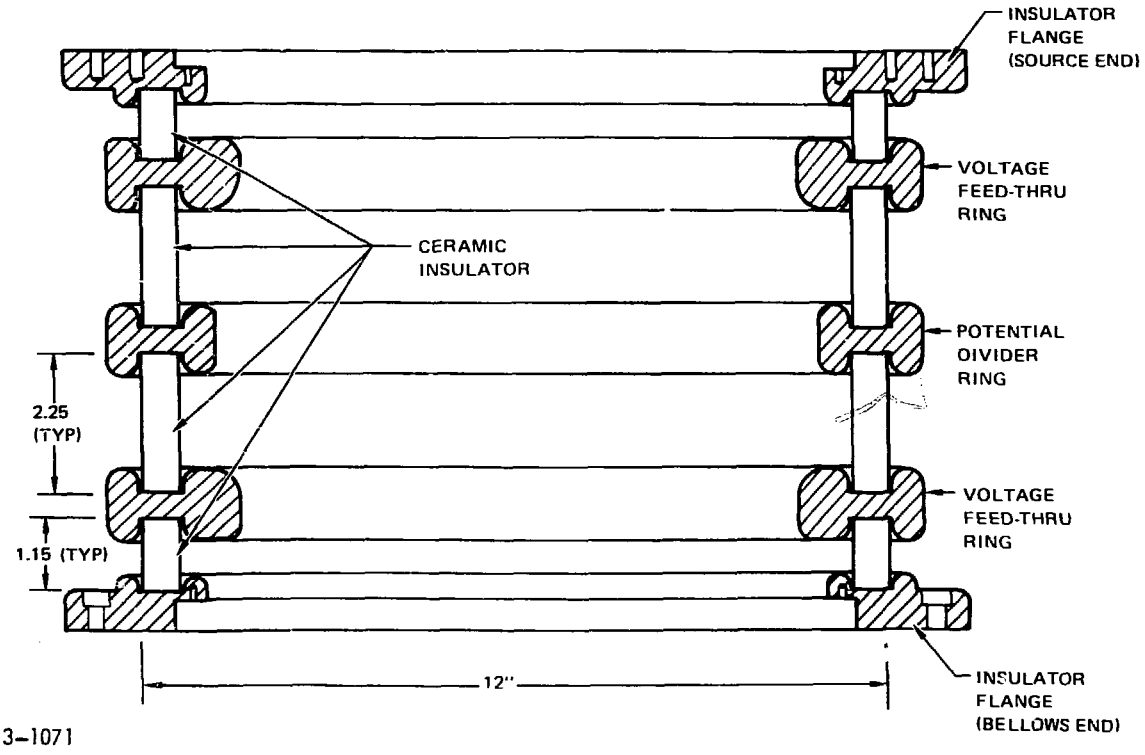

13-1071

FIGURE 1.2.1-1

judged acceptable, with stresses expected to develop as described in the analysis of Section 1.5.

Several brazing techniques were investigated for use in fabricating the Al_2O_3-Nb accelerator. These were a metallized coating on the Al_2O_3 followed by brazing to Nb; a layer of Ti-hydride on the Al_2O_3 during the brazing operation; and utilizing a TICUSIL braze alloy which eliminated the need for the Ti-hydride layer or metalized coating on the ceramic.

The metallized coating on the Al_2O_3 worked well for brazing; however, the procedure for applying the metallized coating was not suitable. There was concern that firing the metallized coating would distort the close tolerance dimensions required on the ring. Also, there was no furnace ideally suited to firing the metallized coating in a wet hydrogen atmosphere at temperatures of approximately 1350°C.

Use of the TICUSIL braze alloy was selected because the process was considered more repeatable than the Ti-hydride process.

A series of tests were conducted to evaluate cleaning procedures, time-temperature cycles, and alloy thicknesses for brazing. Tensile tests were conducted on Al_2O_3 cylinders brazed to Nb to determine joint strengths. The type of specimens utilized for the evaluation are represented in Figure 1.2.1-2. Typically failure was in the Al_2O_3 approximately 0.20 inch from the Nb plate. The stresses developed in the braze joint of cylinders such as these is higher than a direct load/cross-sectional area calculation would indicate. This increased stress is caused by thermal and triaxial stress built up during the tensile tests. The calculated stress at failure of the Al_2O_3 was typically 12 Ksi. The braze alloy thickness selected was 0.003 inch.

Subsequent to development of a brazing procedure, full scale Al_2O_3-Nb rings were brazed. This brazing was accomplished in a clean vacuum furnace capable of 10^{-5} torr. The braze alloy used for this test was 0.004 inch thick. All details were cleaned and prepared per the process specification. The part was instrumented with seven thermocouples to determine the variation in temperature at various locations as shown in Figure 1.2.1-3.

TENSILE TEST BRAZE SPECIMEN

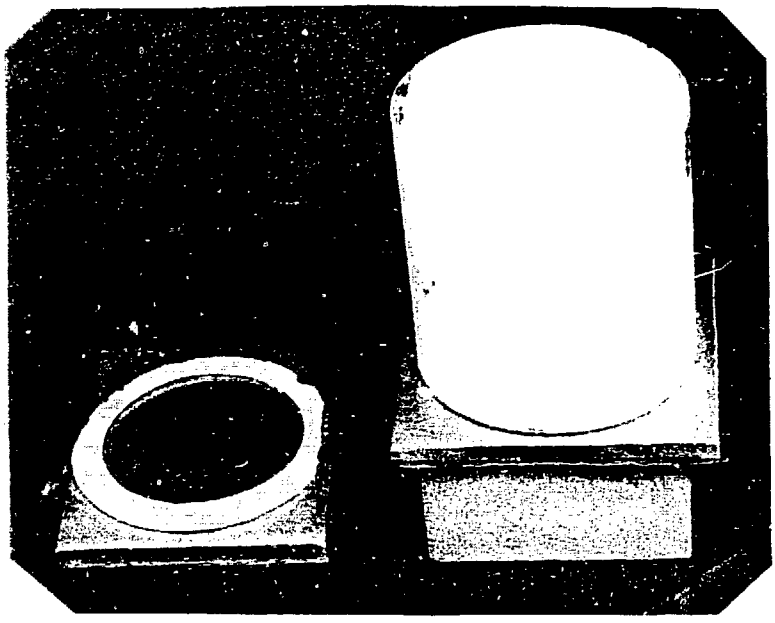

FIGURE 1.2.1-2

THERMOCOUPLE LOCATIONS FOR SIMULATED FULL SCALE RINGS

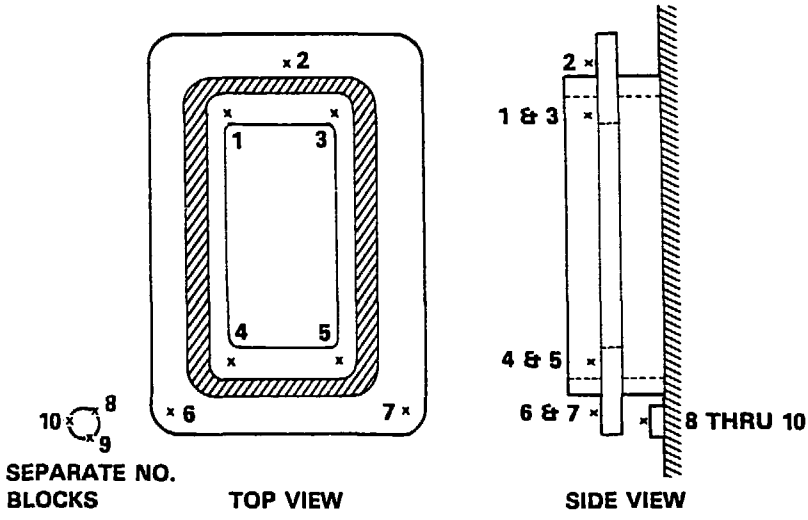

FIGURE 1.2.1-3

Figure 1.2.1-4 shows the time-temperature chart from the vacuum furnace run at brazing temperature. The overall temperature difference was 40°F which was higher than desirable. However, considering the size, different materials, and complexity of the part it was deemed acceptable, especially since the part subsequently passed acceptance test requirements.

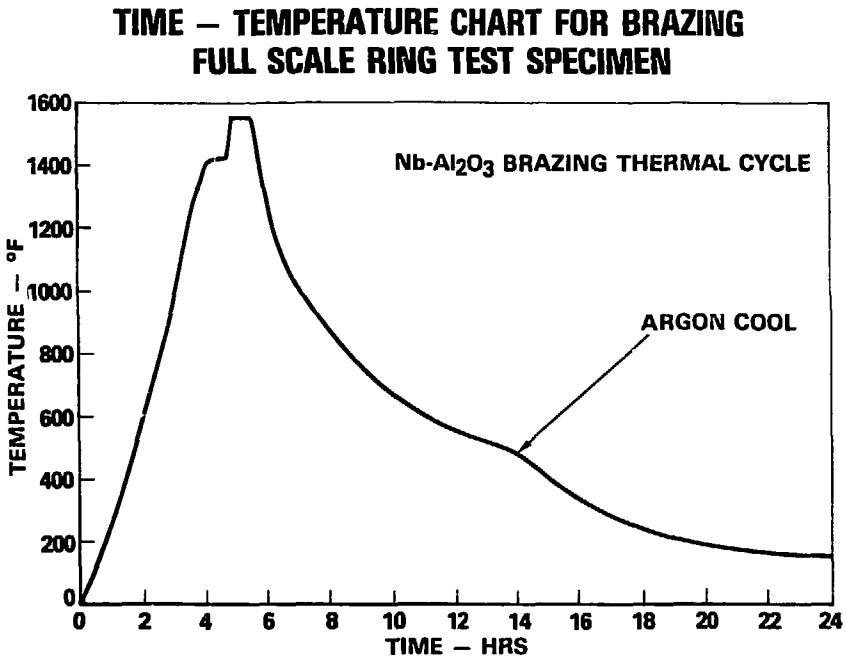

FIGURE 1.2.1-4

The acceptance test requirement was a leak free joint to 10^{-10} std cc/sec helium at a pressure differential of two atmospheres. A vacuum was pulled on the inside of the test part and autoclave pressure was exerted on the outside of the part. The part passed the two atmosphere requirements and finally failed at a pressure differential of approximately 9 atmospheres. Figure 1.2.1-5 shows the part after test with die penetrant showing the cracks that developed.

After successful completion and testing of the part, the techniques developed were utilized to fabricate the production TFTR insulator assembly.

TEST PART AFTER PRESSURE TESTING

FIGURE 1.2.1-5

The insulator assembly was processed for brazing per PB 12-145 of PS 22619. Braze alloy was 0.004 inch thick. The temperature differential during brazing was 40°F. Visual inspection of the insulator after brazing showed several areas where the braze alloy ran down the side of the alumina between the Nb rings and several other areas where puddles of excess alloy developed.

This insulator assembly was leak free to 10^{-10} std cc/sec helium after shipment to St. Louis from the brazing facility. Leaks developed in two diagonally opposite corners of the insulator at the Al_2O_3 to Nb interface during final assembly machining. Ultrasonic inspection revealed that these leaks were cracks along the braze line that propagated into the Al_2O_3.

The failed insulator was disassembled by removing the braze alloy in a 50% HNO_3-H_2O etchant. This etchant did not attack the Al_2O_3 or the Nb, however chips occurred in the Al_2O_3 during disassembly making these rings unusable. The Nb feedthrough rings were reinspected and found to be acceptable.

Stress analysis of the brazeo assembly predicted maximum stresses at the and bending at corners of the outermost niobium rings corners of the insulator. Refer to Section 1.4.2 for details of the analysis. The addition of an Al_2O_3 backup ring on the top and bottom of the assembly lowered the predicted stresses and reduced the bending. Therefore, back-up ceramic rings were added to the second production unit.

The second production insulator assembly was fabricated with new Al_2O_3 rings, including backup rings, and the Nb feedthrough rings from the failed insulator assembly. The braze alloy thickness was reduced to 0.003 inch.

Visual inspection of the insulator after brazing revealed no braze runs or puddles on the Al_2O_3. The insulator assembly was verified to be leak free to 10^{-10} std cc/sec He. A "C-scan" ultrasonic inspection was made on the assembly and showed no regions of questionable bonding.

1.2.2 Hard Vacuum Dielectric Seal Insulators - It is well known that since procelain enamels are glasses, they have high dielectric strength and a smooth impermeable surface for vacuum sealing. Porcelain enamels can be applied as thin coatings on metal surfaces.

Application of Enamel to Large Copper Parts - Enameling of small copper parts is common practice in industry, but enameling of parts as large as those in the plasma source assembly is not common practice and requires special handling. The Thomas C. Thompson Co. supplied MDAC-St. Louis with their #100 pea green copper enamel. This enamel was successfully applied to small test coupons of OFHC copper by spreading the enamel powder evenly over the surface of the specimen and then firing to melt the enamel to a smooth continuous glass layer. The procedure was scaled up to accommodate coating of larger parts with thick coatings of 20 mils or more. Using this method only one side could be coated at a time.

Coating of the thick cathode plate was unsuccessful due to glass disbond on cooling. As the larger part was removed from the furnace and cooled to room temperature, the enamel fractured and small flakes popped from the surface. Repeated attempts at enameling the large part with slower cooling cycles did not improve the adherence of the coating.

A thermal expansion measurement was made by the Coors Spectro-Chemical Laboratory. Figure 1.2.2-1 shows the results in comparison to high purity copper. The thermal expansion mismatch shown is typical of glass metal composites. Since glass is a brittle material and it almost always fails in tension, enamels are designed to be in compression when cooled after firing. This is done by compounding the enamel to give it a lower overall thermal expansion coefficient than the metal, so that upon cooling the enamel layer is placed into compression and the metal in tension. The thermal expansion value for the linear portion of the curve for enamel shown in Figure 1.2.2-1 is 35% lower than the thermal expansion of copper. This difference in expansion proved to be satisfactory for the smaller positive filament electrode copper parts. However, the enamel was put under too great of a stress when it was applied to the larger cathode plate in thick coatings. An enamel that more closely matched the thermal expansion of copper was needed for application to the larger cathode plate. The commercially available copper enamels do not have appreciably higher thermal expansion values than the one shown in Figure 1.2.2-1. Reformulation of a new enamel was not possible because of the expense and time it would involve. Attempts to increase the thermal expansion of #100 pea green enamel through mill additions were not successful.

Application of Porcelain Enamel to 321 Stainless Steel - An alternate design to insulate the large copper parts was to apply porcelain enamel to stainless steel sheets which would then act as insulating gaskets instead of directly applying the enamel to the copper. There are several advantages to using this design as follows:

a) Expensive copper parts are not commited to a heat cycle that would stress relieve the parts and therefore reduce their strength.
b) Thin stainless steel parts are cheaply and easily replaced if damaged.

c) Stainless steel is nonmagnetic.

d) Interchangeability between hard "C" seals and "O" rings is maintained. The disadvantage of using enameled stainless steel is that is doubles the number of vacuum sealing surfaces.

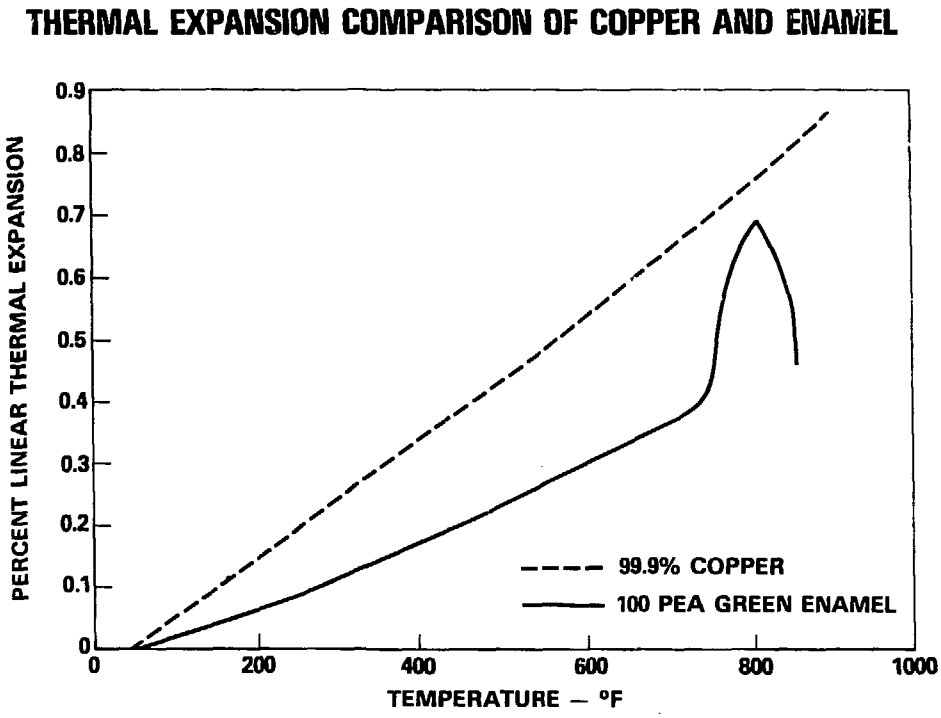

FIGURE 1.2.2-1

Stainless steel alloy 321, 0.032 inches thick, was chosen because of its inhouse availability. Two commercial enamels were chosen that were compatible with 321 stainless steel. Chi-Vit's SG-33766 titanium opacified enamel and O. Hommel's #MF9754 blue enamel. These enamels can be applied to the part using "state-of-the-art" techniques of dipping the part directly into the enamel slurry or using spraying techniques similar to those used for spraying paint. The spraying method was chosen because it provided the more uniform thickness.

Metal parts were cleaned with of Methyl Ethyl Ketone (MEK) and then roughened by grit blasting with size 10 glass beads. The porcelain enamel did not require

any preparation other than thorough mixing or an occasional density adjustment. Application of the enamel to the parts was made using a Devilbiss type EGA Series 502 spray gun. The amount of enamel applied was determined by weight as suggested by the enamel manufacturer. The O. Hommel enamel was applied to a coating weight of 20-23 gm/ft^2. The Chi-Vit enamel was applied to a coating weight of 28-32 gm/ft^2. The firing time used depended largely on the size and thickness of the part and the enamel. Figure 1.2.2-2 illustrates firing time dependency on thickness. Firing temperature for both enamels was 1500°F. Both sides of the parts were coated and fired at one time.

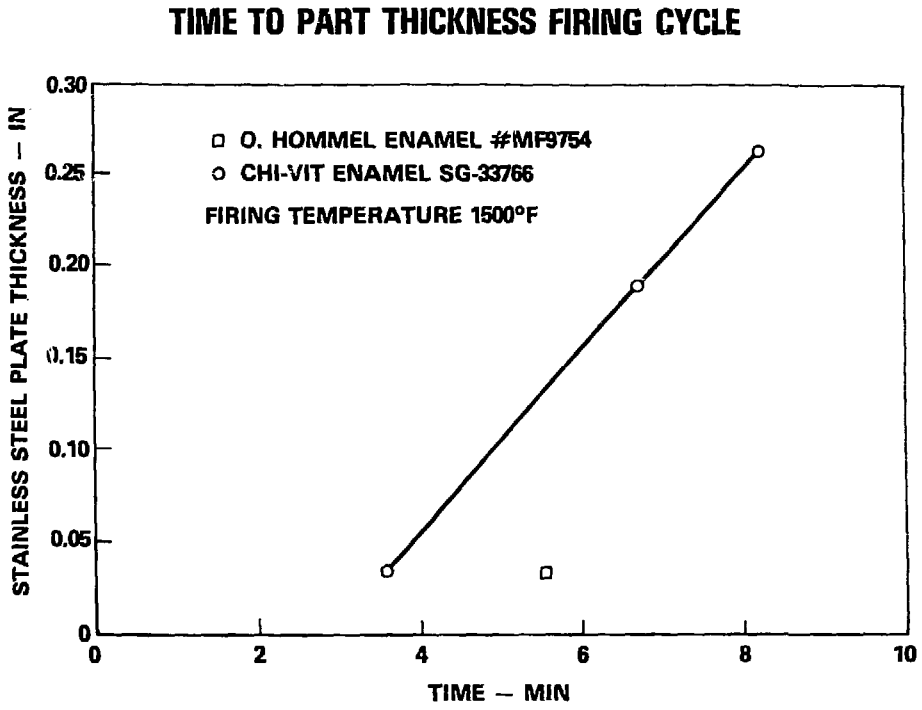

FIGURE 1.2.2-2

After successful application of the porcelain enamels to stainless steel, sample coupons of the two enamels were made and checked for vacuum sealing ability. Both enamels provided vacuum tight seals when rubber "O" rings were used. However, when a metal "C" seal was used on the white enamel from Chi-Vit, the enamel became chipped around some of the holes. The apparent cause was due to

a build-up or meniscus of enamel around holes and edges. When pressure was applied to compress the "C" seal the copper plates came in contact with the enamel causing it to fracture. It was found that by applying a thinner coating the meniscus could be reduced to acceptable levels. Thinner coatings were best applied with the blue enamel from O. Hommel, because it is sprayed at a lower specific gravity.

Figures 1.2.2-3 shows drawings of the 321 stainless steel parts. Complete coverage of all edges on the parts was not possible because the metal was so thin. The tight radius around the edge of .032" thick metal creates excessive stress when the enamel is fired. Minimum radius used in industry for most enamels is 1/8". Enough space was provided between the copper and insulator edge to give adequate electrical insulation.

All finished porcelain enameled plates were electrically checked using ASTM C-743 "Continuity of Porcelain Enamel Coatings". The voltage used in the test was 200V DC. Dielectric strength of the porcelain enamel was found to be 200 v/mil.

1.2.3 Deep Drawn Molybdenum Shields - The original design concept selected for the suppressor and gradient grid shields involved break forming 0.010 inch thick molybdenum sheet metal and welding the four (4) corners to form the rectangular shield. The four corners of the shields were recrystalized during the welding and cracked at one or more of the corners when installed on the grids. Several attempts to weld and reweld the shield only increased the brittle zone and resulted in more severe cracking at the corners. Because of these failures, it was felt that a new, more reliable, lower cost shield fabrication technique was required for future production ion sources. Therefore, a deep draw process was selected and developed under company funds to eliminate the need for welding. The gradient grid shield was redesigned to increase the shield corner radii to simplify forming. The redesigned deep drawn gradient grid shield is shown in Figure 1.2.3-1. The deep drawn suppressor grid shield is shown installed on the suppressor grid in Figure 1.2.3-2. Both deep drawn shields were hydrogen fired in our vacuum/hydrogen brazing furnace prior to installation on the grids.

1.3 Design Changes - During the fabrication several design changes were made as a result of manufacturing problems and reviews with LBL.

STAINLESS STEEL PLATE .032" THICK

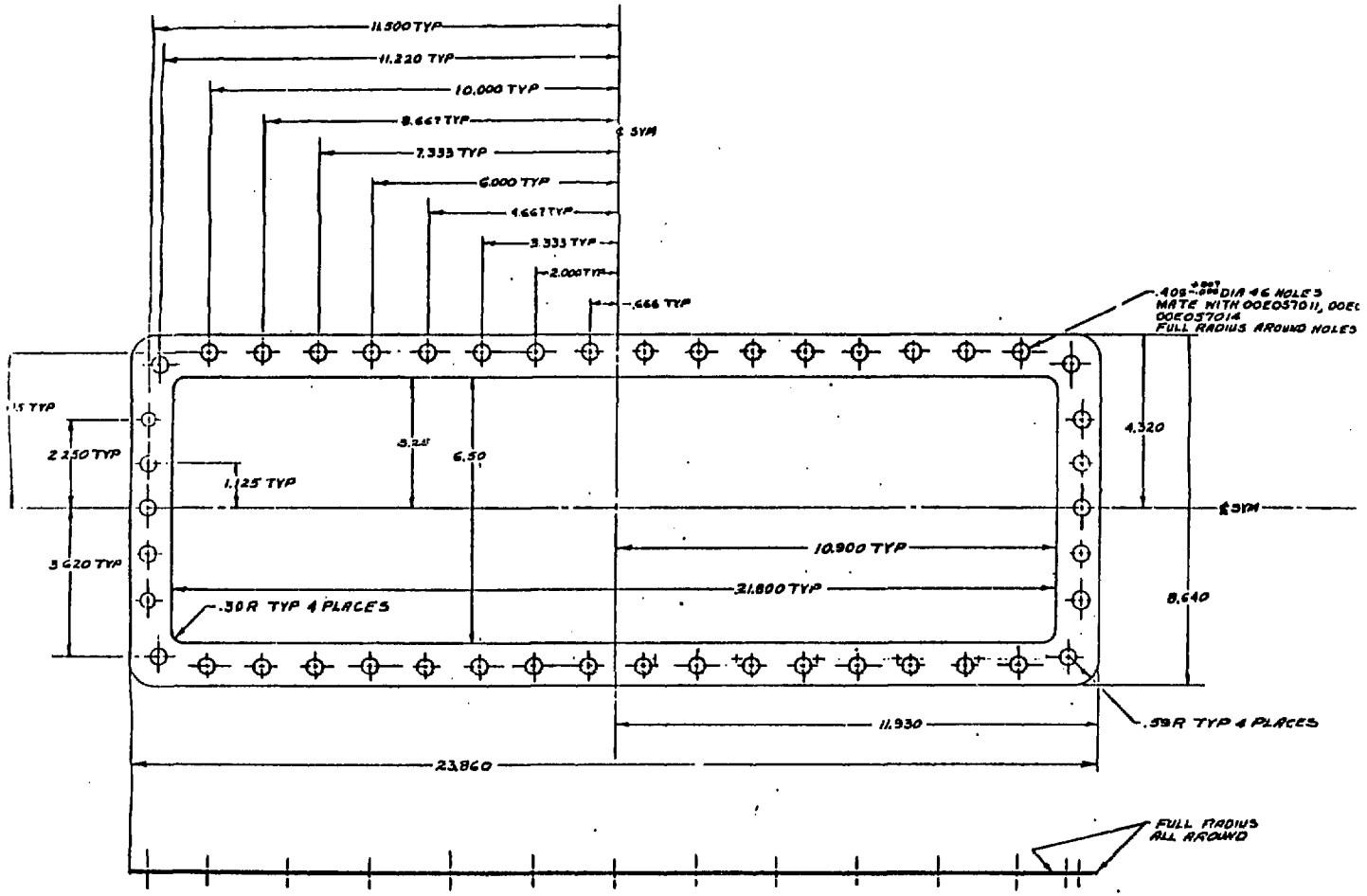

(A)

FIGURE 1.2.2-3

STAINLESS STEEL PLATE .032" THICK

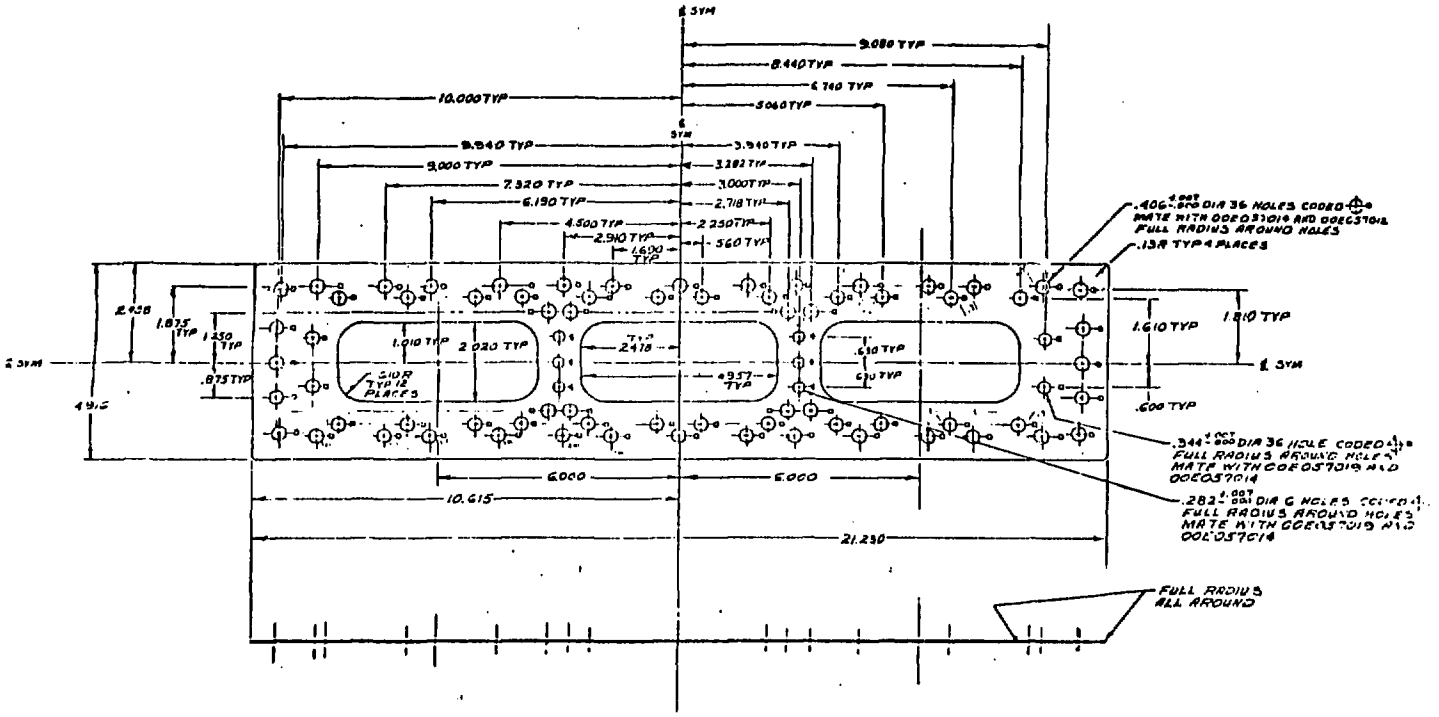

(B)

FIGURE 1.2.2-3 (continued)

DEEP DRAW MOLYBDENUM SHIELD
TFTR ACCELERATOR GRADIENT GRID

13–2643

FIGURE 1.2.3-1

1.3.1 Plasma Generator Changes - Fabrication of plasma generator components and full scale development testing of hard vacuum dielectric seals resulted in two changes to the plasma generator. One involved increasing the number of fasteners required in the anode supports and filament electrodes to be compatible with the hard "C" seals. The second change involved a new concept for the porcelain enameled dielectric seal insulators and was discussed in Paragraph 1.2.2 above.

Development testing of full size hard "C" seals indicated the need for pressures on the order of 260 pounds per linear inch on the straight sides and 500 pounds per linear inch at the corners to achieve the specified leakage rate of 10^{-10} scc/sec of helium. The original fastener design located the attaching bolts on 2.5 inch centers around the periphery of the filament electrodes and four (4) fasteners at each corner of the anode supports. This fastening technique was not sufficient to meet the seal compression requirements as defined by the develop-

TFTR ACCELERATOR DEEP DRAWN MOLYBDNUM SUPPRESSOR GRID SHIELD (INSTALLED)

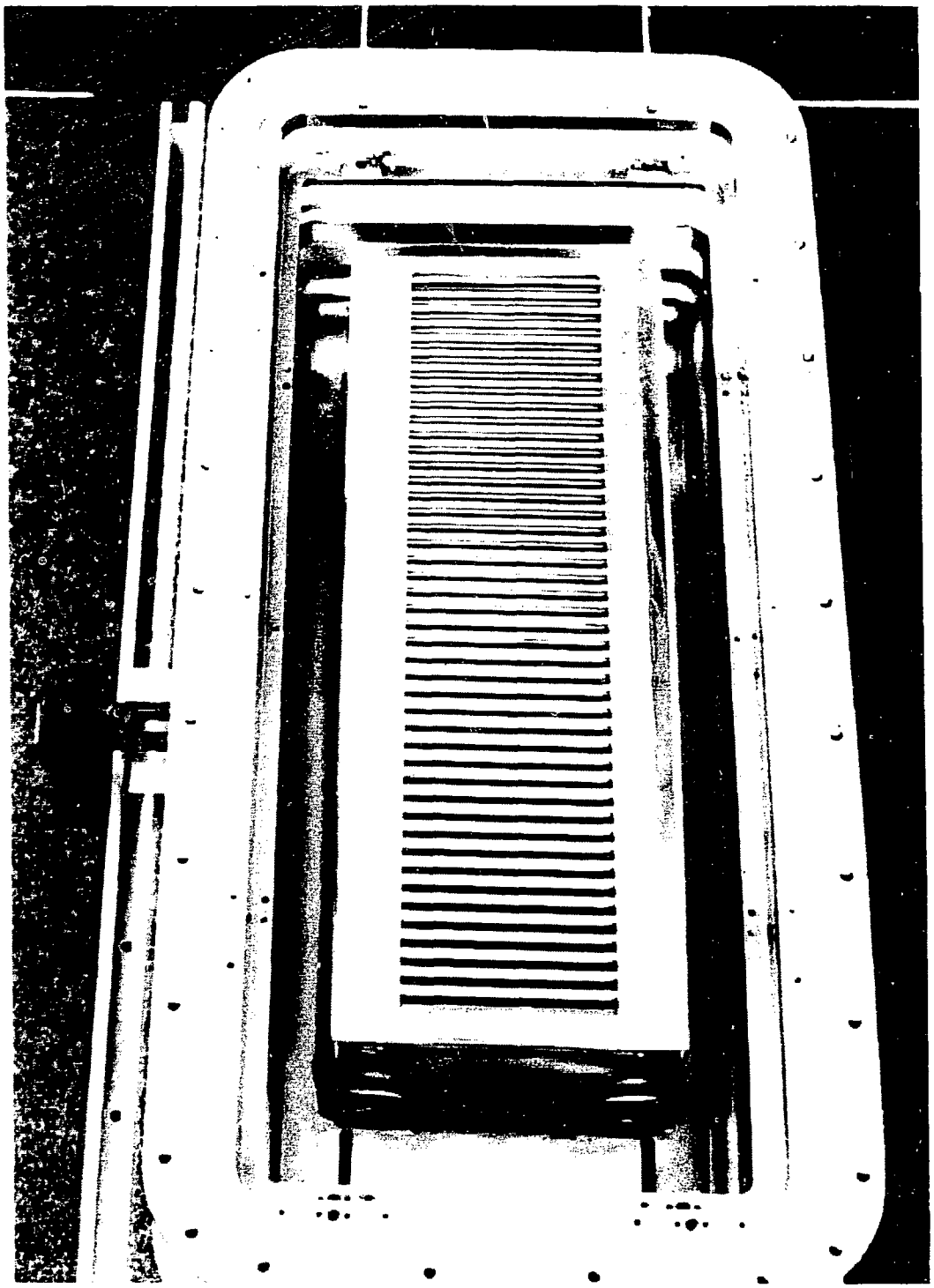

13-2642

FIGURE 1.2.3-2

ment tests. To meet the requirements, additional fasteners were added by remachining the electrodes and anode supports to provide bolt centerline spacings of approximately 1.5 inch. Figure 1.3.1-1 shows the redesigned anode supports and filament electrodes and the added fastener locations.

1.3.2 Accelerator - The accelerator was pre-assembled prior to cleaning and hydrogen firing to insure proper fitup of the components. Disassembly of the unit was witnessed by LBL personnel and the following design changes were made as a result of this review.

(1) A molybdenum shield was added to the probe plate to cover exposed portions of the source grid shield fasteners. The configuration of this shield is shown on Drawing 00E057110.

(2) The ends of the gradient grid rail holders and hats were radiused to eliminate sharp corners.

(3) The exit grid end shims were widened to seal gaps between the hat and water fittings.

(4) A shield was added to the exit grid ends to cover gaps between the end pieces and the hat. The configuration of the shield is shown on Drawing 00E057111.

1.4 STRUCTURAL ANALYSIS - Thermal stress analysis of a straight bar braze assembly was performed to identify the metal/ceramic combination most likely to survive the brazing cycle and mechanical loadings. The material combinations evaluated were also required to satisfy electrical insulating requirements. Evaluation of material combinations was based on axial thermal stresses in the ceramic and shear stresses in the braze resulting from cooldown from brazing temperatures. The evaluation was based on stress in the straight bar and assumed shear stresses occuring uniformly over a one-inch length at each end. Results are shown in Figure 1.4-1 for several material combinations. These stresses are based on a 0.85 inch thick ceramic. This configuration provided representative stresses for comparing material combinations. The best conbination is one that has the lowest axial thermal stress in the ceramic and the lowest shear stress in the

ORIGINAL

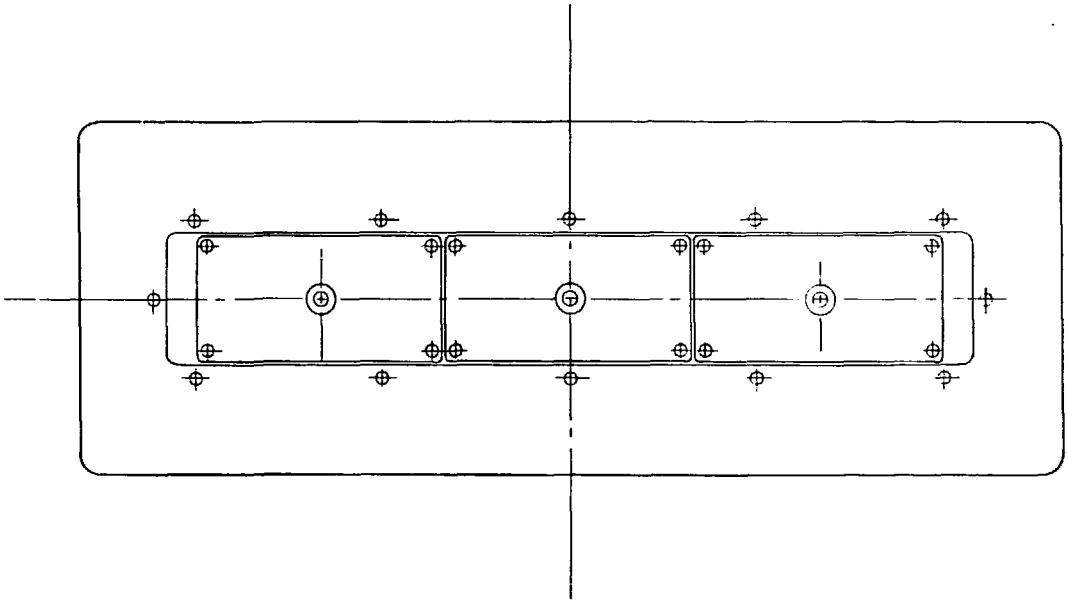

REDESIGN

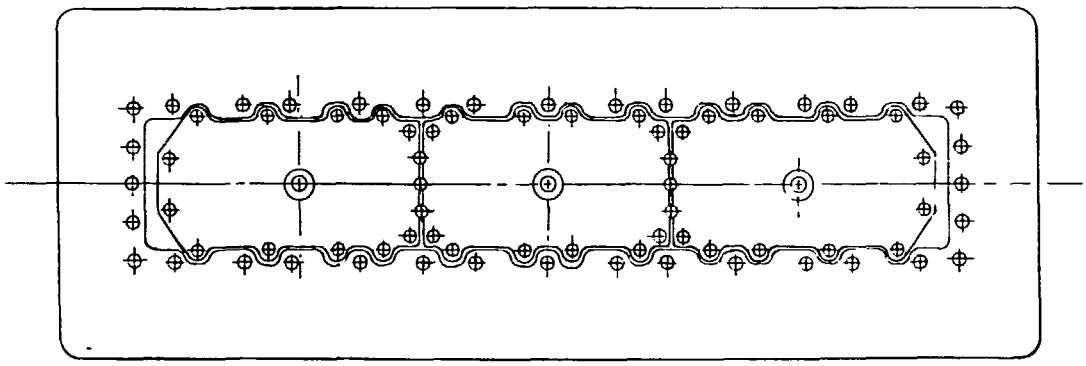

FIGURE 1.3.1-1

AXIAL THERMAL STRESSES IN THE CERAMIC AND BRAZE SHEAR

STRESS FOR VARIOUS MATERIAL COMBINATIONS

METAL/CERAMIC COMBINATION	SHEAR STRESS IN BRAZE ∿psi	AXIAL THERMAL STRESS IN CERAMIC ∿psi
FS 85/ALUMINA 94%	610	480 (TENSION)
COMM PURE Nb/ALUMINA 94%	2670	2120 (COMPRESSION)
FS 85/STD. ELECT. PORC.	4137	3283 (TENSION)
COMM PURE Nb/HIGH STR. ELECT. PORC.	5110	4060 (COMPRESSION)
FS 85/ALUMINA 85%	7400	5880 (COMPRESSION)
COMM PURE Nb/ALUMINA 85%	7840	6220 (COMPRESSION)
COMM PURE Nb/STD. ELECT. PORC.	13700	10860 (COMPRESSION)
FS 85/HIGH STR. ELECT. PORC.	15700	12460 (COMPRESSION)
COMM PURE Ti/MACOR	16580	13100 (TENSION)
COMM PURE Ti/ALUMINA 94%	26100	20700 (COMPRESSION)
COMM PURE Ti/ALUMINA 85%	31300	24900 (COMPRESSION)

FIGURE 1.4-1

braze. Since the compressive strength of the ceramic is higher than the tensile strength, compression in the ceramic is preferred.

Subsequently, more detailed analysis was conducted to determine actual combined stresses in the accelerator assembly. The braze joint was developed to a point where it was stronger than the adjacent ceramic. The ceramic wall thickness was then sized for the combined thermal and mechanical loadings.

Thickness of the ceramic wall was sized considering the cross sectional areas, moments of inertia, modulus of elasticity, and load sharing of the metal and ceramic frames. The two atmosphere external pressure load is shared between the ceramic and metal frames according to their relative bending stiffnesses. As ceramic thicknesses increases, bending stresses in the ceramic decrease even though more load is carried in the ceramic. This variation with thickness is shown in Figure 1.4-2. Also shown in the figure is the 4375 psi design stress of 85% alumina. This allowable stress level is based on vendor supplied average tensile strength data with a reduction factor of 0.50 to account for scatter. A factor of safety of 2.0 was also used to reduce the design stress level. Similar analysis of FS85/94% alumina and commercially pure niobium/94% alumina under combined loading gave maximum tensile stresses very near that found for the chosen material combination 85% alumina and commercially pure niobium.

The ceramic wall thickness chosen was 0.75 inch. This wall thickness results in a bending stress of 4150 psi which is slightly below the design stress level. The 0.75 inch ceramic wall thickness provides the required room for remote handling equipment to reach and remove the attachment bolts as a maintenance operation.

A NASTRAN finite element model was constructed using beam elements to determine thermal stresses in the corners of the accelerator subassembly. The model for the bellows end, with a ceramic backup ring is shown in Figure 1.4-3. Analysis was conducted both with and without the ceramic backup ring to evaluate the reduction in stresses that result from using the backup ring. The ceramic and niobium rings were modeled from the center of the long side of the subassembly to the center of the short side. The beams in the longitudinal (X) ring direction represent the axial and bending stiffnesses of the niobium and ceramic

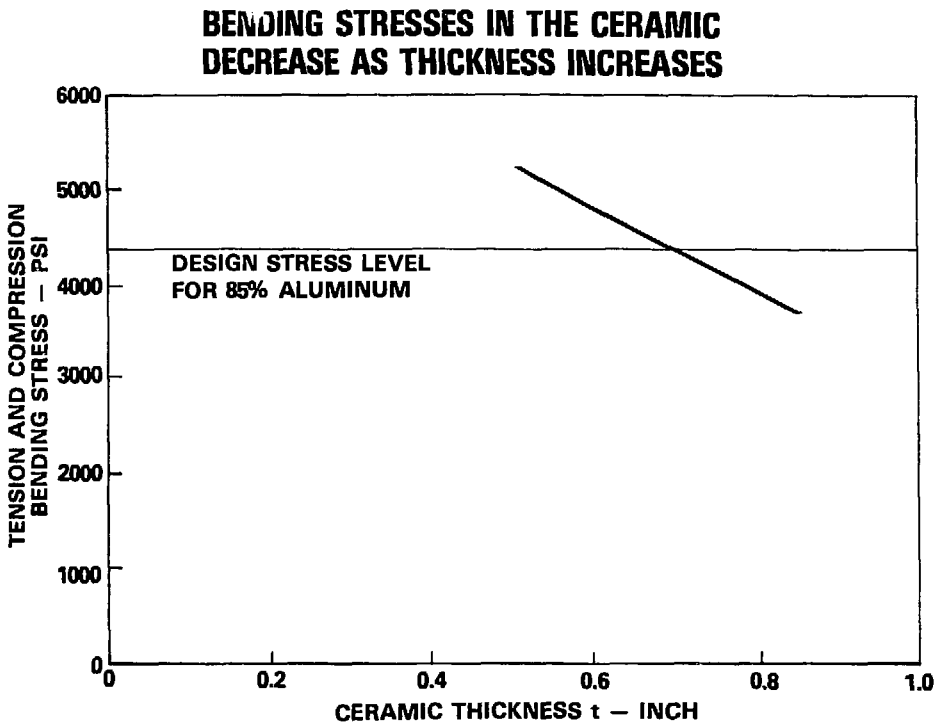

FIGURE 1.4-2

rings. Beams in the vertical (Z) direction represent the axial and bending stiffness of the ceramic. The beam element allows the shear center and neutral axes to be located in their actual location instead of at the grid point. The model was restrained from rotation about the Z axis at the ends (center of the spans) and from rotation about the X axis at the centerline of the top niobium frame. A temperature of -823°C was applied to represent cooldown from the braze temperature.

The finite element analyses gives the radial running shear forces and tipping moments between the end niobium and ceramic frames at the corner and are shown in Figure 1.4-4. Addition of the backup frame reverses the direction of the tipping moment carried across the braze and reduces it by approximately a factor

NASTRAN FINITE ELEMENT MODEL OF ACCELERATOR SUBASSEMBLY CORNER AT BELLOWS END

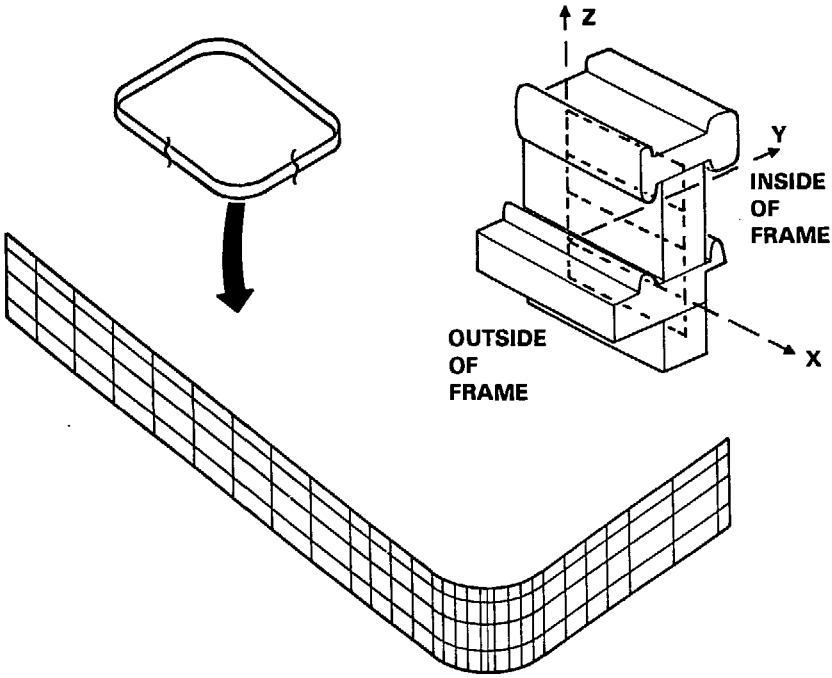

FIGURE 1.4-3

of two. Shear stresses are reduced by approximately 20%. The maximum tipping moment between the end niobium and end ceramic frame is 420 in-lbs/in. At the braze between the end niobium frame and ceramic backup frame the bending moment is approximately the same. The maximum shear load of 3800 lbs/in corresponds to a stress of 4.0 ksi and a bending moment of 420 in-lb/in corresponds to a maximum tensile stress across the braze of approximately 4.5 ksi.

A 2 atmosphere differential pressure will be applied to the accelerator subassembly during operation. To calculate combined stresses in the ceramic, the external pressure was applied to the NASTRAN thermal stress model. Resulting stresses in the ceramic due to the external pressure and cooldown from braze temperature are shown in Figure 1.4-5(a). These stresses and shears are at the center of the corner.

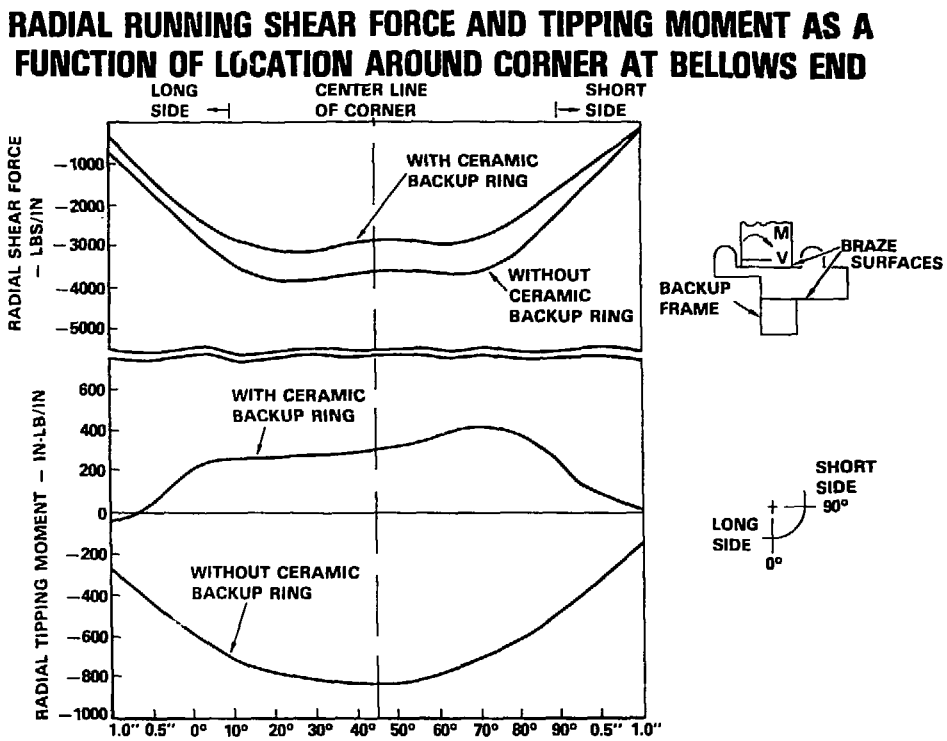

FIGURE 1.4-4

Ceramics will most likely fail by brittle fracture. Therefore, the applicable theory of failure in analyzing the ceramic is the maximum strain theory of failure. According to this theory the maximum equivalent axial stress in the corner of the ceramic is 5600 psi, as shown in Figure 1.4-5(b). With a failure stress of 7200 psi, a margin of safety of +.3 results based on actual loads. A margin of safety of +1.0 was desired.

1.4.1 Ceramic/Niobium Test Specimens - Large variations in strengths exist for the ceramics and brazes for joining ceramics to metals. To increase confidence in the material combination and braze selected for the accelerator subassembly design, several 85% alumina to niobium braze specimens were fabricated and tested. Initially straight bar assemblies were brazed successfully. Then three ceramic cylinders with niobium plates brazed to each end were fabricated and

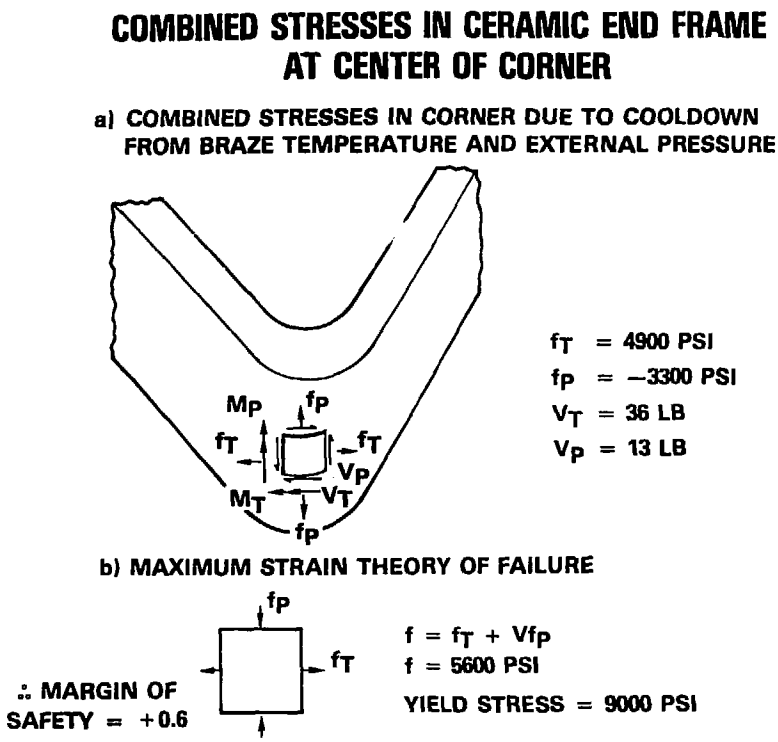

FIGURE 1.4-5

mechanically tested. A corner specimen was also successfully brazed to determine the compatibility of the commercially pure niobium, 85% alumina and braze material. Finally a full scale rectangular configuration, shown in Figure 1.4-6, was fabricated.

Each of the cylindrical ceramic to niobium braze specimens were mechanically tested to failure. Two specimens were tested by applying an axial tension load. Failure occurred at an axial load level corresponding to apparent low axial stress levels (P/A = 0.94 ksi and 2.43 ksi). An internal pressure was applied to the third specimen and failure occurred at an apparent hoop stress level of pr/t = 3.1 ksi. Detailed stress analysis taking into account thermal stresses, resulting from cool down, shows that a combined equivalent axial stress level of approximately 12 ksi was attained in the two weakest specimens. While stress levels of approximately 11 ksi were attained at the braze, none of the specimens failed in

FULL SCALE ALUMINA/NIOBIUM/ALUMINA
BRAZE ASSEMBLY

FIGURE 1.4-6

the braze. Therefore, it was believed that the braze choice and processing procedures developed gave brazes that exceed the strength of the ceramic. The cylindrical test specimen geometry and the combined stress levels attained in the two weakest specimens are shown in Figure 1.4-7(a).

Stress components in three directions were combined along the length and through the thickness of the ceramic cylinders to determine critical locations and equivalent axial stress levels at failure. The combined stress levels at these critical locations are shown in Figures 1.4-7(b), -7(c), and -7(d) for thermal stress only, thermal stress plus axial load, and thermal stress plus pressuriza-

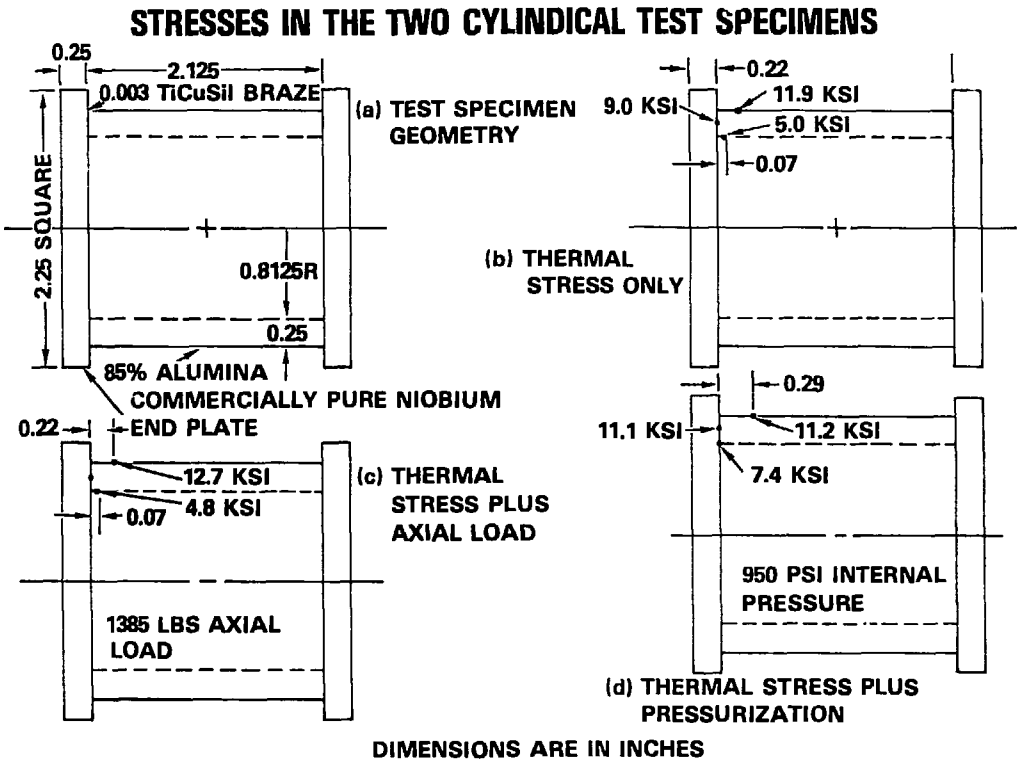

FIGURE 1.4-7

tion, respectively. Comparison of the stresses shown in Figures 1.4-7(b), -7(c), and -7(d) indicates that most of the stress in the ceramic was due to the thermal contraction. The combined stress level of 12.7 ksi in the ceramic in the axially loaded specimens is in the range of the expected strength of the ceramic. This stress level occurs over the length .15 to .22 inches from the ends. Analysis of the membrane and discontinuity mechanical and thermal stresses in the pressurized test specimen indicates that the ceramic was sustaining tensile stresses on the order of 11.2 ksi over the first 0.37 inches from the ends. Approximately equal peaks were found at two locations. On the outside surface a peak occurs at 0.27 inches from the ends with essentially constant stress over the length 0.22 to 0.34 inches from the ends. The largest component is a longitudinal stress from the discontinuity (cylinder to end plate) shear force. On the midplane of the ceramic at the ends there is a peak combined stress equivalent to 11.1 ksi. This stress is primarily a result of the shear stresses at the ends along with large

compression hoop stress (elastic foundation) from the differential thermal contraction. Because ceramics are flaw sensitive, the actual failure location does not necessarily coincide with the peak stress location.

Most of the strength of the test specimens was utilized in sustaining the geometry dependent thermal stresses. The end plates in the test specimens are quite stiff and greatly contribute to the discontinuity stresses. Thermal stresses at the corners of the accelerator subassembly's rectangular frames are considerably less because a full hoop (ring) restraint doesn't exist there. Lower thermal stresses in the full size ceramic frames allow higher mechanical stresses to be sustained.

A full scale alumina/niobium/alumina braze assembly was made to demonstrate that a vacuum tight brazed accelerator subassembly was feasible. The brazing operation was successful and gave a crack-free, vacuum tight assembly.

The full scale alumina/niobium/alumina braze assembly was subjected to external pressure loads to verify the structural integrity of a representative test article at design pressures. The open ends of the test article were sealed by thick aluminum plates with rubber seals and a differential collapse pressure was applied in an autoclave. The test article was fully instrumented to verify load sharing and distribution and failure. Instrumentation of the test article included thirteen strain gages and an internal pressure gage. Strain gages were placed at critical locations on the ceramic and niobium rings.

The external pressure on the test article was increased above the 2-atmosphere operating level until leakage of the seals overtook the autoclave pressurization. A plot of the test article internal gage pressure versus autoclave gage pressure is shown in Figure 1.4-8. The maximum pressure differential attained between the inside and outside of the test article was 145 psi (10 atm), as shown in Figure 1.4-8. The combined mechanical/thermal stress levels attained with 145 psi differential pressure were well above the combined stress level consistant with a factor of safety of 2.0.

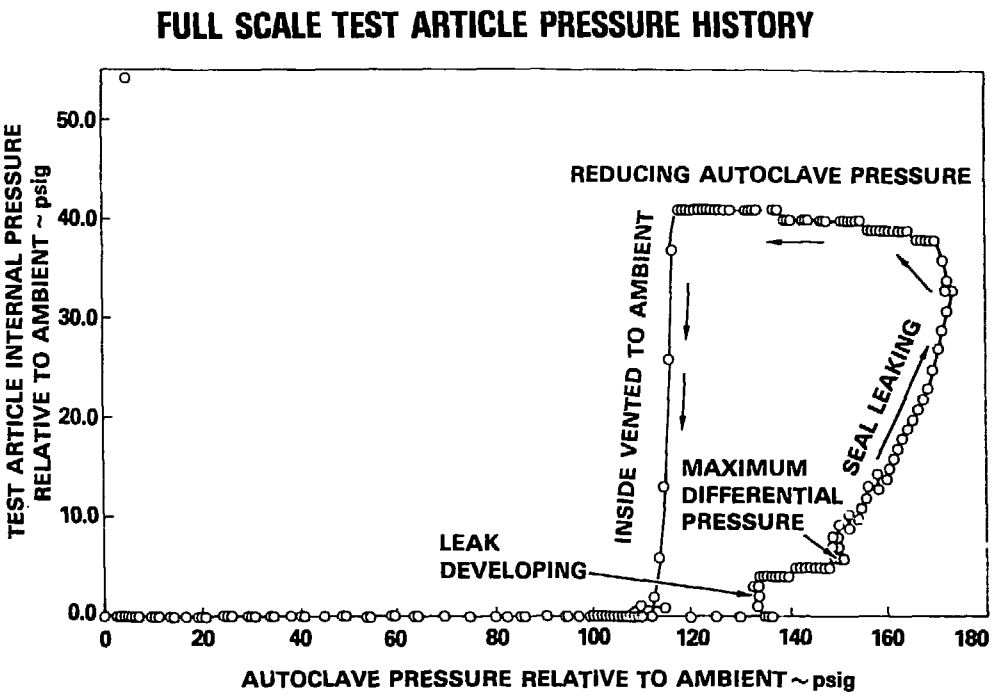

FIGURE 1.4-8

Examination of the test article after pressurization indicated that the braze withstood the differential pressure without failure. Cracks had developed in the ceramic frames near the center of the long sides and at the corners, as expected. Cracks at the center of the long sides propagated to the neutral axis of the composite (ceramic/metal) beam where they gradually turned 90 degrees and stopped. Cracks at the corners of the ceramic went through the thickness and may have leaked. However, the main source of leakage in the assembly was from the rubber seal on the closure dates being sucked in at the higher pressures.

Strain gage data and the corresponding stress for the inside surfaces of the ceramic and niobium frames at the center of the long side is shown in Figure 1.4-9. At both locations the strain increased linearly with increasing external pressure until at an autoclave pressure of 152 psig, the strain jumped at both locations, indicating some sort of structural adjustment. The differential pressure at that

STRAIN GAGE DATA AT INSIDE CENTER OF LONGSIDE INDICATES CRACKING OCCURRED AT AN AUTOCLAVE PRESSURE OF 152 psig

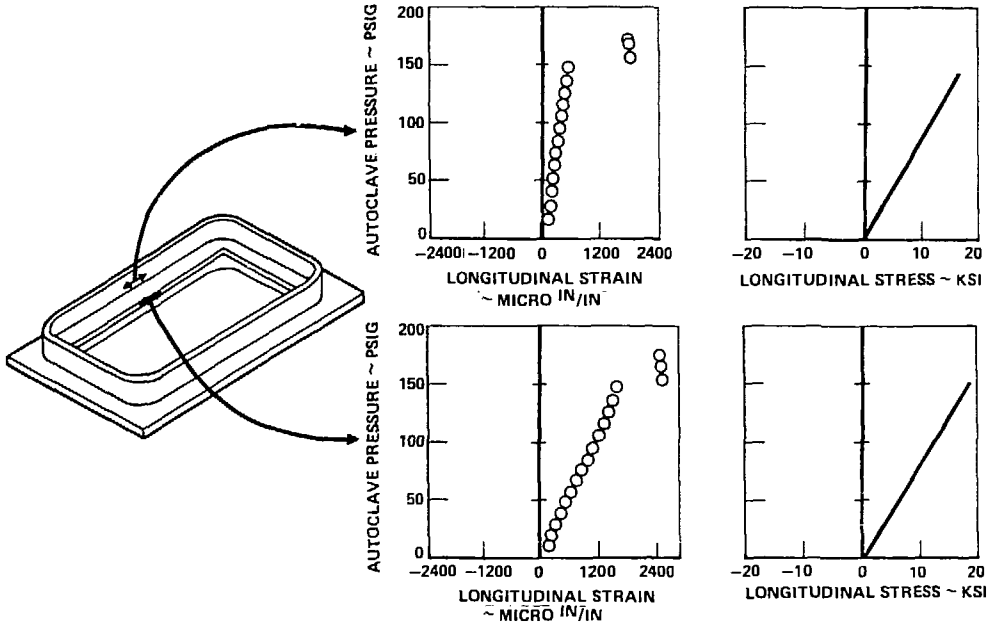

FIGURE 1.4-9

time was the maximum value reached (145 psi). The strain in the ceramic jumped from 550 micro in/in to 1800 micro in/in. In the niobium ring the strain jumped from 1600 micro in/in to 2500 micro in/in.

The conclusion drawin from the test was that a full scale accelerator sub-assembly of these material and braze combinations would work for the actual geometry, loads, and metal/ceramic area and bending resistance ratios involved.

2.0 MANUFACTURING

In keeping with the "Industrialization" concept, the fabrication of the TFTR ion source was established at the outset as a full production program within the manufacturing departments of MDAC-St. Louis. In this manner, all organizations were provided the program visibility necessary to insure that materials, manpower and facilities were available resulting in a nucleous of trained production personnel with hands-on experience in fabricating TFTR ion sources. Below is a detailed description of the manufacturing process used and problems encountered and their solutions. The TFTR Neutral Beam Source has been completed and delivered to LBL for operational testing.

2.1 Manufacturing Process - The MDAC-St. Louis approach used to fabricate the detailed parts and assemblies and the sequence of machining and assembling these components is presented below. Manufacturing work orders and sequential manufacturing flow diagrams were first developed for the plasma source and the accelerator (extractor) showing the sequencial steps, tooling requirements and quality assurance inspection points. A detailed description of the sequential manufacturing sequences is presented along with the flow diagrams. These flow diagrams identify long lead material, tooling, manufacturing sources, scheduling conflicts and capital equipment requirements.

2.1.1 Plasma Source Assembly - The plasma source subassembly negative filament electrode, positive filament electrode, and the cathode plate were rough machined on all surfaces, alternating the rough machining between both sides of the copper plates to minimize distortion.

The negative filament electrode was finish machined after roughing with the exception of the filament chuck support flanges. These flanges were left oversize until the 204 holes were taped. The flanges were then machined to drawing tolerances to eliminate tap break-out on the side walls of the flanges. All mounting holes were drilled to pilot size only to accommodate mate drilling with the other electrodes at final assembly.

The positive filament electrode, cathode plate and anode supports were finish machined using standard machining procedures, after which, the mounting holes were pilot drilled for later mate drilling at final assembly.

The wall tank electrode was hogged out of a 3-inch thick plate of OFHC copper to eliminate the need for brazing. Structural support gussets were machined from aluminum with a slip fit between the upper and lower wall tank flanges. The gussets were held in place by long bolts which passed through the entire assembly ending in a tapped hole in the lower wall tank flage. Holes in the flanges were pilot drilled followed by mate drilling at plasma source final assembly.

The hard vacuum dielectric seal insulators were machined from 304 stainless steel, deburred and inspected. Following cleaning, porcelain enamel was applied to the steel substrate and inspected for proper thickness and finish. This was a change to the basic design approach of applying enamel directly to the copper electrodes. A description of the problems encountered and the solutions are presented in Paragraph 2.2.1.

The anode plates, gas divertors and filament chucks were fabricated from molybdenum. The filaments were made from tungsten and formed over a form die to provide uniform contours and filament length.

The plasma source machined parts were preassembled and inspected to assure proper fit-up and then mate drilled. Following disassembly, the parts were cleaned and reassembled in a clean room. All parts were handled with surgical gloves to maintain cleanliness.

The assembly sequence of the plasma source was as follows:

(1) Assemble wall tank electrode, porcelain insulators, cathode plate, filament electrodes and gussets using insulating bushings and screws. The mating screws were torqued to specified levels in a controlled sequence to prevent warping and insure vacuum sealing integrity.
(2) Install anode supports.
(3) Install anode plates.

(4) Install filament chucks in positive and negative filament electrodes.
(5) Install filaments.

The plasma source assembly manufacturing flow is depicted in Figure 2.1.1-1.

After assembly of the plasma source, a series of manufacturing tests were performed to assure proper assembly prior to final assembly to the accelerator. These tests included a vacuum leak check and an electrical continuity check before filament installation. Problems with the hard "C" seals were encountered in final assembly which are discussed in Paragraph 2.2.2.

2.1.2 Accelerator Grid Assemblies - Grid rail alignment was critical to the functional operation of the neutral beam ion source. The methods and techniques used to achieve the precision alignment requirements began with the fabrication of the detail parts and continued through final assembly and inspection. In order to maintain final accelerator assembly tolerances, early attention was given to the fabrication and quality control of the grid rails and rail holders. Manufacturing flow diagrams of the source, gradient, suppressor and exit grid assemblies are shown in Figures 2.1.2-1 through 2.1.2-4.

Grid Rails - The grid rails were fabricated by a cold rolling manufacturing method. Each rail was inspected for proper cross-sectional dimensions and straightness. A non-contact probe in conjunction with our coordinate measuring machine was used to check each rail for straightness in both axis.

Grid Rail Holders - The rail holder is a complex part requiring precise machining to insure precision rail to rail alignment. The gradient suppressor and exit rail holders were machined using special form cutters and machined in pairs to achieve the tolerance between rail slots of ± 0.001 inch. The source grid rail holders were EDM machined. The holders were rough machined and the cross section contour finished machined prior to drilling holes and machining of the slots for the grid rails. The grid rail slots were rough machined leaving approximately 0.010 inch on each side of the slots. Finishing passes were made on one side of each slot at a time. This routine eliminated cutter deflection which could result in a buildup of tolerance. No attempt was made to mill the slot to final tolerance

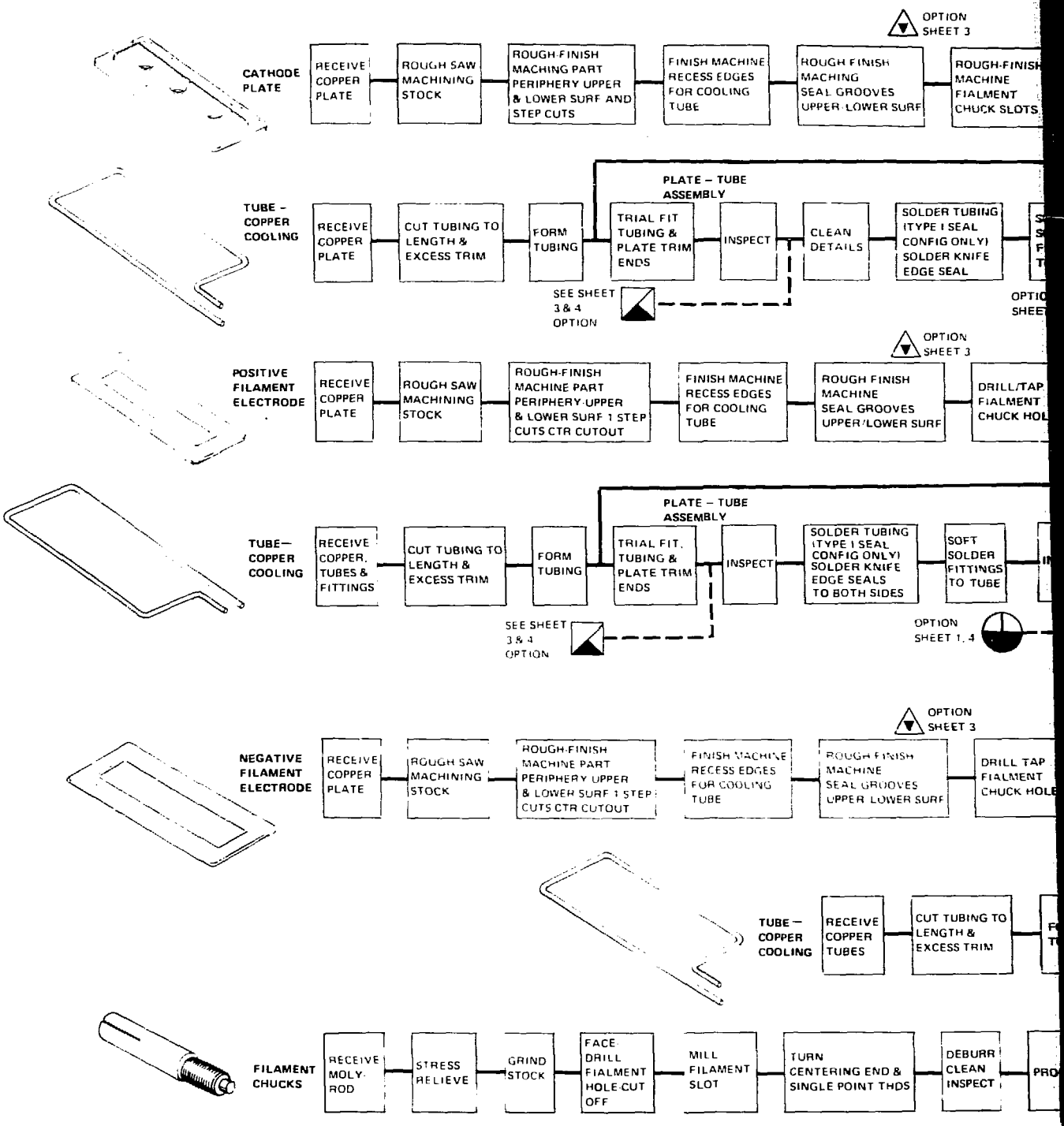

13-1305

FIGURE 2.1.1-1 (A)

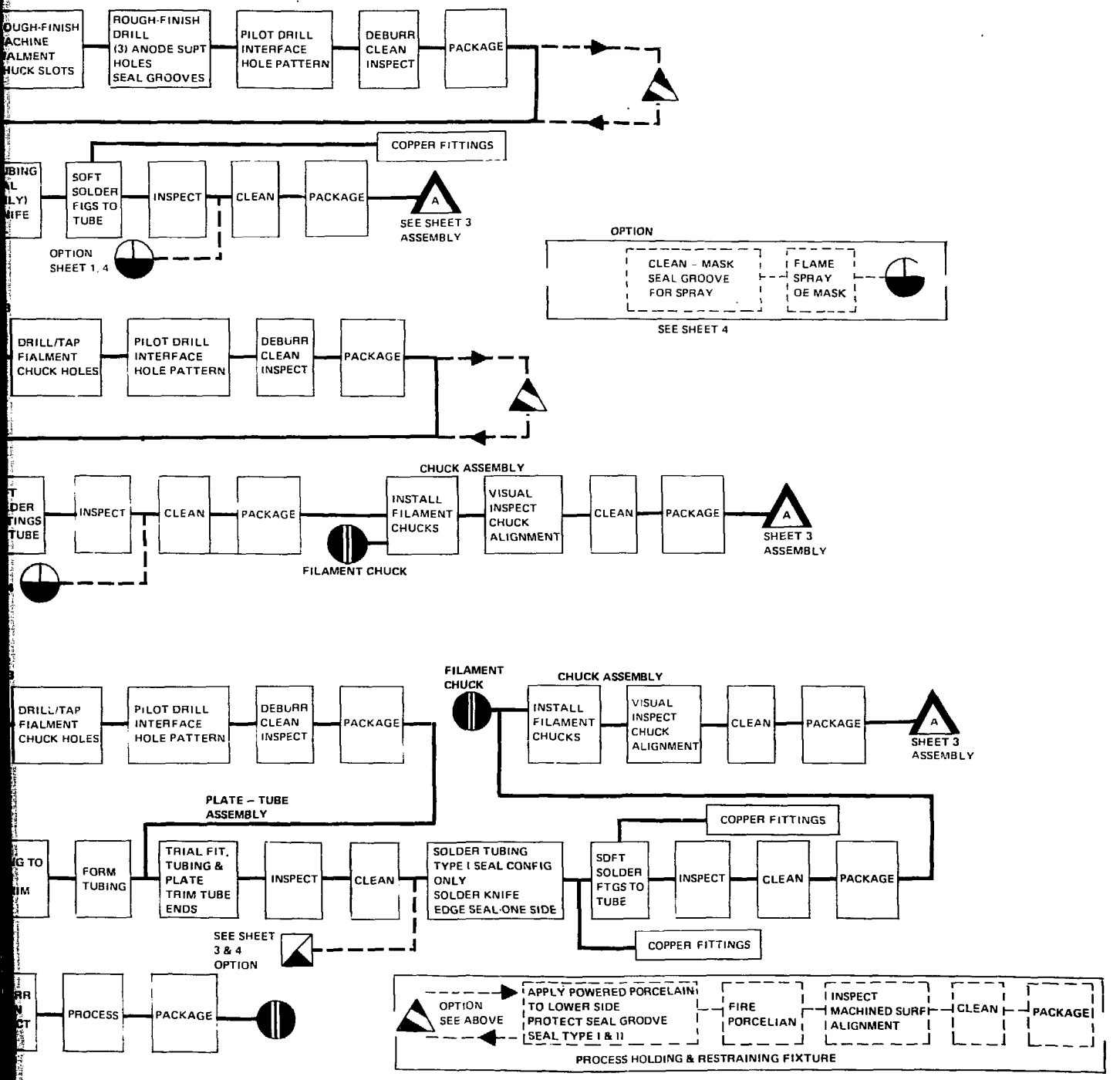
OUGH-FINISH
ACHINE
ALMENT
HUCK SLOTS
ROUGH-FINISH DRILL (3) ANODE SUPT HOLES SEAL GROOVES
PILOT DRILL INTERFACE HOLE PATTERN
DEBURR CLEAN INSPECT
PACKAGE
COPPER FITTINGS
BING
AL
LY)
IFE
SOFT SOLDER FIGS TO TUBE
INSPECT
CLEAN
PACKAGE
A
SEE SHEET 3 ASSEMBLY
OPTION SHEET 1, 4
OPTION
CLEAN - MASK SEAL GROOVE FOR SPRAY
FLAME SPRAY OE MASK
SEE SHEET 4
DRILL/TAP FIALMENT CHUCK HOLES
PILOT DRILL INTERFACE HOLE PATTERN
DEBURR CLEAN INSPECT
PACKAGE
CHUCK ASSEMBLY
T
DER
TINGS
TUBE
INSPECT
CLEAN
PACKAGE
INSTALL FILAMENT CHUCKS
VISUAL INSPECT CHUCK ALIGNMENT
CLEAN
PACKAGE
A
SHEET 3 ASSEMBLY
FILAMENT CHUCK
DRILL/TAP FIALMENT CHUCK HOLES
PILOT DRILL INTERFACE HOLE PATTERN
DEBURR CLEAN INSPECT
PACKAGE
FILAMENT CHUCK
CHUCK ASSEMBLY
INSTALL FILAMENT CHUCKS
VISUAL INSPECT CHUCK ALIGNMENT
CLEAN
PACKAGE
A
SHEET 3 ASSEMBLY
PLATE – TUBE ASSEMBLY
COPPER FITTINGS
G TO
IM
FORM TUBING
TRIAL FIT, TUBING & PLATE TRIM TUBE ENDS
INSPECT
CLEAN
SOLDER TUBING TYPE I SEAL CONFIG ONLY SOLDER KNIFE EDGE SEAL-ONE SIDE
SDFT SOLDER FTGS TO TUBE
INSPECT
CLEAN
PACKAGE
COPPER FITTINGS
SEE SHEET 3 & 4 OPTION
RR
N
CT
PROCESS
PACKAGE
OPTION SEE ABOVE
APPLY POWERED PORCELAIN TO LOWER SIDE PROTECT SEAL GRODVE SEAL TYPE I & II
FIRE PORCELIAN
INSPECT MACHINED SURF ALIGNMENT
CLEAN
PACKAGE
PROCESS HOLDING & RESTRAINING FIXTURE

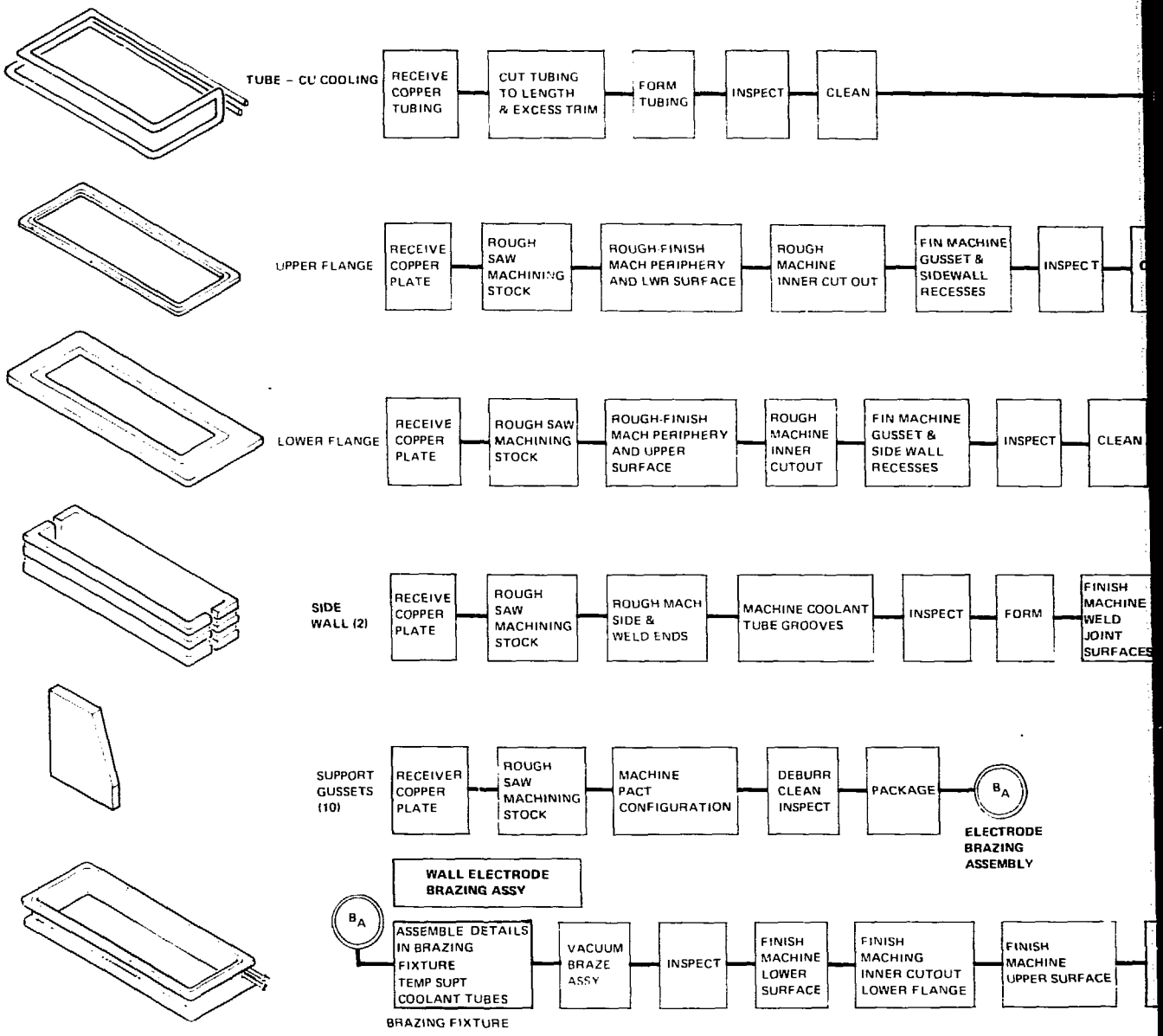

13–1304

FIGURE 2.1.1-1 (B)

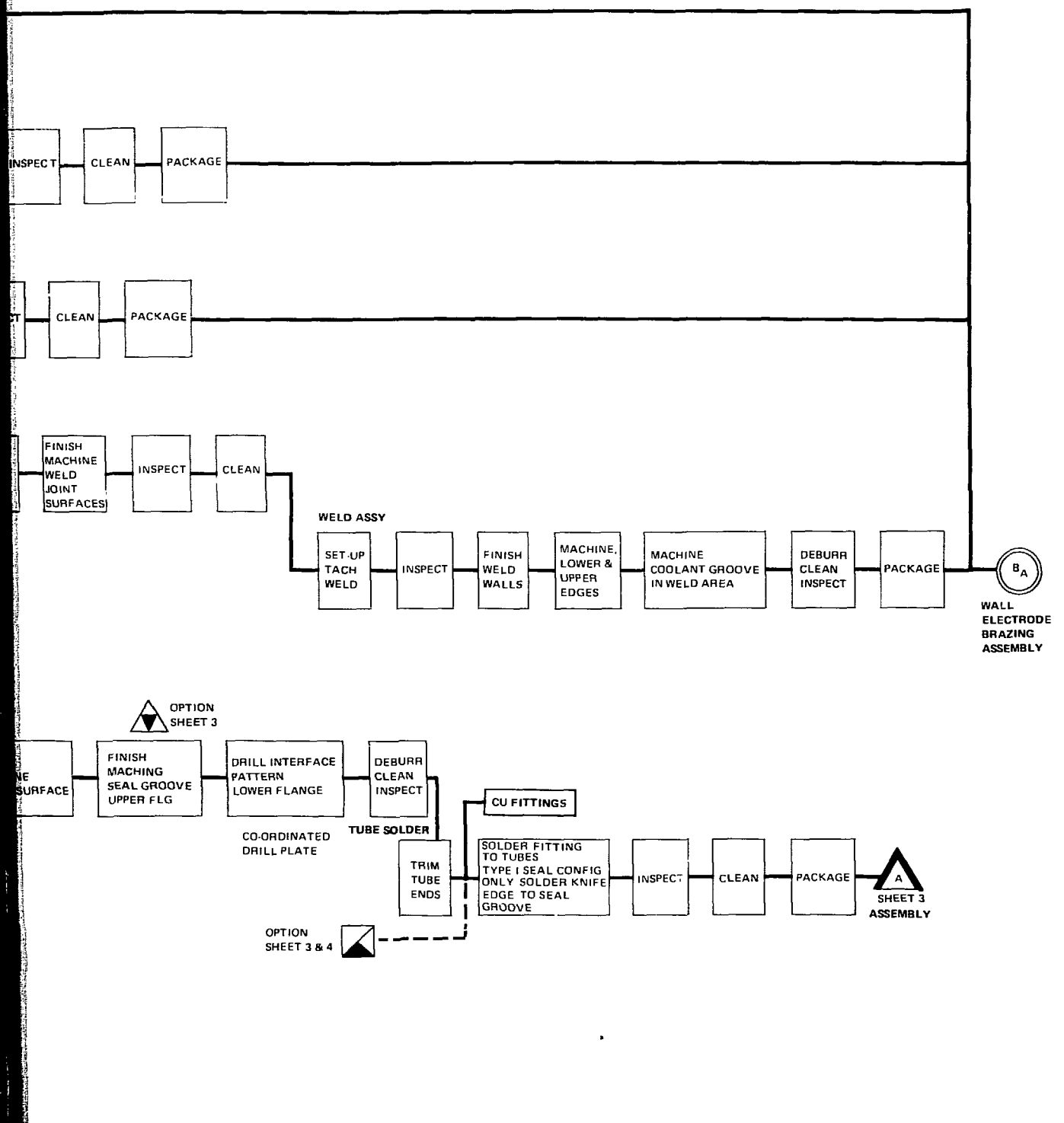
INSPECT
CLEAN
PACKAGE
CLEAN
PACKAGE
FINISH MACHINE WELD JOINT SURFACES
INSPECT
CLEAN
WELD ASSY
SET-UP TACH WELD
INSPECT
FINISH WELD WALLS
MACHINE, LOWER & UPPER EDGES
MACHINE COOLANT GROOVE IN WELD AREA
DEBURR CLEAN INSPECT
PACKAGE
B A
WALL ELECTRODE BRAZING ASSEMBLY
OPTION SHEET 3
SURFACE
FINISH MACHING SEAL GROOVE UPPER FLG
DRILL INTERFACE PATTERN LOWER FLANGE
DEBURR CLEAN INSPECT
CO-ORDINATED DRILL PLATE
TUBE SOLDER
CU FITTINGS
TRIM TUBE ENDS
SOLDER FITTING TO TUBES TYPE I SEAL CONFIG ONLY SOLDER KNIFE EDGE TO SEAL GROOVE
INSPECT
CLEAN
PACKAGE
A
SHEET 3 ASSEMBLY
OPTION SHEET 3 & 4

SOURCE GRID ASSEMBLY MANUFACTURING FLOW

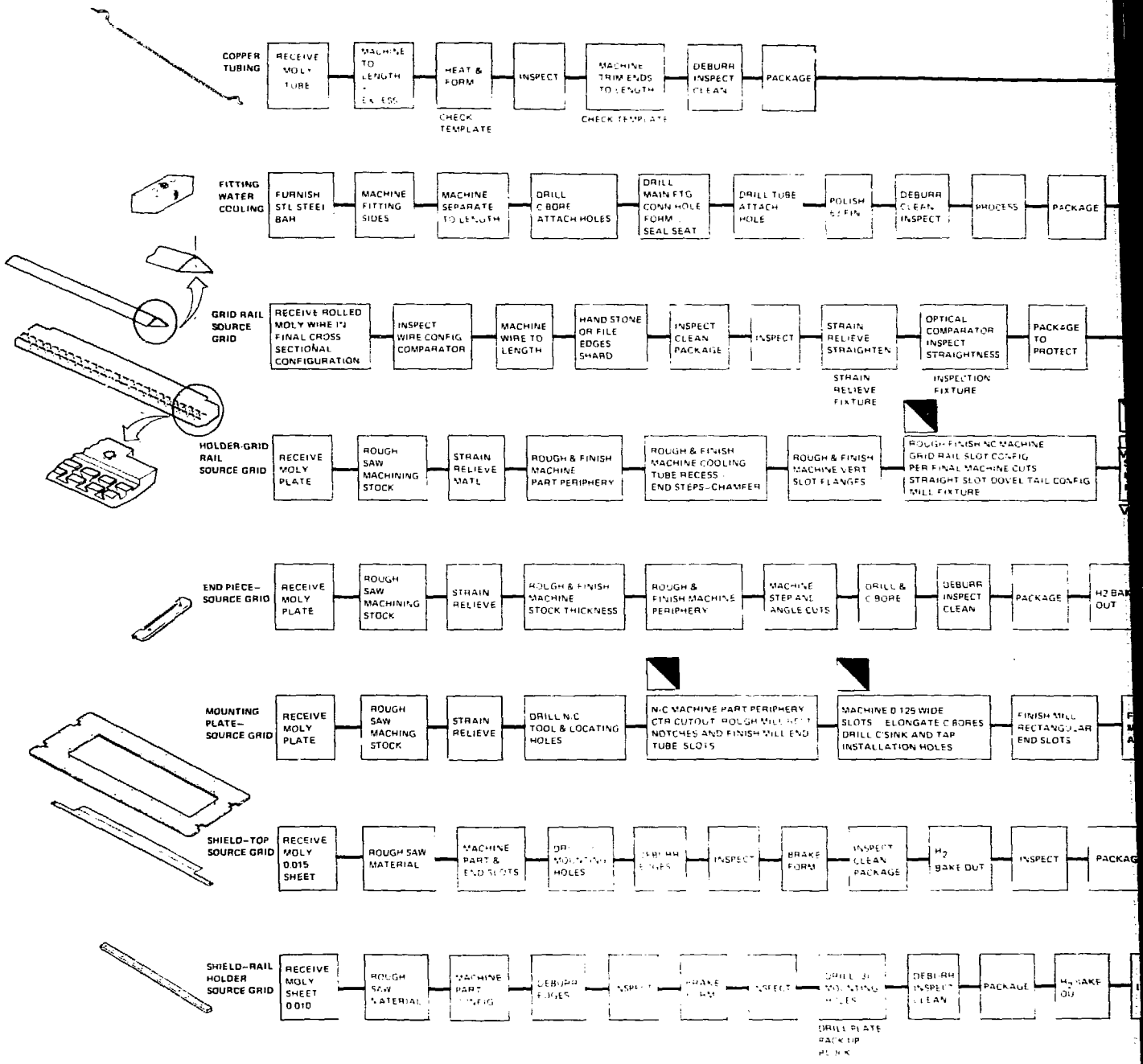

13-1308

FIGURE 2.1.2-1

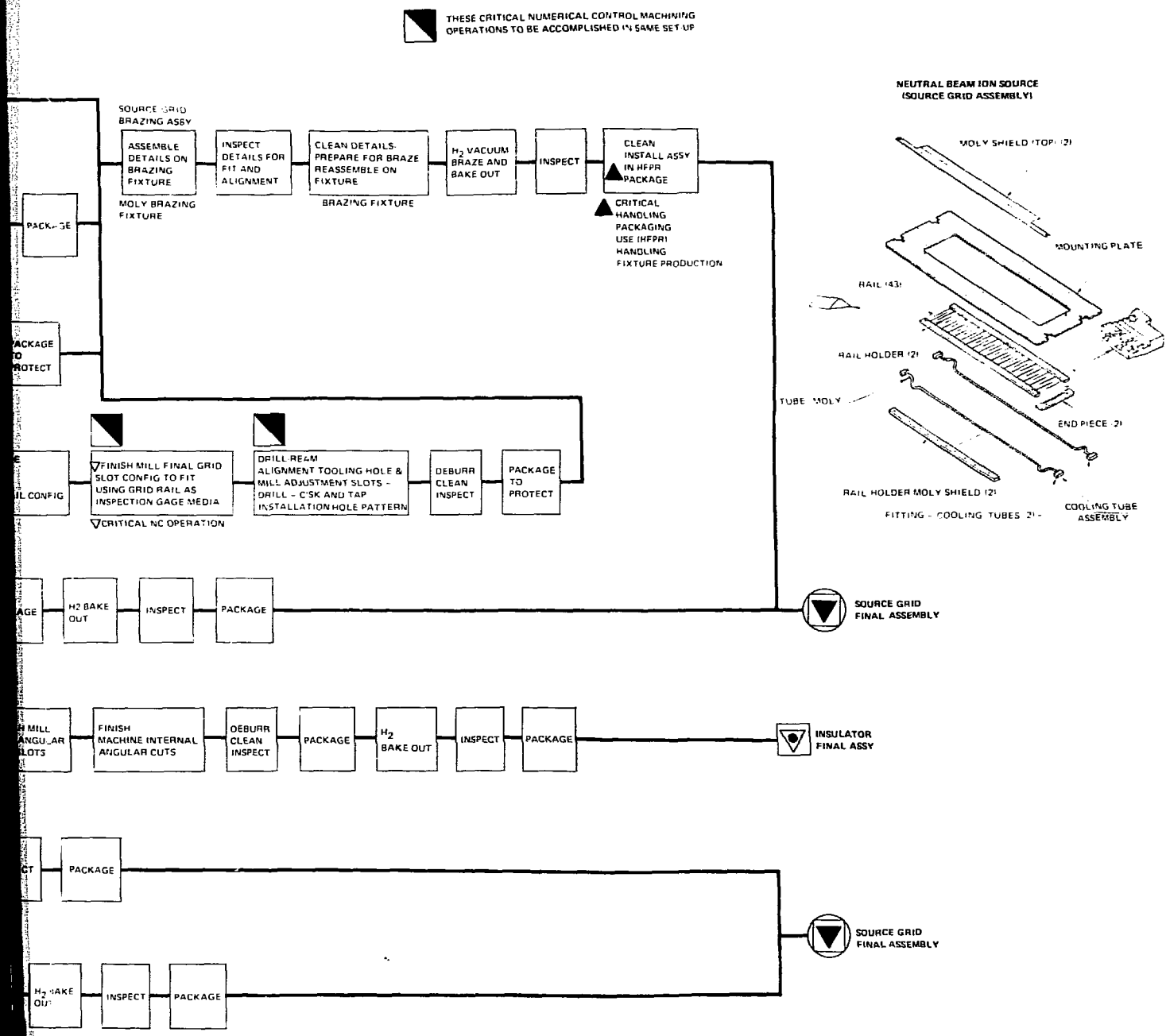
THESE CRITICAL NUMERICAL CONTROL MACHINING OPERATIONS TO BE ACCOMPLISHED IN SAME SET-UP
NEUTRAL BEAM ION SOURCE (SOURCE GRID ASSEMBLY)
SOURCE GRID BRAZING ASSY
ASSEMBLE DETAILS ON BRAZING FIXTURE
MOLY BRAZING FIXTURE
INSPECT DETAILS FOR FIT AND ALIGNMENT
CLEAN DETAILS. PREPARE FOR BRAZE REASSEMBLE ON FIXTURE
BRAZING FIXTURE
H_2 VACUUM BRAZE AND BAKE OUT
INSPECT
CLEAN INSTALL ASSY IN HFPR PACKAGE
CRITICAL HANDLING PACKAGING USE (HFPR) HANDLING FIXTURE PRODUCTION
PACKAGE
PACKAGE TO PROTECT
FINISH MILL FINAL GRID SLOT CONFIG TO FIT USING GRID RAIL AS INSPECTION GAGE MEDIA
CRITICAL NC OPERATION
DRILL REAM ALIGNMENT TOOLING HOLE & MILL ADJUSTMENT SLOTS - DRILL - C'SK AND TAP INSTALLATION HOLE PATTERN
DEBURR CLEAN INSPECT
PACKAGE TO PROTECT
H2 BAKE OUT
INSPECT
PACKAGE
SOURCE GRID FINAL ASSEMBLY
FINISH MILL ANGULAR SLOTS
FINISH MACHINE INTERNAL ANGULAR CUTS
DEBURR CLEAN INSPECT
PACKAGE
H_2 BAKE OUT
INSPECT
PACKAGE
INSULATOR FINAL ASSY
PACKAGE
H_2 BAKE OUT
INSPECT
PACKAGE
SOURCE GRID FINAL ASSEMBLY
MOLY SHIELD (TOP) (2)
MOUNTING PLATE
RAIL (43)
RAIL HOLDER (2)
TUBE MOLY
END PIECE (2)
RAIL HOLDER MOLY SHIELD (2)
FITTING - COOLING TUBES (2)
COOLING TUBE ASSEMBLY

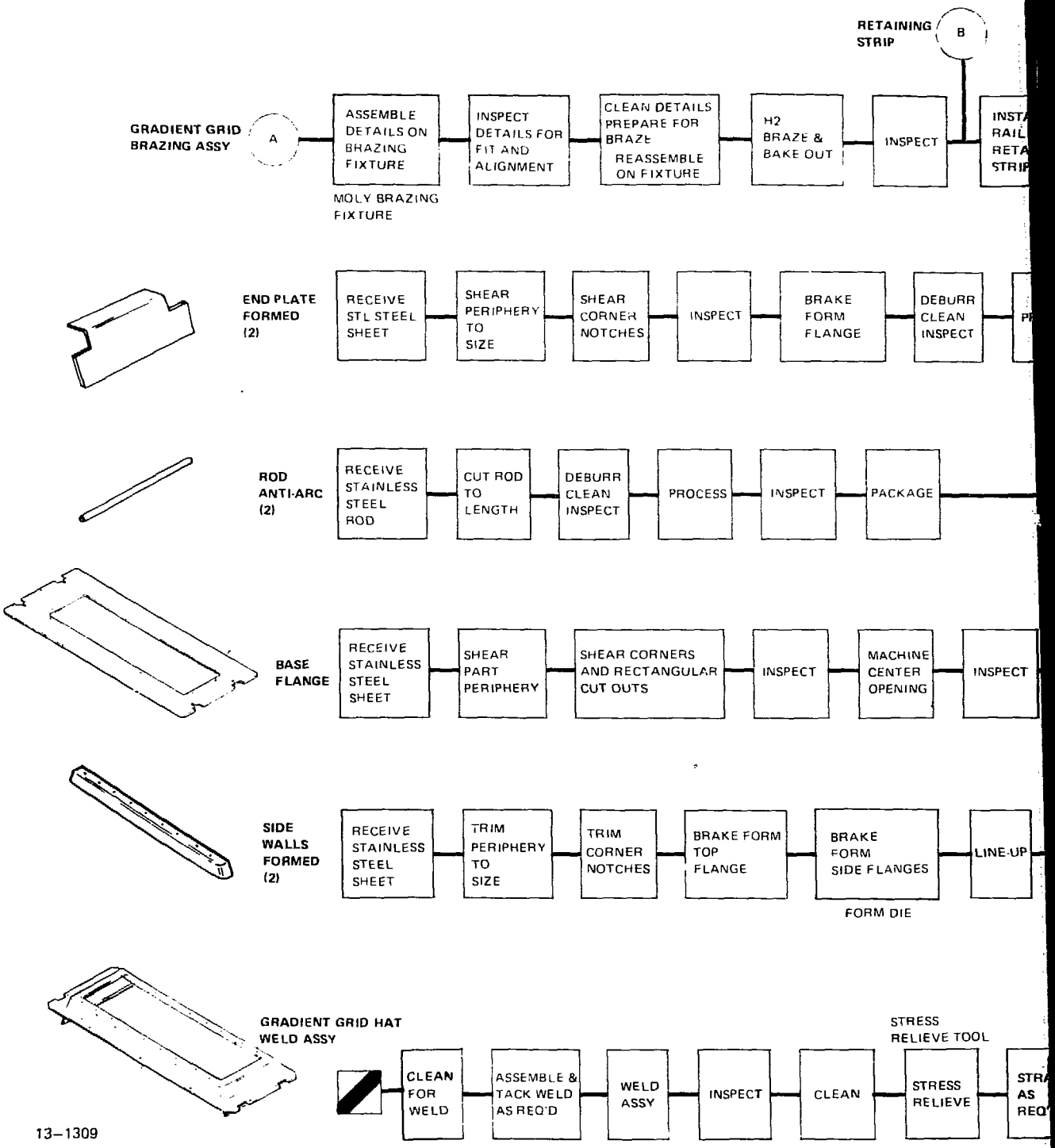

13–1309

FIGURE 2.1.2-2 (A)

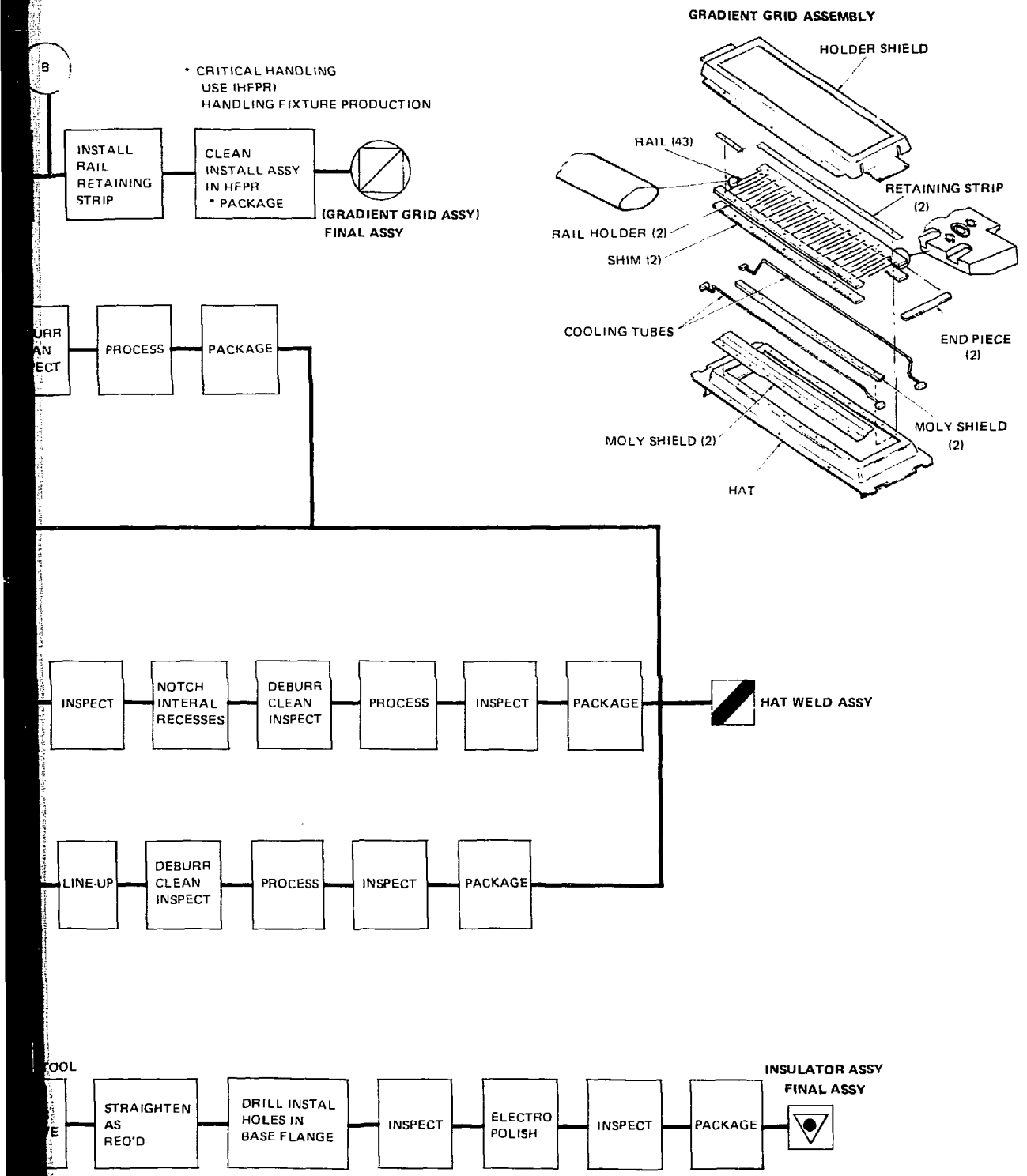
GRADIENT GRID ASSEMBLY
HOLDER SHIELD
RAIL (43)
RETAINING STRIP (2)
RAIL HOLDER (2)
SHIM (2)
COOLING TUBES
END PIECE (2)
MOLY SHIELD (2)
MOLY SHIELD (2)
HAT
B
• CRITICAL HANDLING USE (HFPR) HANDLING FIXTURE PRODUCTION
INSTALL RAIL RETAINING STRIP
CLEAN INSTALL ASSY IN HFPR • PACKAGE
(GRADIENT GRID ASSY) FINAL ASSY
URR AN ECT
PROCESS
PACKAGE
INSPECT
NOTCH INTERAL RECESSES
DEBURR CLEAN INSPECT
PROCESS
INSPECT
PACKAGE
HAT WELD ASSY
LINE-UP
DEBURR CLEAN INSPECT
PROCESS
INSPECT
PACKAGE
TOOL
E
STRAIGHTEN AS REQ'D
DRILL INSTAL HOLES IN BASE FLANGE
INSPECT
ELECTRO POLISH
INSPECT
PACKAGE
INSULATOR ASSY FINAL ASSY

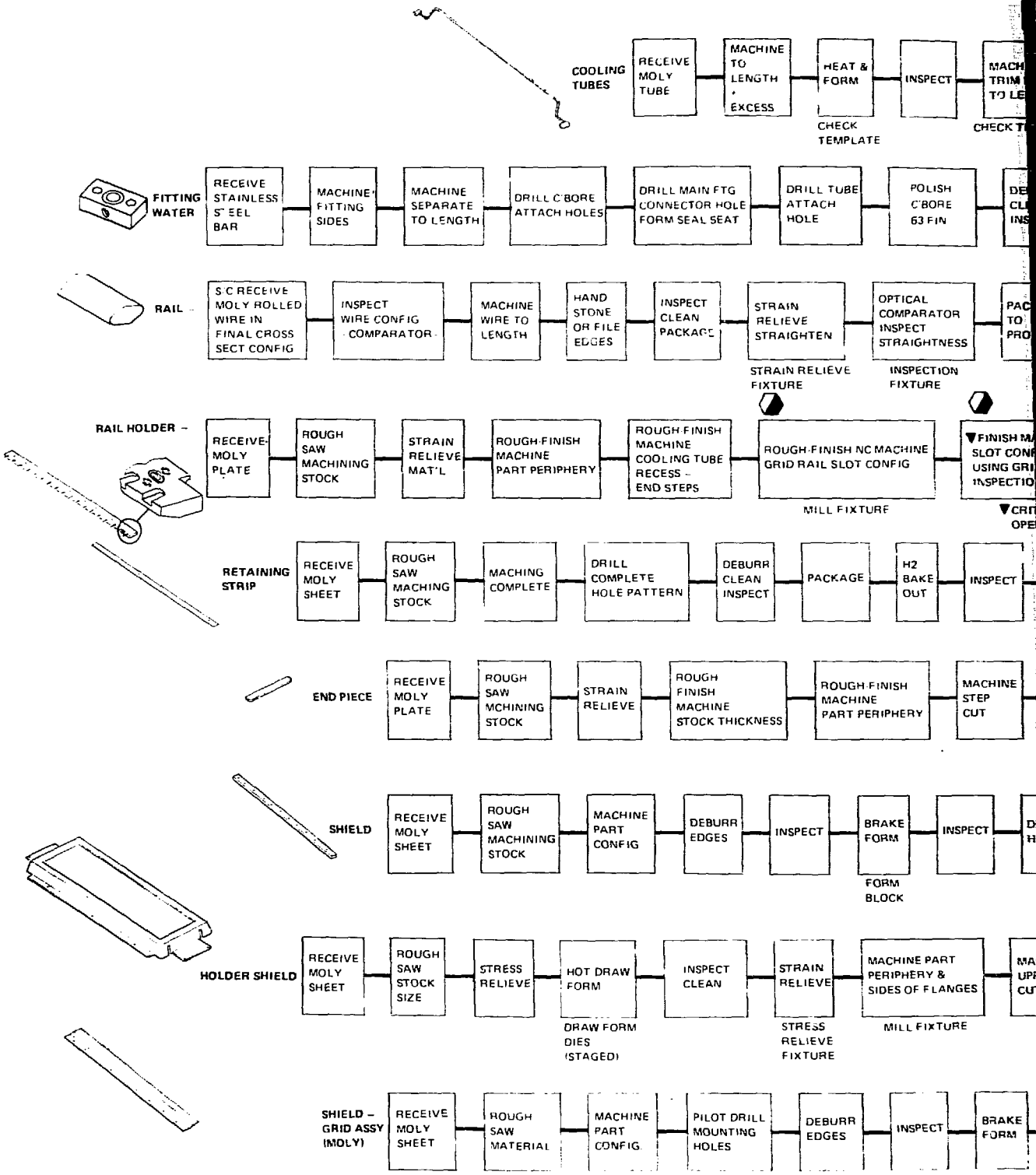

13-1310

FIGURE 2.1.2-2 (B)

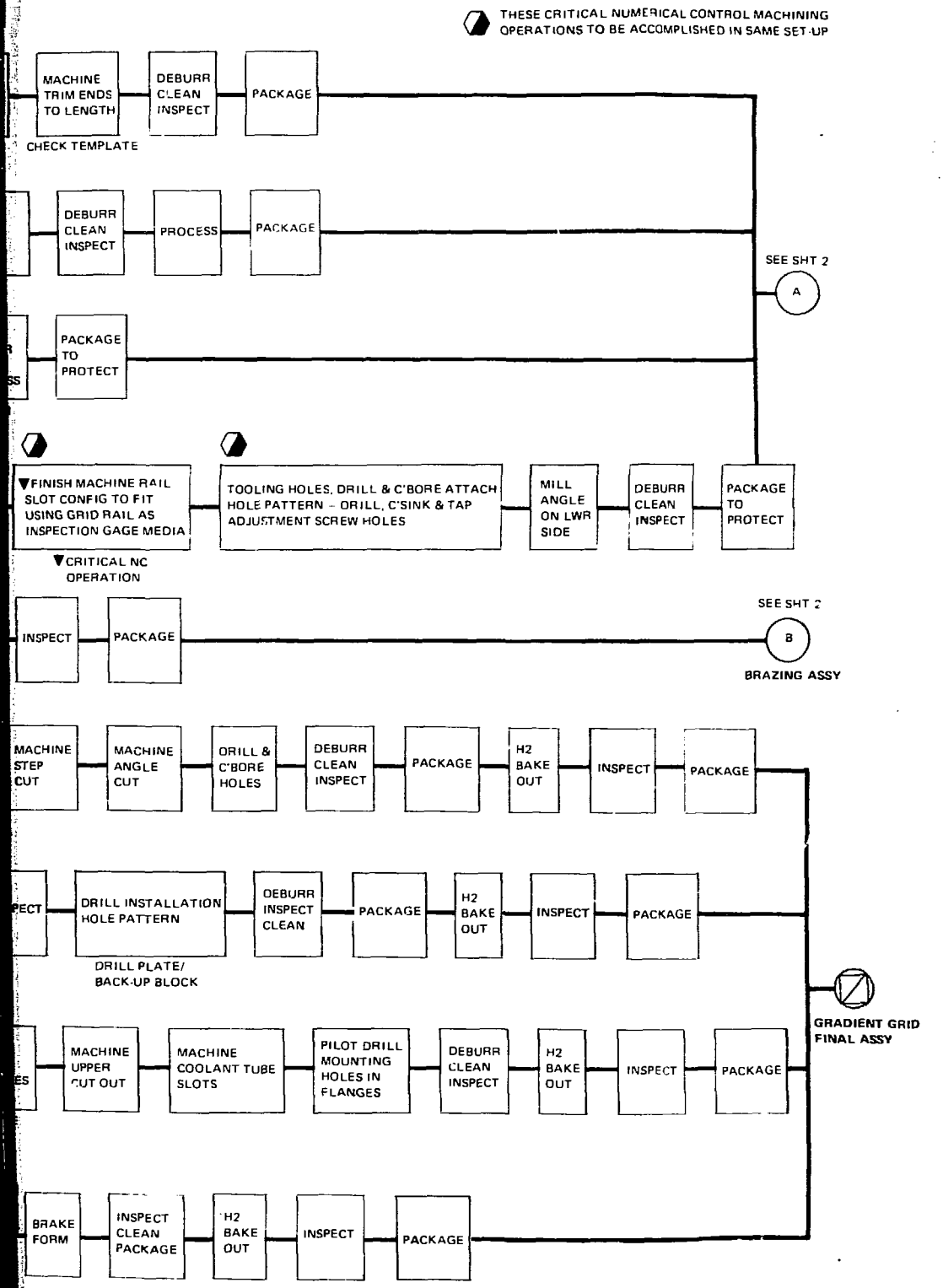
THESE CRITICAL NUMERICAL CONTROL MACHINING OPERATIONS TO BE ACCOMPLISHED IN SAME SET-UP
MACHINE TRIM ENDS TO LENGTH
CHECK TEMPLATE
DEBURR CLEAN INSPECT
PACKAGE
DEBURR CLEAN INSPECT
PROCESS
PACKAGE
PACKAGE TO PROTECT
SEE SHT 2
A
FINISH MACHINE RAIL SLOT CONFIG TO FIT USING GRID RAIL AS INSPECTION GAGE MEDIA
CRITICAL NC OPERATION
TOOLING HOLES, DRILL & C'BORE ATTACH HOLE PATTERN - DRILL, C'SINK & TAP ADJUSTMENT SCREW HOLES
MILL ANGLE ON LWR SIDE
DEBURR CLEAN INSPECT
PACKAGE TO PROTECT
INSPECT
PACKAGE
SEE SHT 2
B
BRAZING ASSY
MACHINE STEP CUT
MACHINE ANGLE CUT
DRILL & C'BORE HOLES
DEBURR CLEAN INSPECT
PACKAGE
H2 BAKE OUT
INSPECT
PACKAGE
DRILL INSTALLATION HOLE PATTERN
DRILL PLATE/ BACK-UP BLOCK
DEBURR INSPECT CLEAN
PACKAGE
H2 BAKE OUT
INSPECT
PACKAGE
MACHINE UPPER CUT OUT
MACHINE COOLANT TUBE SLOTS
PILOT DRILL MOUNTING HOLES IN FLANGES
DEBURR CLEAN INSPECT
H2 BAKE OUT
INSPECT
PACKAGE
BRAKE FORM
INSPECT CLEAN PACKAGE
H2 BAKE OUT
INSPECT
PACKAGE
GRADIENT GRID FINAL ASSY

SUPPRESSOR GRID ASSEMBLY MANUFACTURING FLOW

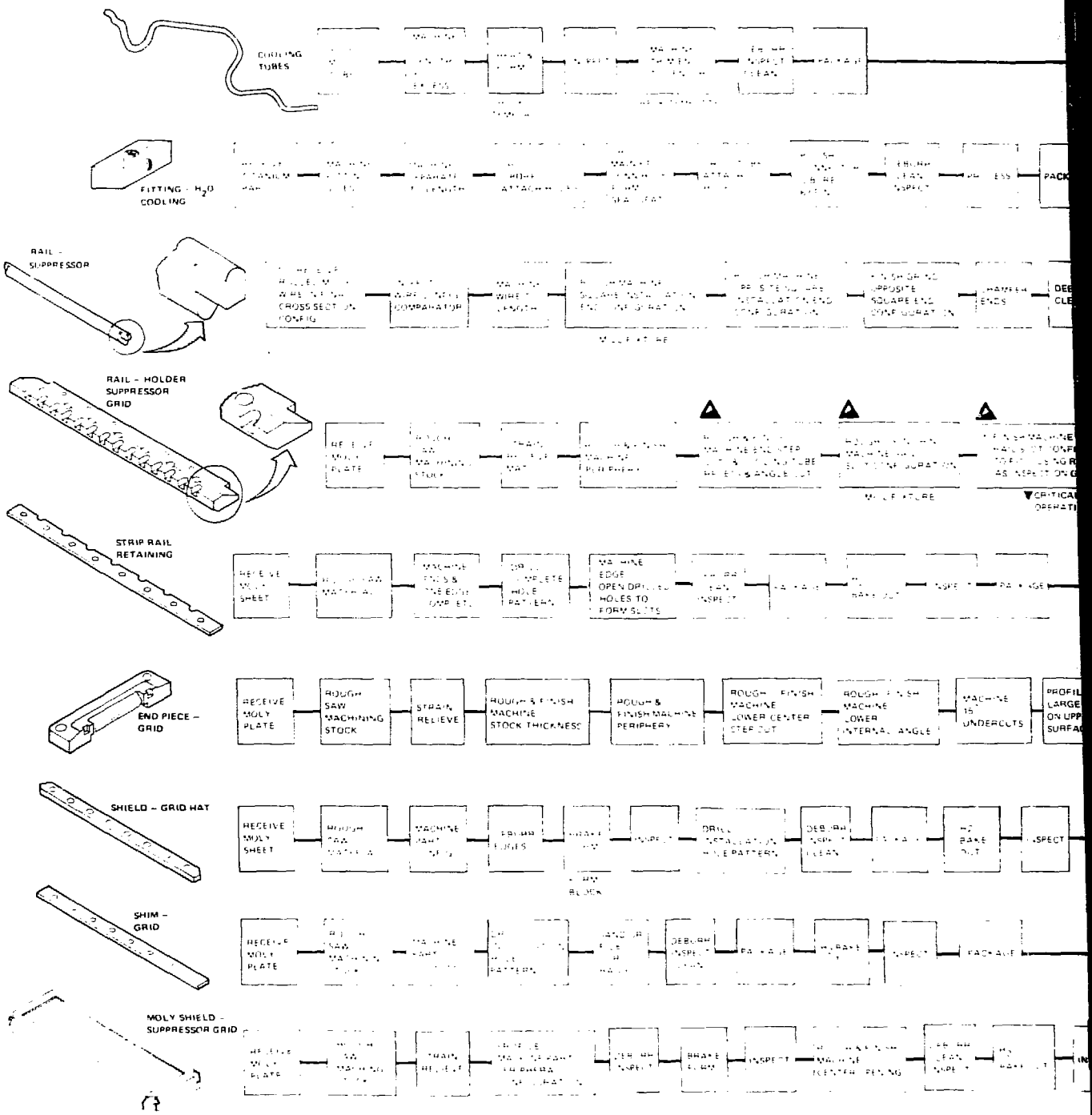

FIGURE 2.1.2-3 (A)

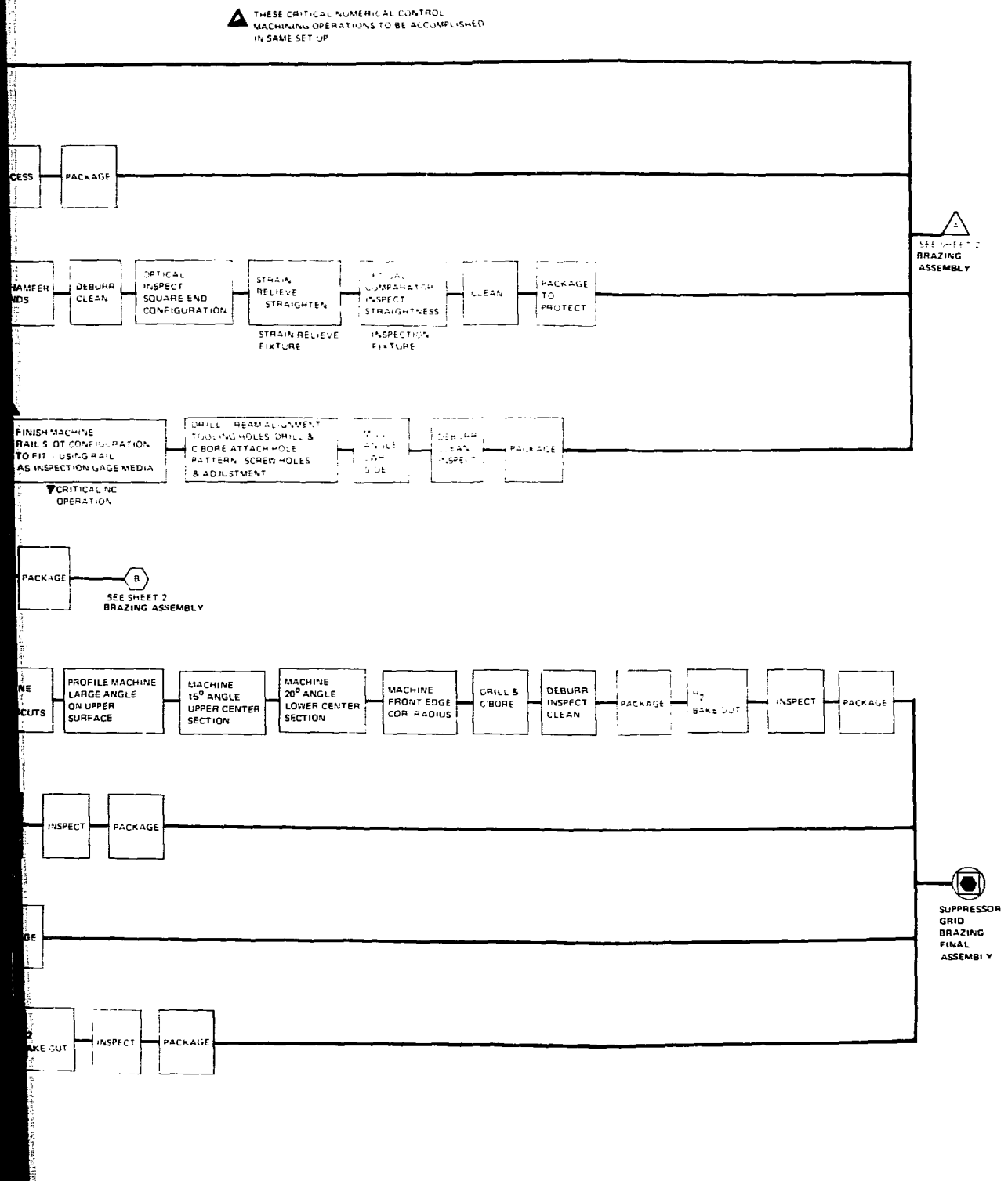
THESE CRITICAL NUMERICAL CONTROL MACHINING OPERATIONS TO BE ACCOMPLISHED IN SAME SET UP
CESS
PACKAGE
A
SEE SHEET 2
BRAZING ASSEMBLY
AMFER
NDS
DEBURR CLEAN
OPTICAL INSPECT SQUARE END CONFIGURATION
STRAIN RELIEVE STRAIGHTEN
STRAIN RELIEVE FIXTURE
COMPARATOR INSPECT STRAIGHTNESS
INSPECTION FIXTURE
CLEAN
PACKAGE TO PROTECT
FINISH MACHINE RAIL SLOT CONFIGURATION TO FIT - USING RAIL AS INSPECTION GAGE MEDIA
CRITICAL NC OPERATION
DRILL - REAM ALIGNMENT TOOLING HOLES DRILL & C BORE ATTACH HOLE PATTERN SCREW HOLES & ADJUSTMENT
PACKAGE
PACKAGE
B
SEE SHEET 2
BRAZING ASSEMBLY
NE
CUTS
PROFILE MACHINE LARGE ANGLE ON UPPER SURFACE
MACHINE 15° ANGLE UPPER CENTER SECTION
MACHINE 20° ANGLE LOWER CENTER SECTION
MACHINE FRONT EDGE COR RADIUS
DRILL & C'BORE
DEBURR INSPECT CLEAN
PACKAGE
H_2 BAKE OUT
INSPECT
PACKAGE
INSPECT
PACKAGE
GE
AKE OUT
INSPECT
PACKAGE
SUPPRESSOR GRID BRAZING FINAL ASSEMBLY

SUPPRESSOR GRID ASSEMBLY (Continued)
MANUFACTURING FLOW

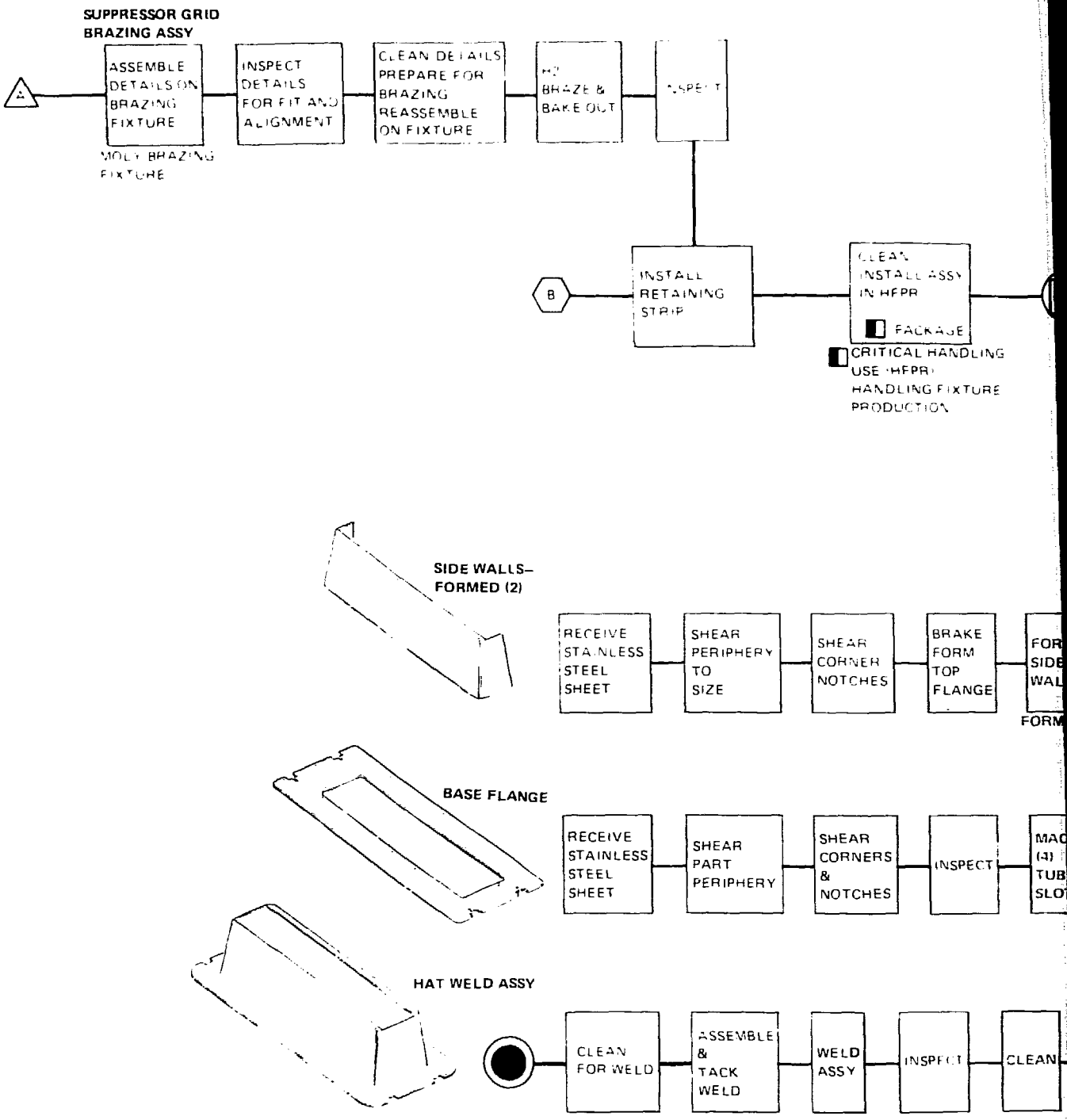

13-1312

FIGURE 2.1.2-3 (B)

SUPPRESSOR GRID ASSEMBLY

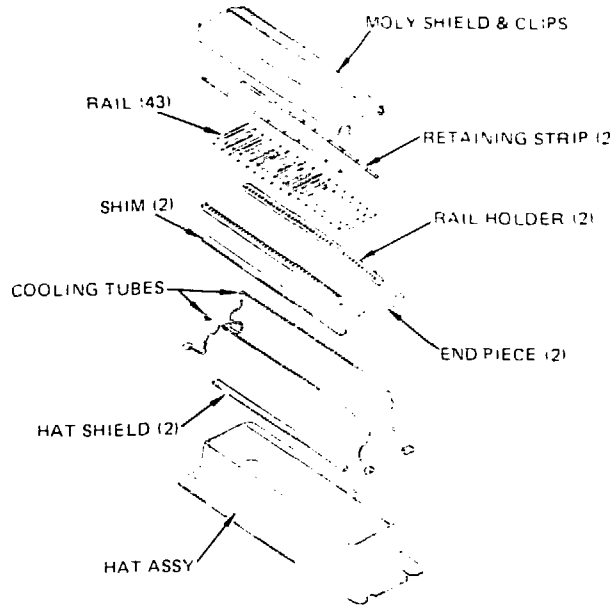

SUPPRESSOR GRID FINAL ASSEMBLY

LING

URE

E

GE

FORM SIDE WALLS — FORM DIE — LINE UP — DEBURR INSPECT — PROCESS — INSPECT — PACKAGE

HAT WELD ASSY

CT

MACHINE (4) TUBE SLOTS — MACHINE CENTER OPENING — DEBURR CLEAN INSPECT — PROCESS — INSPECT — PACKAGE

STRESS RELIEVE TOOL

CLEAN — STRESS RELIEVE — STRAIGHTEN AS REQ'D — DRILL INSTALLATION HOLES IN BASE FLANGE — INSPECT — PACKAGE

INSULATOR FINAL ASSY

EXIT GRID ASSEMBLY MANUFACTURING FLOW

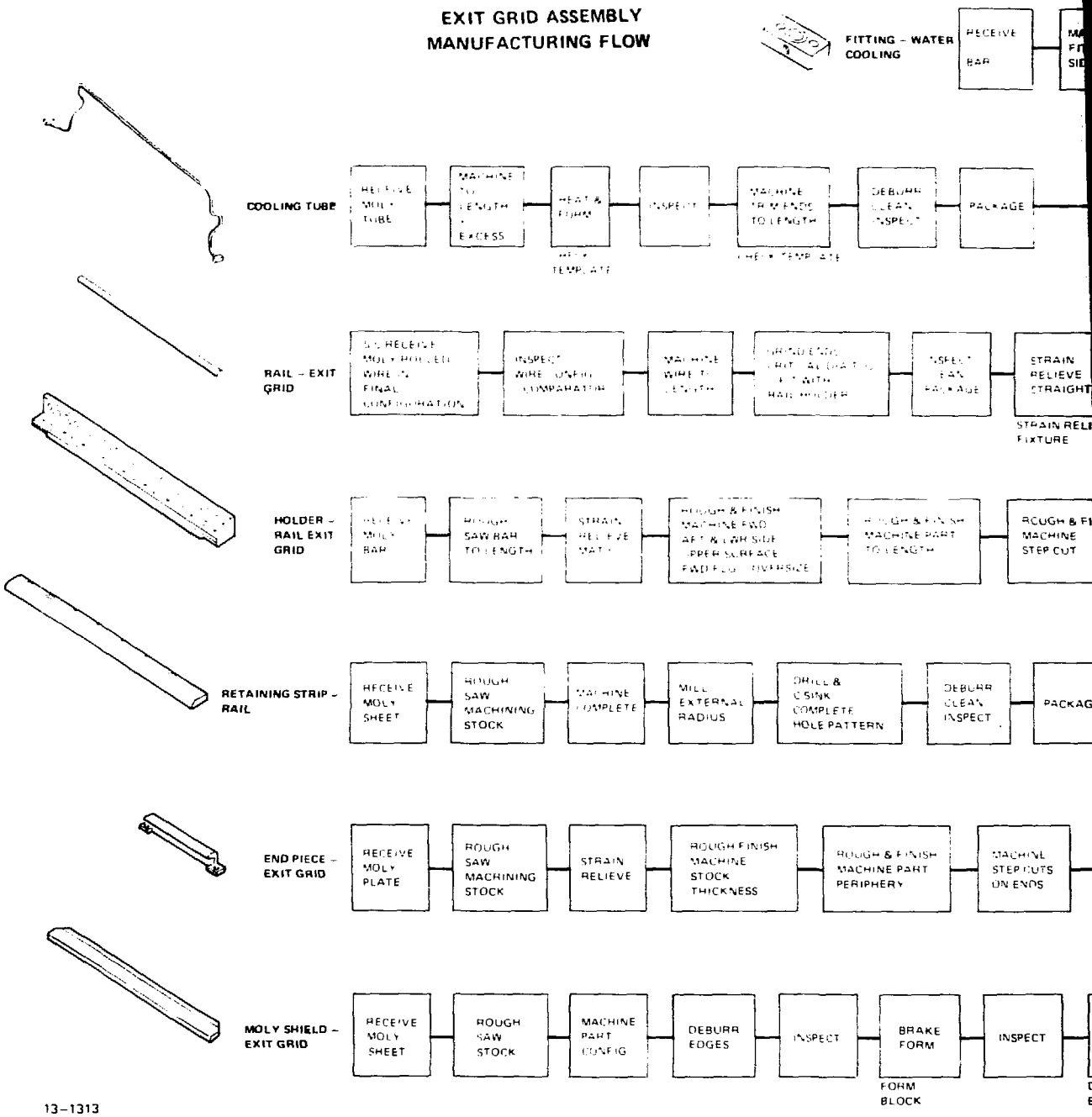

FIGURE 2.1.2-4 (A)

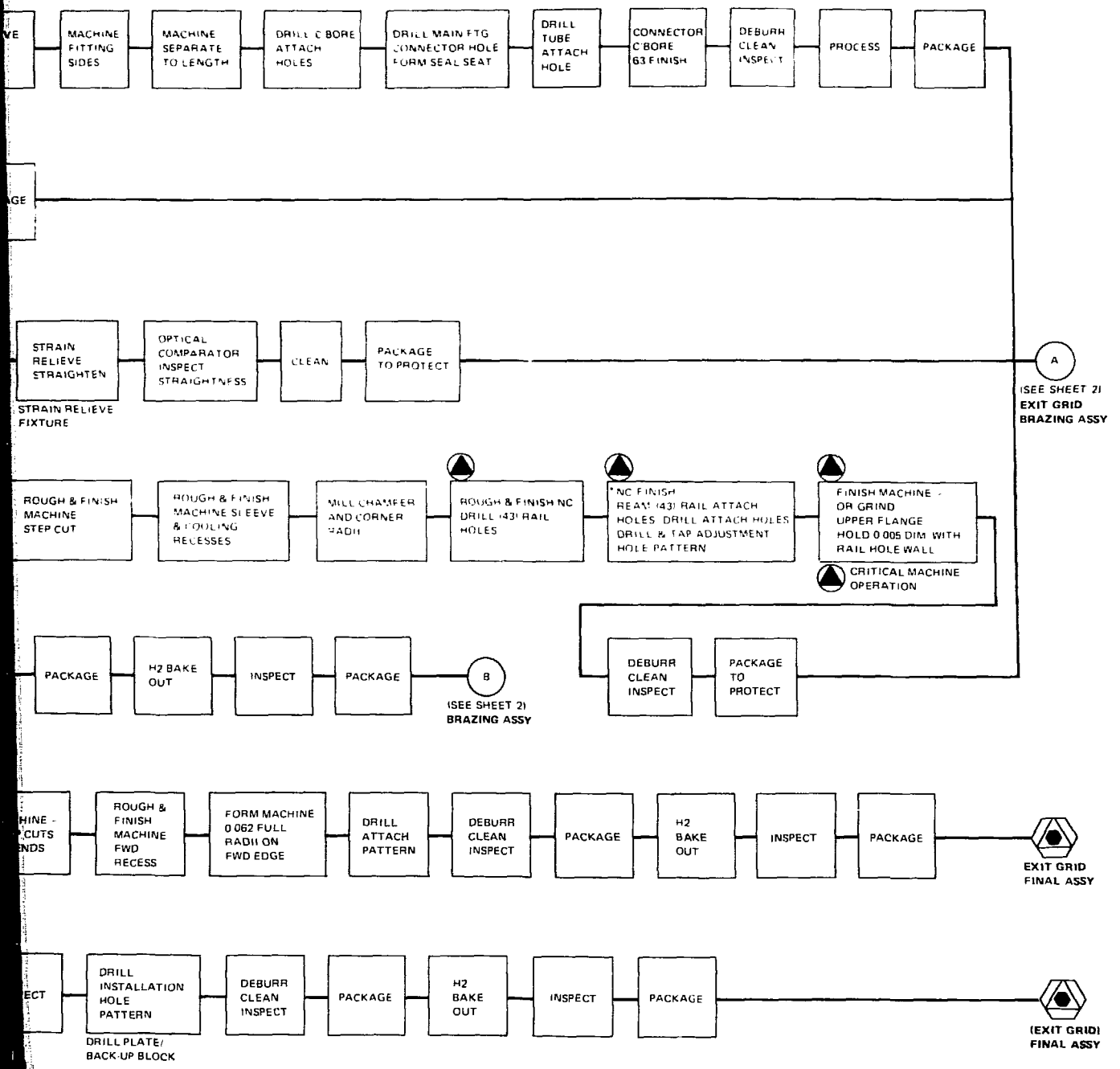
VE
MACHINE FITTING SIDES
MACHINE SEPARATE TO LENGTH
DRILL C BORE ATTACH HOLES
DRILL MAIN FTG CONNECTOR HOLE FORM SEAL SEAT
DRILL TUBE ATTACH HOLE
CONNECTOR C'BORE 63 FINISH
DEBURR CLEAN INSPECT
PROCESS
PACKAGE
AGE
STRAIN RELIEVE STRAIGHTEN
STRAIN RELIEVE FIXTURE
OPTICAL COMPARATOR INSPECT STRAIGHTNESS
CLEAN
PACKAGE TO PROTECT
A
(SEE SHEET 2)
EXIT GRID BRAZING ASSY
ROUGH & FINISH MACHINE STEP CUT
ROUGH & FINISH MACHINE SLEEVE & COOLING RECESSES
MILL CHAMFER AND CORNER RADII
ROUGH & FINISH NC DRILL (43) RAIL HOLES
NC FINISH REAM (43) RAIL ATTACH HOLES DRILL ATTACH HOLES DRILL & TAP ADJUSTMENT HOLE PATTERN
FINISH MACHINE - OR GRIND UPPER FLANGE HOLD 0.005 DIM WITH RAIL HOLE WALL
CRITICAL MACHINE OPERATION
DEBURR CLEAN INSPECT
PACKAGE TO PROTECT
PACKAGE
H2 BAKE OUT
INSPECT
PACKAGE
B
(SEE SHEET 2)
BRAZING ASSY
HINE - CUTS NDS
ROUGH & FINISH MACHINE FWD RECESS
FORM MACHINE 0.062 FULL RADII ON FWD EDGE
DRILL ATTACH PATTERN
DEBURR CLEAN INSPECT
PACKAGE
H2 BAKE OUT
INSPECT
PACKAGE
EXIT GRID FINAL ASSY
ECT
DRILL INSTALLATION HOLE PATTERN
DRILL PLATE/ BACK-UP BLOCK
DEBURR CLEAN INSPECT
PACKAGE
H2 BAKE OUT
INSPECT
PACKAGE
(EXIT GRID) FINAL ASSY

EXIT GRID ASSEMBLY MANUFACTURING FLOW (CONTINUED)

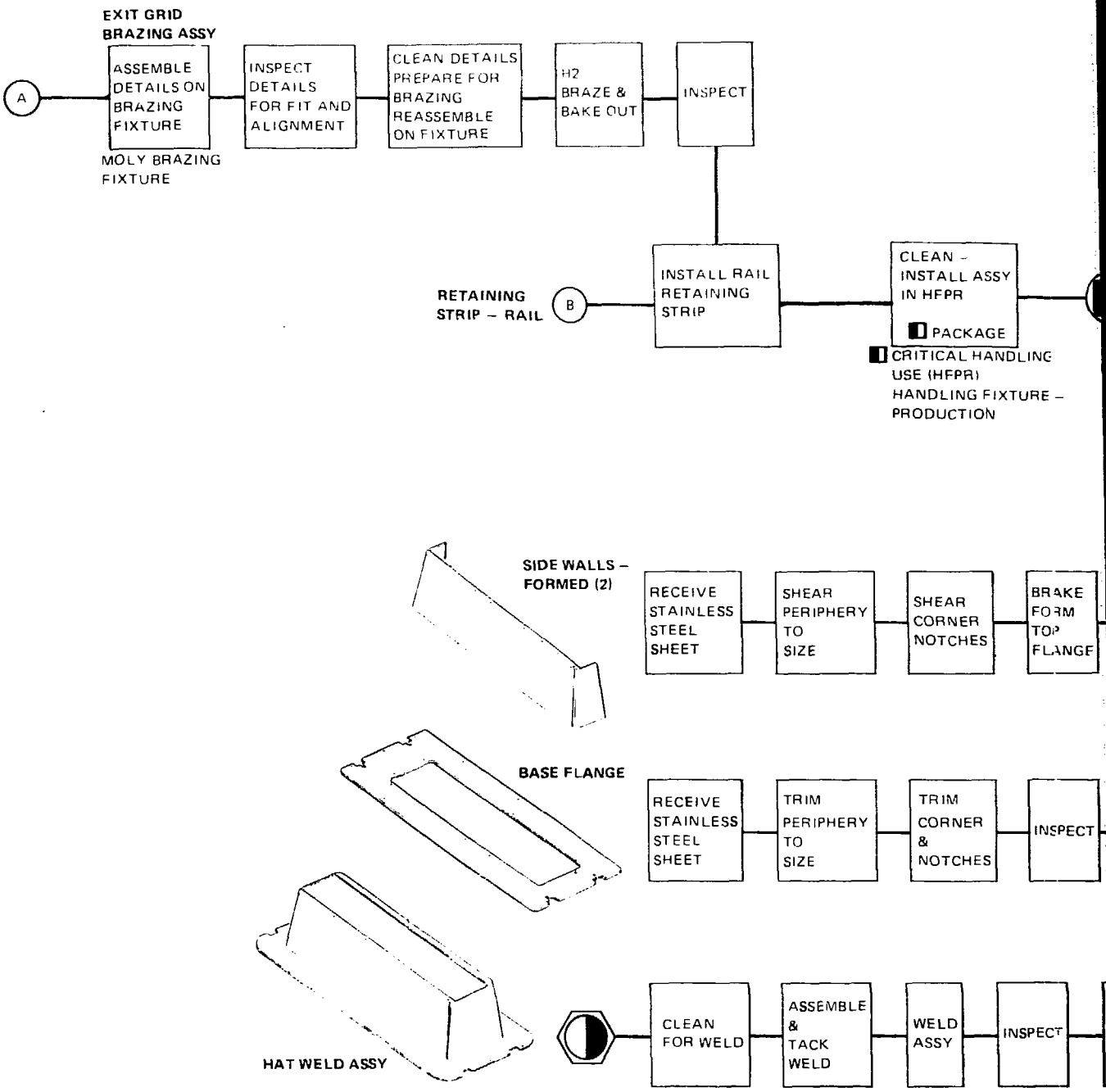

13-1314

FIGURE 2.1.2-4 (B)

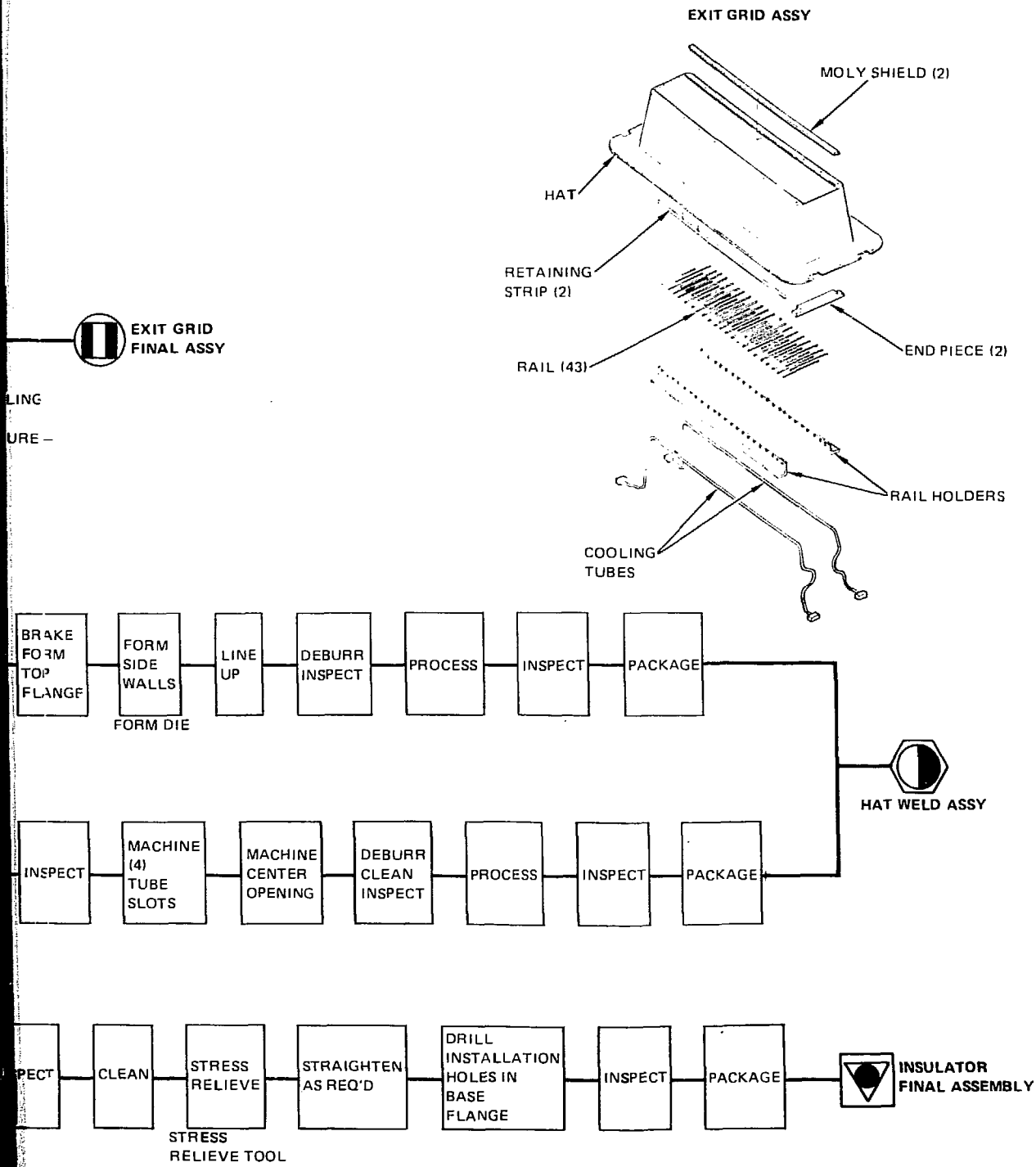
EXIT GRID ASSY
MOLY SHIELD (2)
HAT
RETAINING STRIP (2)
RAIL (43)
END PIECE (2)
RAIL HOLDERS
COOLING TUBES
EXIT GRID FINAL ASSY
LING
URE –
BRAKE FORM TOP FLANGE
FORM SIDE WALLS
FORM DIE
LINE UP
DEBURR INSPECT
PROCESS
INSPECT
PACKAGE
HAT WELD ASSY
INSPECT
MACHINE (4) TUBE SLOTS
MACHINE CENTER OPENING
DEBURR CLEAN INSPECT
PROCESS
INSPECT
PACKAGE
PECT
CLEAN
STRESS RELIEVE
STRESS RELIEVE TOOL
STRAIGHTEN AS REQ'D
DRILL INSTALLATION HOLES IN BASE FLANGE
INSPECT
PACKAGE
INSULATOR FINAL ASSEMBLY

with the first finishing pass and the slot was intentionally left undersize at this point. Grid rails were trial fit in the slots and if proper fit was not obtained other finishing passes were made removing 0.0002 to 0.0003 inch per side per pass until the desired fit was achieved between the grid rails and the slots in the rail holders. Tooling holes were then machined in relation to the center lines of the grid rail slots. The holders were inspected on the coordinate measuring machine to assure compliance to design tolerances.

Grid Hats - The accelerator gradient grid, suppressor grid and exit grid hats were fabricated from stainless steel sheet metal. The overall thickness of the hats was 0.063 inch except for the top grid mounting flange which was 0.250 inch. The thicker top grid mounting flange was required to accommodate installation of the grid mounting dowel pins. All of the hats were electropolished to remove sharp edges and burrs that might effect voltage holding.

Molybdenum Shields - The molybdenum shields were manufactured from sheet stock and formed at warm temperatures (less than 200°C) by brake forming with the exception of the gradient and suppressor grid hat shields which were deep drawn at room temperature. A detailed description of the deep drawing process developed for these shields is presented in paragraph 1.2.3. The shields were drilled during accelerator preassembly and hydrogen fired before final assembly.

There are certain problems unique to forming sheet metal molybdenum which was avoided by controlling the raw material microstructure and by controlling the fabrication processes. One of the major problems is that of cracking and delamination. Cracking and delamination tends to occur more frequently in cutting, shearing, punching or drilling operations used to prepare blanks and tend to propagate when the defective area is stressed in a subsequent forming operation. Therefore, extreme importance is placed on the blanking and edge preparation procedure used.

Grid Brazing - The rails, rail holders, molybdenum cooling tubes and fittings were brazed simultaneously in molybdenum braze fixtures. The brazing fixtures positioned the machined rail holders using dowel pin locators to provide proper alignment. The rails were positioned and aligned by the accurately machined slots

in the grid rail holders. The suppressor grid mounted on its molybdenum braze fixture is shown in Figure 2.1.2-5. The source grid, gradient grid and exit grid molybdenum brazing fixture are similar to the suppressor grid brazing fixture.

TFTR ACCELERATOR SUPPRESSOR GRID

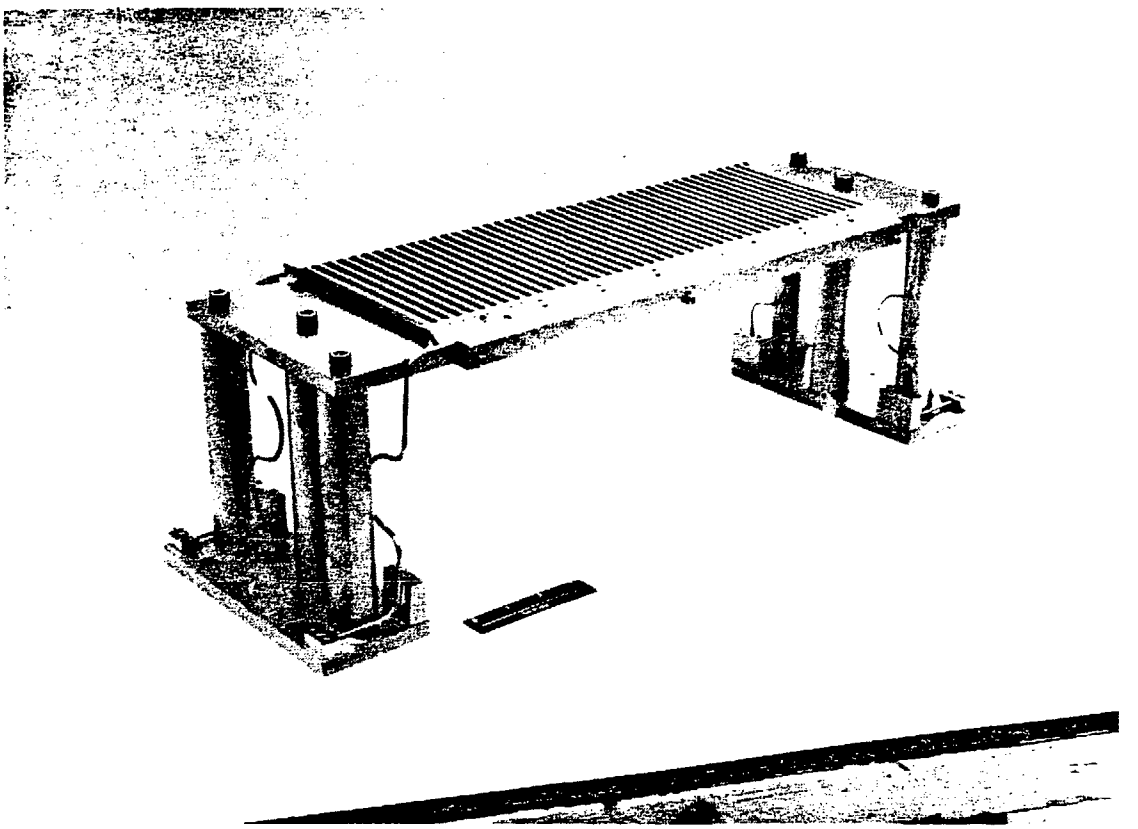

13–2754

FIGURE 2.1.2-5

The detail grid parts were assembled and located on their respective braze fixtures and inspected for fit and alignment. Rail to rail center distances and flatness checks were made prior to brazing. Following this insepction, the parts were disassembled, cleaned and reassembled applying the braze alloy and braze stop-off as required. Brazing was accomplished in a hydrogen atmosphere holding at 850°C for 30 minutes to provide a hydrogen bake-out and then advanced to the brazing temperature as specified on the engineering drawings. Slow heating and cooling were used to prevent thermal shock.

Extremely high operating temperatures are not anticipated for the neutral beam ion source so that assemblies can be brazed at or below 1100°C, and the embrittlement which accompanies the recrystallization of molybdenum can be avoided. There are a number of commercially available copper-base and precious metal-base alloys which have been used successfully to braze molybdenum at temperatures between 820°C and 1100°C. These alloys range from the 72 Ag-28 Cu eutectic alloy which melts at 780°C to pure copper which melts at 1083°C and include Wesco's Palcusil 25 (54 Ag-21 Cu-25 Pd) which was selected for brazing the molybdenum components.

Although the selection of brazing alloys and brazing conditions did not present problems, the low coefficient of thermal expansion of molybdenum does require special attention. For example, tooling materials must also have low thermal expansion coefficients to maintain close dimensional tolerances. This ruled out the use of conventional materials such as steels. Stainless and carbon steels above their transformation temperature (725°C) will expand 3 to 4 times more rapidly than molybdenum. Therefore, braze and stress relief tooling for the molybdenum components was made from molybdenum.

2.1.3 Accelerator Insulator Assembly - The niobium voltage feed through and flange rings were machined using standard manufacturing practices. Plates were rough sawed to stock sizes and tooling holes drilled and reamed on the centerline to facilitate NC machining. The rings were machined alternating from one side of the plate to the other to minimize distortion using the tooling holes to position the part in relation to the NC program.

The ceramic insulator was procured as a completed item.

The details were preassembled and visually inspected for fit and alignment. The parts were then cleaned, reassembled and brazed. A titanium-copper-silver braze alloy foil was selected and trimmed to the appropriate width. The braze alloy foil was cut to fit the straight sides and the corner radii of the insulator. The corner alloy pieces were trimmed to overlap the straight side alloy pieces by approximately 0.125 inch. The thickness of the alloy selected, 0.003 inch, was critical in that an excess amount of alloy would result in puddling or wicking up

the sides of the ceramic insulators. A description of this process is discussed in Paragraph 1.2.1.

Interface hole paterna and mating surfaces were machined prior to brazing to eliminate any undue stress to the assembly following brazing. The brazed insulator assembly was inspected for dimensional accuracy and a vacuum leak test performed. See manufacturing flow, Figure 2.1.3-1.

2.1.4 Final Assembly - The individual alignment of each grid assembly within the accelerator represents a time consuming and expensive portion of accelerator fabrication. In the event an accelerator must be disassembled, the grids must be realigned using the same techniques that were used for initial build-up.

Tooling holes in the rail holders and matching holes in the mounting plate and grid hats, Figure 2.1.4-1, were used to assist in the alignment from one set of grid rails to another. A tooling hole and two slots were machined into the rail holders within the same setup used to machine the slots which position the rails. This method of machining assured an accurate and direct relationship between the grid rail slots and the tooling holes. The combination of one round tooling hole and two slots establishes parallelism of rail holders but still allowed for thermal expansion.

The mating dowel pin holes in the mounting plate and grid hats were drilled after these parts had been preassembled within the accelerator assembly and pinned in position. An assembly drill jig (Figure 2.1.4-2) was used to drill all of the tooling holes in the mounting plate and grid hats in one setup. By drilling all tooling holes in the structure that holds, supports and positions the grid rail assemblies with one common assembly drill jig, an accumulation of tolerance was eliminated, a positive relationship was maintained from grid to grid, and the assembly and disassembly of grids was possible without extensive realignment.

Other advantages of this system are:

- o Simplified alignment and thereby shorter alignment time. Less cost.
- o Slots for hold down screws in the rail holders, used for adjustment are no longer required. Round holes will do. Less cost.

INSULATOR ASSEMBLY
MANUFACTURING FLOW

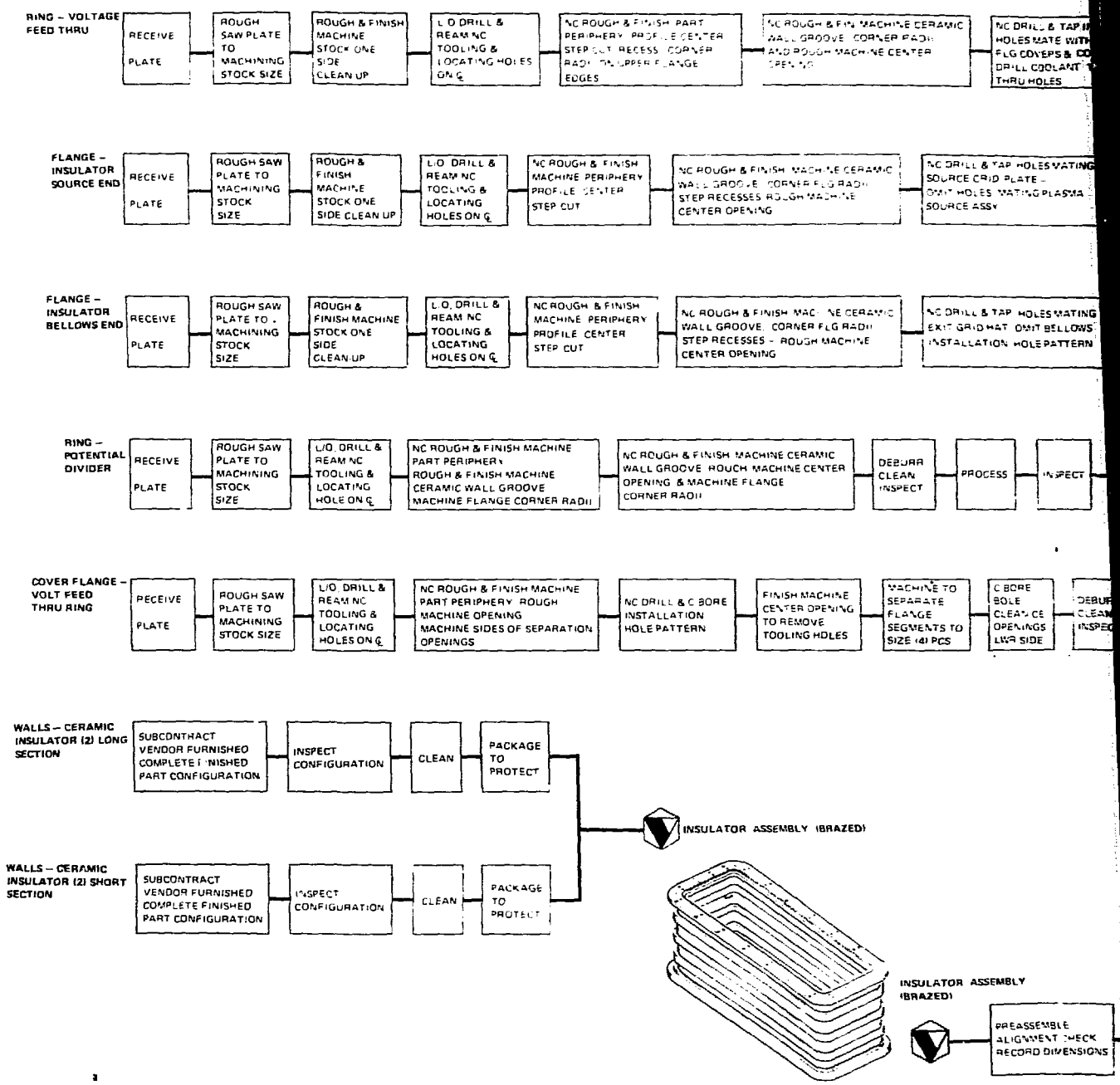

13–1315

FIGURE 2.1.3-1

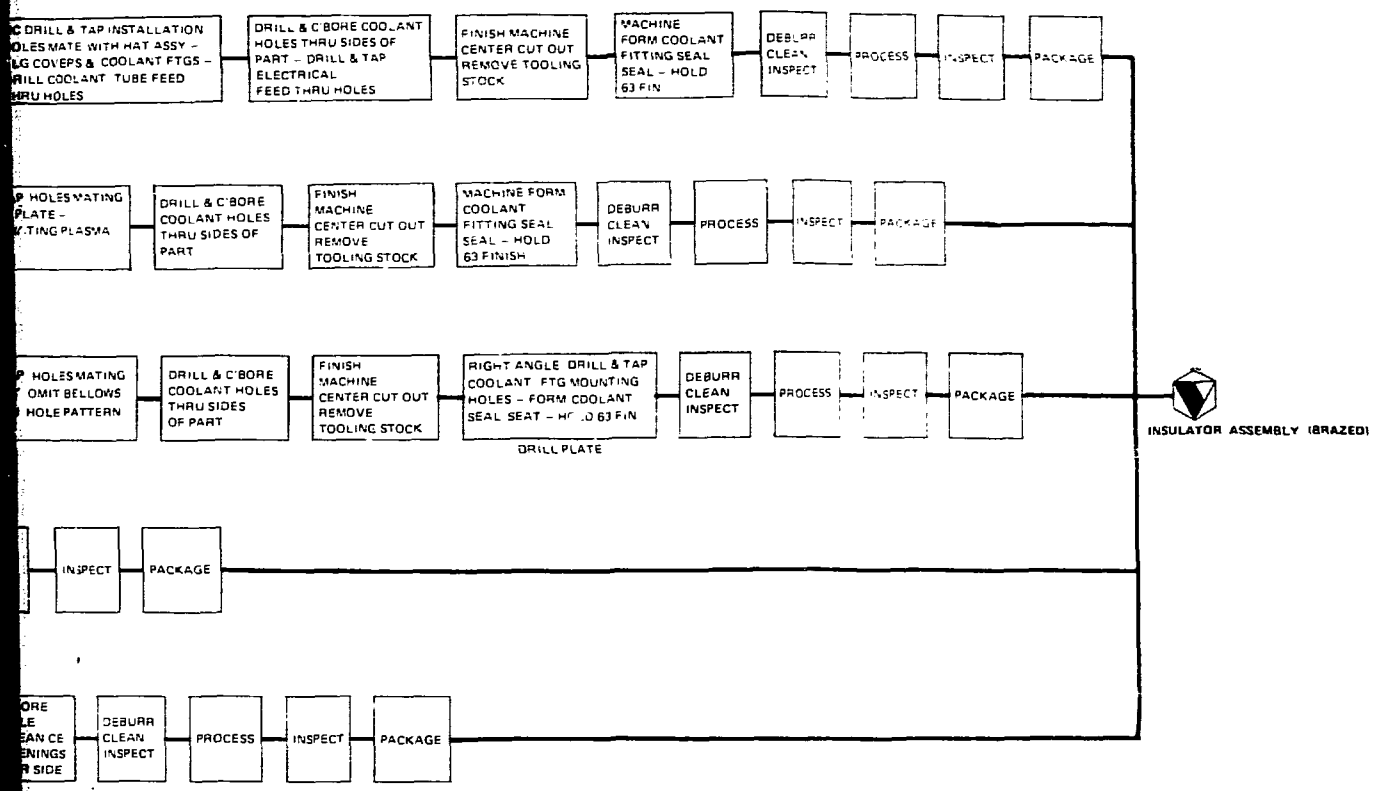
C DRILL & TAP INSTALLATION
OLES MATE WITH HAT ASSY –
LG COVEPS & COOLANT FTGS –
RILL COOLANT TUBE FEED
HRU HOLES
DRILL & C'BORE COOLANT HOLES THRU SIDES OF PART – DRILL & TAP ELECTRICAL FEED THRU HOLES
FINISH MACHINE CENTER CUT OUT REMOVE TOOLING STOCK
MACHINE FORM COOLANT FITTING SEAL SEAL – HOLD 63 FIN
DEBURR CLEAN INSPECT
PROCESS
INSPECT
PACKAGE
HOLES MATING
PLATE –
TING PLASMA
DRILL & C'BORE COOLANT HOLES THRU SIDES OF PART
FINISH MACHINE CENTER CUT OUT REMOVE TOOLING STOCK
MACHINE FORM COOLANT FITTING SEAL SEAL – HOLD 63 FINISH
DEBURR CLEAN INSPECT
PROCESS
INSPECT
PACKAGE
HOLES MATING
OMIT BELLOWS
HOLE PATTERN
DRILL & C'BORE COOLANT HOLES THRU SIDES OF PART
FINISH MACHINE CENTER CUT OUT REMOVE TOOLING STOCK
RIGHT ANGLE DRILL & TAP COOLANT FTG MOUNTING HOLES – FORM COOLANT SEAL SEAT – HOLD 63 FIN
DRILL PLATE
DEBURR CLEAN INSPECT
PROCESS
INSPECT
PACKAGE
INSPECT
PACKAGE
ORE
LE
EAN CE
ENINGS
R SIDE
DEBURR CLEAN INSPECT
PROCESS
INSPECT
PACKAGE
INSULATOR ASSEMBLY (BRAZED)

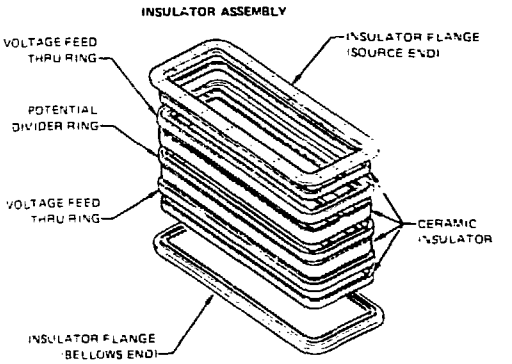
INSULATOR ASSEMBLY
VOLTAGE FEED THRU RING
INSULATOR FLANGE (SOURCE END)
POTENTIAL DIVIDER RING
VOLTAGE FEED THRU RING
CERAMIC INSULATOR
INSULATOR FLANGE (BELLOWS END)

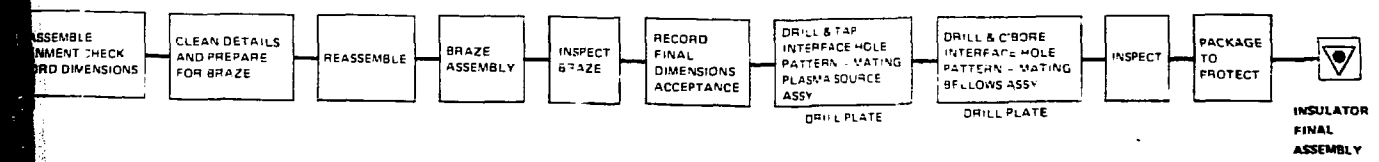
SSEMBLE
NMENT CHECK
RD DIMENSIONS
CLEAN DETAILS AND PREPARE FOR BRAZE
REASSEMBLE
BRAZE ASSEMBLY
INSPECT BRAZE
RECORD FINAL DIMENSIONS ACCEPTANCE
DRILL & TAP INTERFACE HOLE PATTERN – MATING PLASMA SOURCE ASSY
DRILL PLATE
DRILL & C'BORE INTERFACE HOLE PATTERN – MATING BELLOWS ASSY
DRILL PLATE
INSPECT
PACKAGE TO PROTECT
INSULATOR FINAL ASSEMBLY

RAIL ALIGNMENT USING TOOLING HOLES

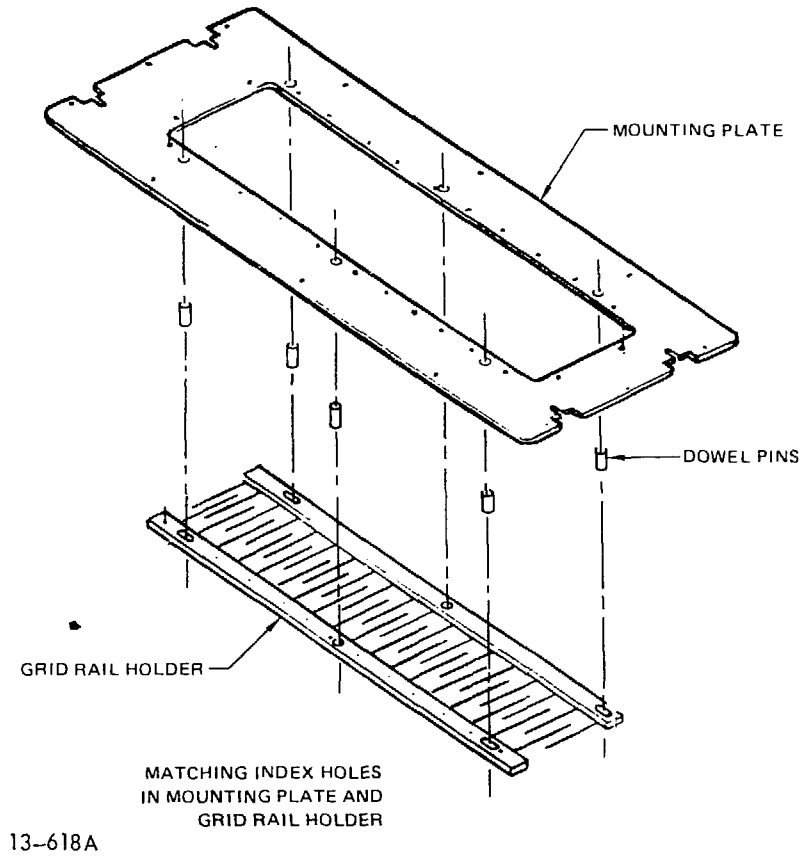

FIGURE 2.1.4-1

- Equipment used for alignment will not be tied up for long periods of time. If higher production rates are required, duplicate tools will not be necessary.
- If a minor adjustment is required to a grid, the center dowel pins in each rail holder will be removed, the minor adjustment made, the center dowel pin hole is redrilled and the next largest dowel pin size installed.

The previously described sequence of operations aligned one accurately constructed grid assembly to another. As each grid was installed in its correct

ASSEMBLY DRILL JIG – FOR RAIL ALIGNMENT USING INDEXING PINS

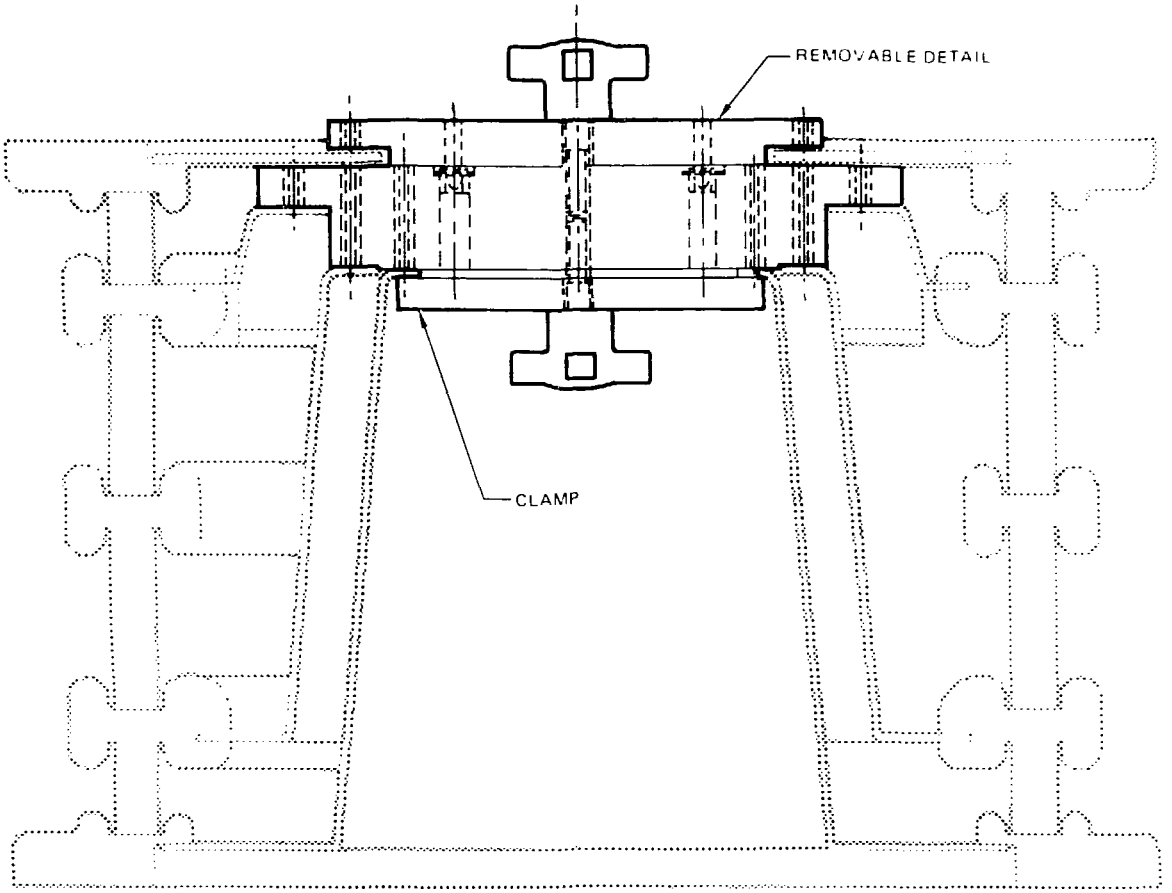

13–1019

FIGURE 2.1.4-2

location, an inspection was made to verify rail to rail dimensions, squareness, parallelism, and that one grid assembly was aligned with other grid assemblies. All dimensions in the "X" and "Y" directions had been accounted for.

Alignment in the "Z" direction is dependent upon the ability to measure the height of each grid rail. Before final assembly the individual grid assemblies had been inspected to insure that each grid rail was at its proper height within the grid rail holders. The grid rail holders were adjustable in the "Z" axis using shims at the hat to insulator interface and jack screws within each grid

rail holder. The source and gradient rails were very delicate. For example, as little as five grams of pressure in the center of a gradient grid rail would deflect the rail approximately 0.001 inch as shown in Figure 2.1.4-3. This deflection represents more than half of the alignment tolerance in one direction. For this reason we used a noncontact probe for measurements of rail height. Each grid assembly was inspected and adjusted to the desired height before the next grid assembly was installed.

CENTER DEFLECTION OF GRID RAILS DUE TO MEASURING INSTRUMENT'S STYLUS FORCE

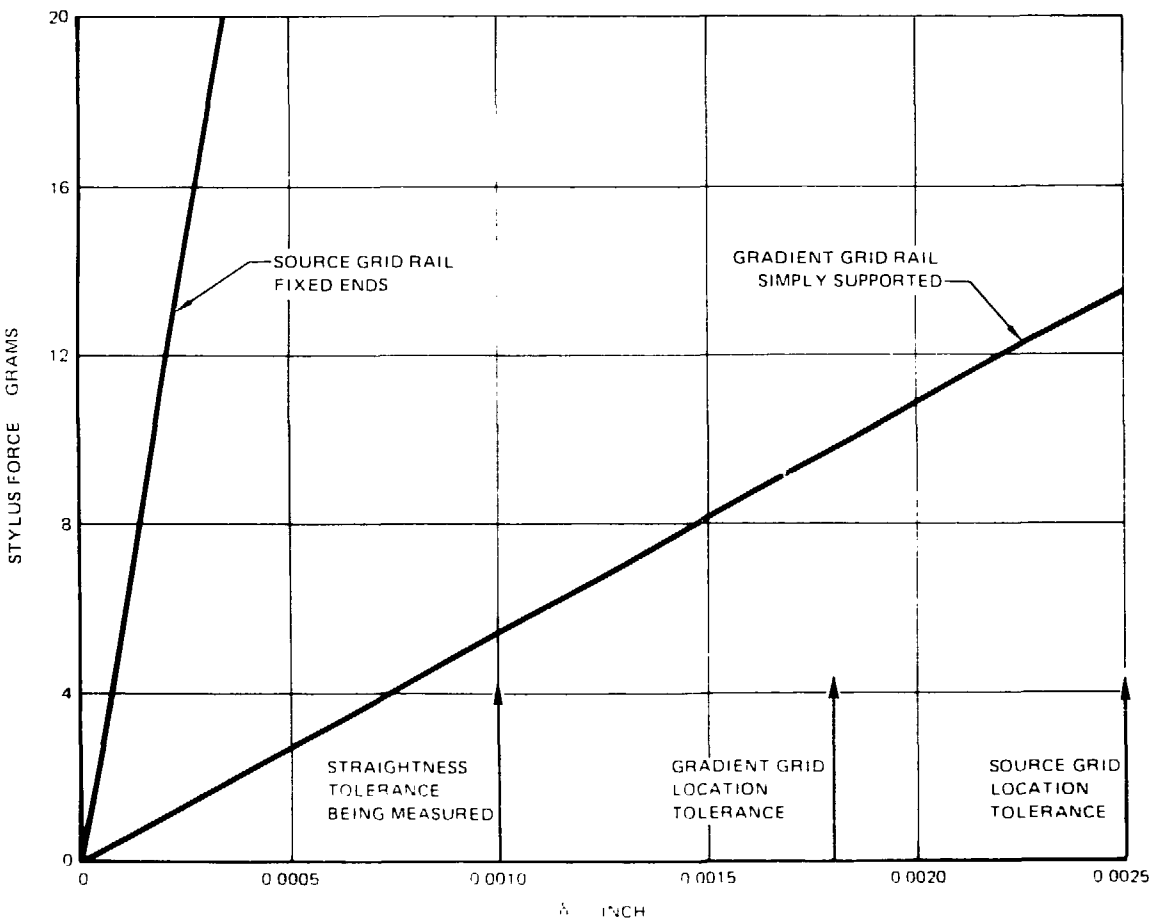

13–1078

FIGURE 2.1.4-3

The approach used for final assembly accelerator grid alignment was a computer assisted coordinate measuring machine with a three axis readout. The equipment offered fast and reliable measurement with the following advantages:

- o Elimination of human error
- o Provided permanent records
- o Improved utility of machine
- o Simplified inspection procedures
- o Greatly reduced off line analysis
- o Automatic alignment shortens setup time.

Final assembly of the accelerator was accomplished in a clean room and all detail parts and subassemblies were inspected, cleaned and packaged prior to entering the final assembly area. Subsequent handling was with surgical gloves.

The source assembly was then mated to the accelerator assembly and demonstration tests performed to verify compliance of the final assembly to LBL requirements and engineering drawings. The completed ion source was placed in a specially designed and fabricated shipping container to maintain cleanliness and shipped to LBL for further e aluation. The manufacturing flow for the neutral beam ion source final assembly is presented in Figure 2.1.4-4.

2.2 Manufacturing Problems and Solutions - The fabrication and assembly of the TFTR Neutral Beam Ion Source was a very challenging effort that required a great deal of learning. In that the TFTR ion source was the first source built by our company, manufacturing problems were encountered as a result of this learning process. Mistakes were made both in design and fabrication which required a dedicated effort by our engineering and manufacturing team to see the job through to completion. Discussed below are the major problems that were encountered and the solutions used to overcome these problems.

2.2.1 Hard Vacuum Dielectric Seal Insulators - The initial design selected for the hard vacuum dielectric seal insulators involved the application of porcelain enamel directly to the copper electrodes. Early development testing indicated

FINAL ASSEMBLY MANUFACTURING FLOW

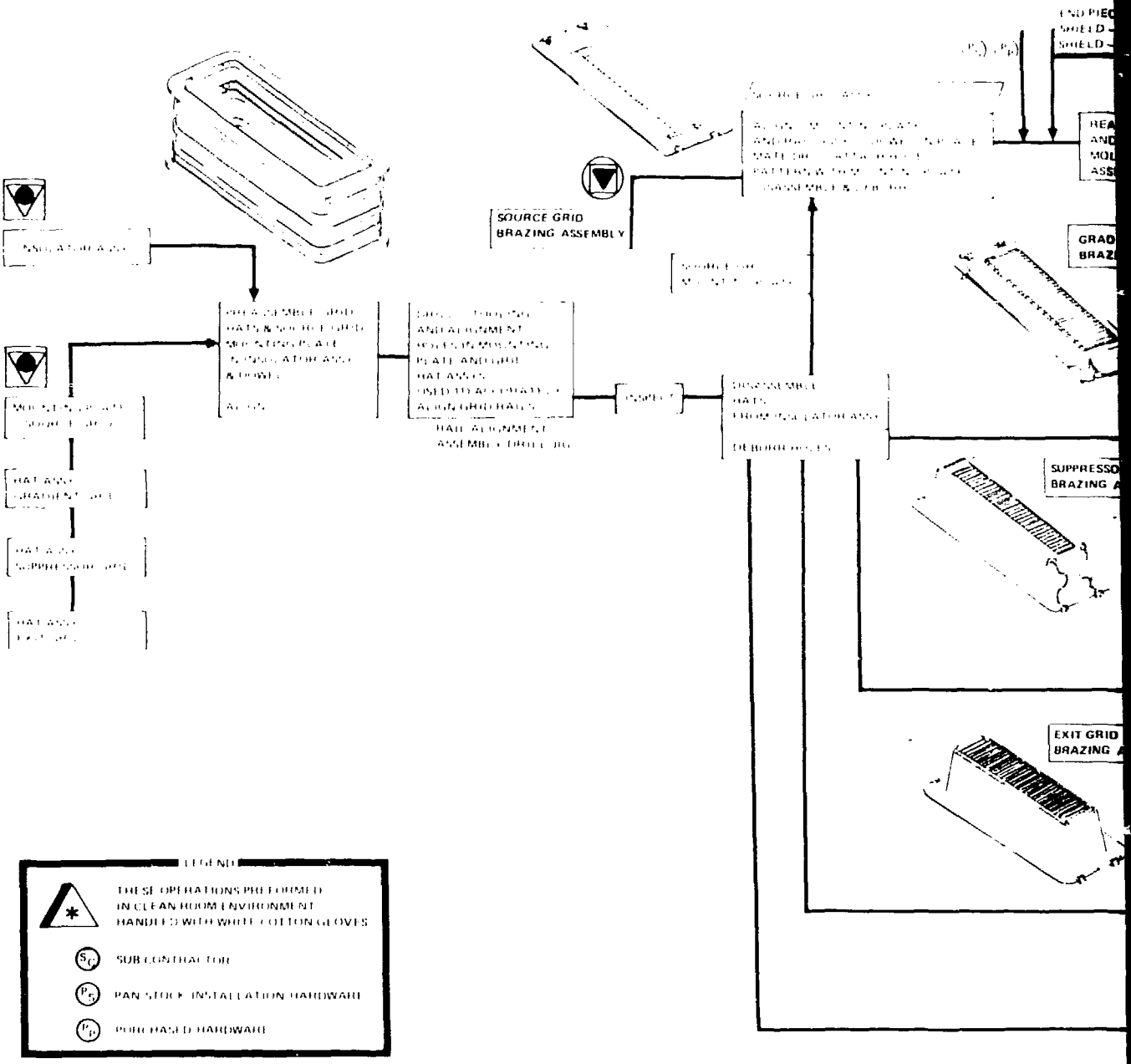

13 1416

FIGURE 2.1.4-4

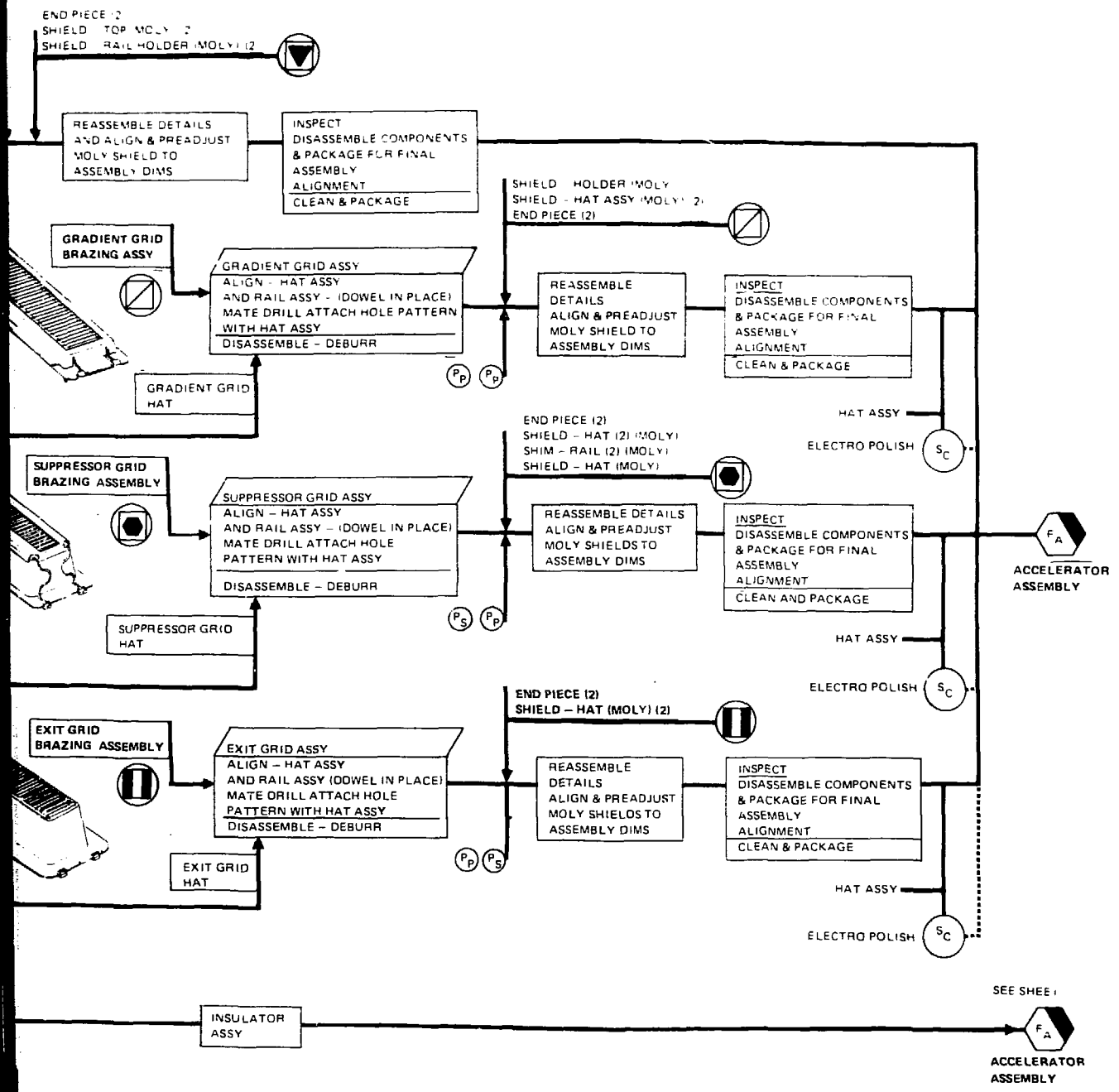
END PIECE (2)
SHIELD – TOP (MOLY) (2)
SHIELD – RAIL HOLDER (MOLY) (2)
REASSEMBLE DETAILS AND ALIGN & PREADJUST MOLY SHIELD TO ASSEMBLY DIMS
INSPECT
DISASSEMBLE COMPONENTS & PACKAGE FOR FINAL ASSEMBLY
ALIGNMENT
CLEAN & PACKAGE
SHIELD – HOLDER (MOLY)
SHIELD – HAT ASSY (MOLY) (2)
END PIECE (2)
GRADIENT GRID BRAZING ASSY
GRADIENT GRID ASSY
ALIGN – HAT ASSY
AND RAIL ASSY – (DOWEL IN PLACE)
MATE DRILL ATTACH HOLE PATTERN WITH HAT ASSY
DISASSEMBLE – DEBURR
GRADIENT GRID HAT
REASSEMBLE DETAILS ALIGN & PREADJUST MOLY SHIELD TO ASSEMBLY DIMS
INSPECT
DISASSEMBLE COMPONENTS & PACKAGE FOR FINAL ASSEMBLY
ALIGNMENT
CLEAN & PACKAGE
HAT ASSY
ELECTRO POLISH
END PIECE (2)
SHIELD – HAT (2) (MOLY)
SHIM – RAIL (2) (MOLY)
SHIELD – HAT (MOLY)
SUPPRESSOR GRID BRAZING ASSEMBLY
SUPPRESSOR GRID ASSY
ALIGN – HAT ASSY
AND RAIL ASSY – (DOWEL IN PLACE)
MATE DRILL ATTACH HOLE PATTERN WITH HAT ASSY
DISASSEMBLE – DEBURR
SUPPRESSOR GRID HAT
REASSEMBLE DETAILS ALIGN & PREADJUST MOLY SHIELDS TO ASSEMBLY DIMS
INSPECT
DISASSEMBLE COMPONENTS & PACKAGE FOR FINAL ASSEMBLY
ALIGNMENT
CLEAN AND PACKAGE
HAT ASSY
ELECTRO POLISH
ACCELERATOR ASSEMBLY
END PIECE (2)
SHIELD – HAT (MOLY) (2)
EXIT GRID BRAZING ASSEMBLY
EXIT GRID ASSY
ALIGN – HAT ASSY
AND RAIL ASSY (DOWEL IN PLACE)
MATE DRILL ATTACH HOLE PATTERN WITH HAT ASSY
DISASSEMBLE – DEBURR
EXIT GRID HAT
REASSEMBLE DETAILS ALIGN & PREADJUST MOLY SHIELDS TO ASSEMBLY DIMS
INSPECT
DISASSEMBLE COMPONENTS & PACKAGE FOR FINAL ASSEMBLY
ALIGNMENT
CLEAN & PACKAGE
HAT ASSY
ELECTRO POLISH
SEE SHEET
INSULATOR ASSY
ACCELERATOR ASSEMBLY

FINAL ASSEMBLY CONTINUED

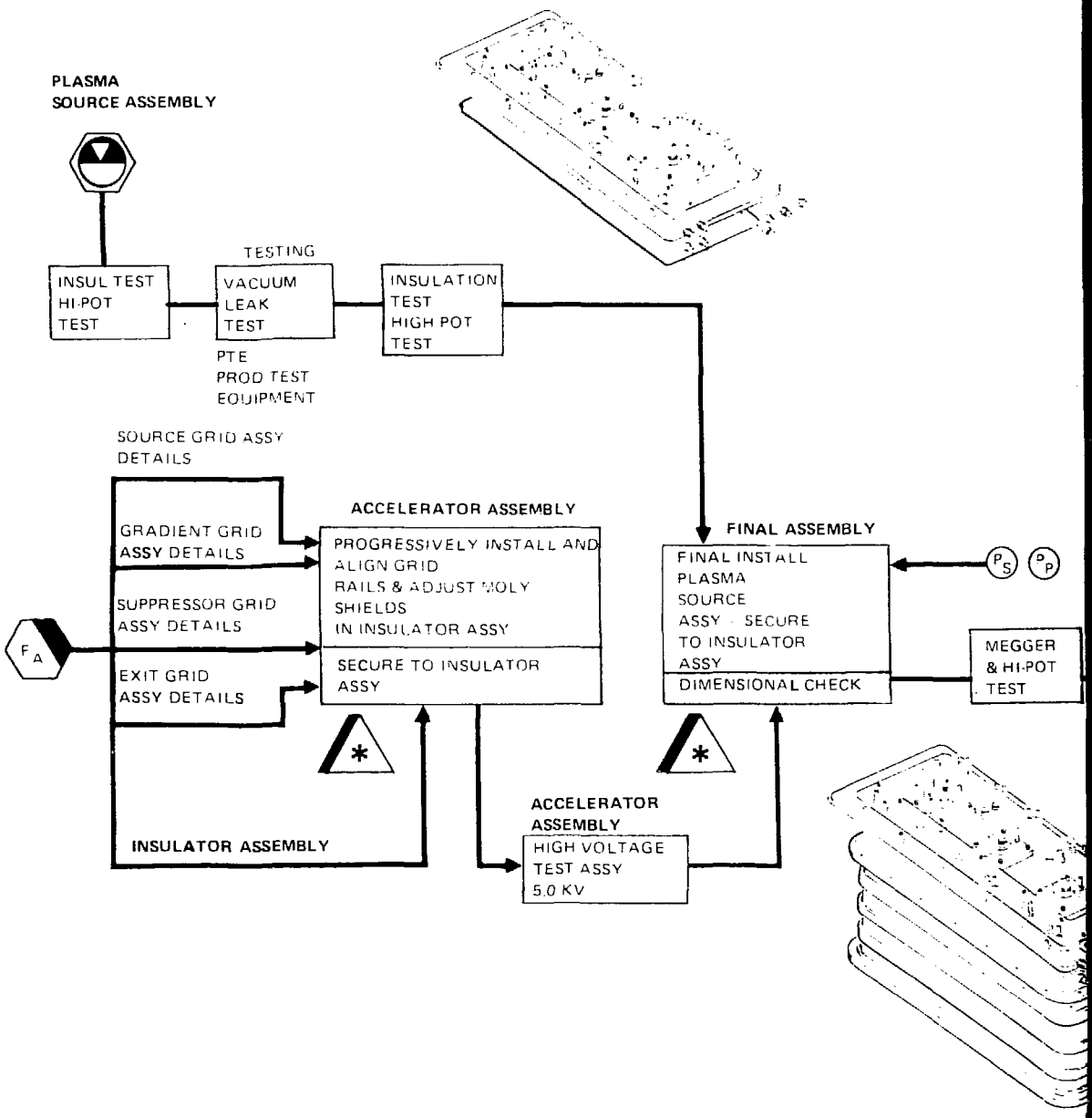

FIGURE 2.1.4-4 (CONTINUED)

13-1317

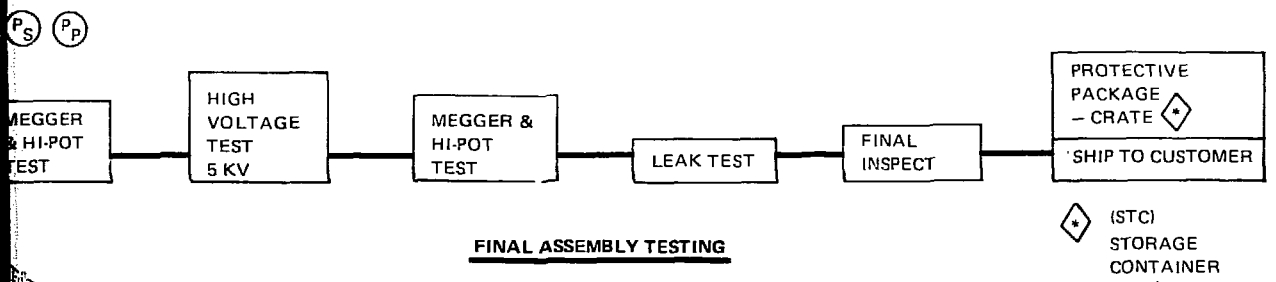

FINAL ASSEMBLY TESTING

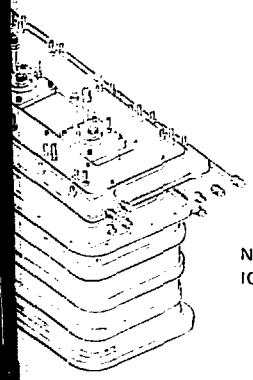

NEUTRAL BEAM
ION SOURCE ASSY

that such a technique would work in that the copper electrodes would yield during cooldown to compensate for the differences in expansion coefficients between the copper and enamel. However, when enamel was applied to the thicker cathode plate, the enamel began popping off during cooldown indicating high stresses. Further analysis indicated the 34% difference in expansion coefficient was too great for the thicker cathode plate. The copper would not yield, thereby exceeding the enamel's compression strength. Adjustment of the enamel formulation to increase its expansion coefficient was too time consuming so an alternate insulator design approach using a stainless steel "gasket" with a porcelain coating was used. This concept still enabled the interchangeability between hard "C" seals and "O" rings and also allowed replacement of a damaged insulator without replacing an electrode. The only drawback was that the number of hard "C" seals required was doubled over the original concept. A detailed description of the development effort is presented in Paragraph 1.2.2.

2.2.2 Hard "C" Seals - The hard vacuum dielectric seal concept utilizes a hard "C" seal to provide vacuum sealing against a porcelain enameled insulator. The "C" seal is made from stainless steel with a lead coating. A total of fourteen (14) hard "C" seals is required for the ion source assembly. Twelve (12) seals are used in the plasma generator, one (1) seal between the probe plate and the accelerator bellows flange and one (1) between the accelerator bellows flange and the stainless steel interface flange.

The plasma source was fully assembled for the final time but would not hold vacuum. A leak was detected at one of the hard seals to insulator interfaces. Disassembly and inspection revealed one of the hard "C" seals was improperly manufactured. A three (3) inch segment of the seal had not been fully formed into the "C" shape and during compression, resulted in a leak path. The source was recleaned and re-assembled using the backup set of "C" seals. Although vacuum integrity had been maintained, an electrical short was discovered between the negative filament electrode and the cathode plate and between one anode support and the cathode plate. Disassembly and inspection revealed that the shorts occurred around two (2) holes in the insulator where gaps in the porcelain enamel shorted the electrodes. The faulty insulator was scrapped and a second insulator was fabricated for subsequent assembly.

Re-assembly of the plasma source was completed using rubber "O" ring seals in place of the hard "C" seals to avoid further schedule delays. The delivery lead time for additional hard "C" seals would delay ion source delivery and subsequent testing at LBL. Additional seals have been purchased and will be installed at LBL following initial testing.

2.2.3 Increased Plasma Source Fasteners - Full scale development testing of the hard vacuum dielectric seals revealed that the fastener design was not adequate to compress the hard "C" seals. Additional fasteners were required to increase the compressive force. The negative and positive filament electrodes,anode supports, cathode plate and wall tank electrodes were remachined to accommodate the increased fasteners. Paragraph 1.3.1 describes the redesigned components and the additional machining that was required.

2.2.4 Accelerator Grid Rail Blushing - The accelerator grid assemblies are brazed molybdenum structures consisting of forty three (43) rails and two rail holders. The rails are hydrogen brazed to the rail holders on one end of the rail only to allow for thermal expansion without distortion of the rail. The quantity and application of the braze alloy is important to prevent the braze alloy from blushing (wicking) out onto the grid rails. The gradient and exit grid assemblies which were the first grids brazed exhibited this blushing on the rails. The blushing was not apparent until after several days exposure to air when the alloy which had wicked out onto the rails became slightly oxidized. Rather than scrap the assemblies, a chemical cleaning technique was used to remove the blushed braze material from the rails. The chemical formula used was a nitric acid solution which contained no halogens or sulfur. The assemblies were inspected after the cleaning process and no detrimental affects on grid rail dimensions or alignment were noted. The assemblies were acceptable and installed in the accelerator. The quantity of braze alloy applied to the remaining two grid assemblies was reduced and no rail blushing occurred.

2.2.5 Repair of Broken Suppressor Grid - One of the suppressor grid rails was inadvertently broken during disassembly of the brazed grid from the brazing fixture. To prevent scraping of the brazed assembly, the broken remains of the

rail was machined from the holder and a new backup rail hydrogen brazed in its place. A lower temperature PalCuSil 10 braze alloy was used to prevent remelting of the other grid rails. The brazed grid assembly was inspected and no degradation to rail alignment was noted. The repaired suppressor grid was acceptable and installed in the accelerator.

2.2.6 Brazed Accelerator High Voltage Insulator Leaks - The Accelerator High Voltage insulator is a brazed assembly of niobium voltage feed through rings and alumina ceramic insulators. The buildup consists of five (5) niobium rings which are vacuum brazed to four alumina ceramic insulator rings. Source and bellows niobium flanges provide structural support for the source and exit grids respectively and two voltage feedthrough niobium rings support the gradient and suppressor grid voltage feedthrough rings. The brazed assembly is a 25 inch by 12 inch rectangular structure approximately 9 inches high.

Two production insulators were brazed during the program. The first production insulator was helium leak tight after vacuum brazing but developed leaks at one corner of the two end flanges later during final assembly operations. Ultrasonic testing of the assembly showed braze separation and cracks in the ceramic at the leaking corners (Figure 2.2.6-1). All brazed joints at the other flange corners and center niobium feedthrough rings were good with no voids or separations. A structural analysis to determine the exact cause for the failure was performed. The results of the analysis indicated radial shear and tipping moments existed between the end niobium and ceramic rings at the subassembly corner. The solution to the problem was the addition of a backup ceramic ring to the two end flanges. The added backup rings tend to reverse the direction of the bending moment across the braze and reduce it by approximately a factor of two. Shear stresses are reduced by approximately 20%. A detail description of the analysis is presented in Paragraph 1.4 above.

The second insulator was brazed with backup ceramic rings added to the end flanges.

A technique was developed for "hard" (non-organic) repair of brazed insulators and involved a chemical separation of all the ceramic/niobium rings followed

CERAMIC INSULATOR VACUUM LEAKS

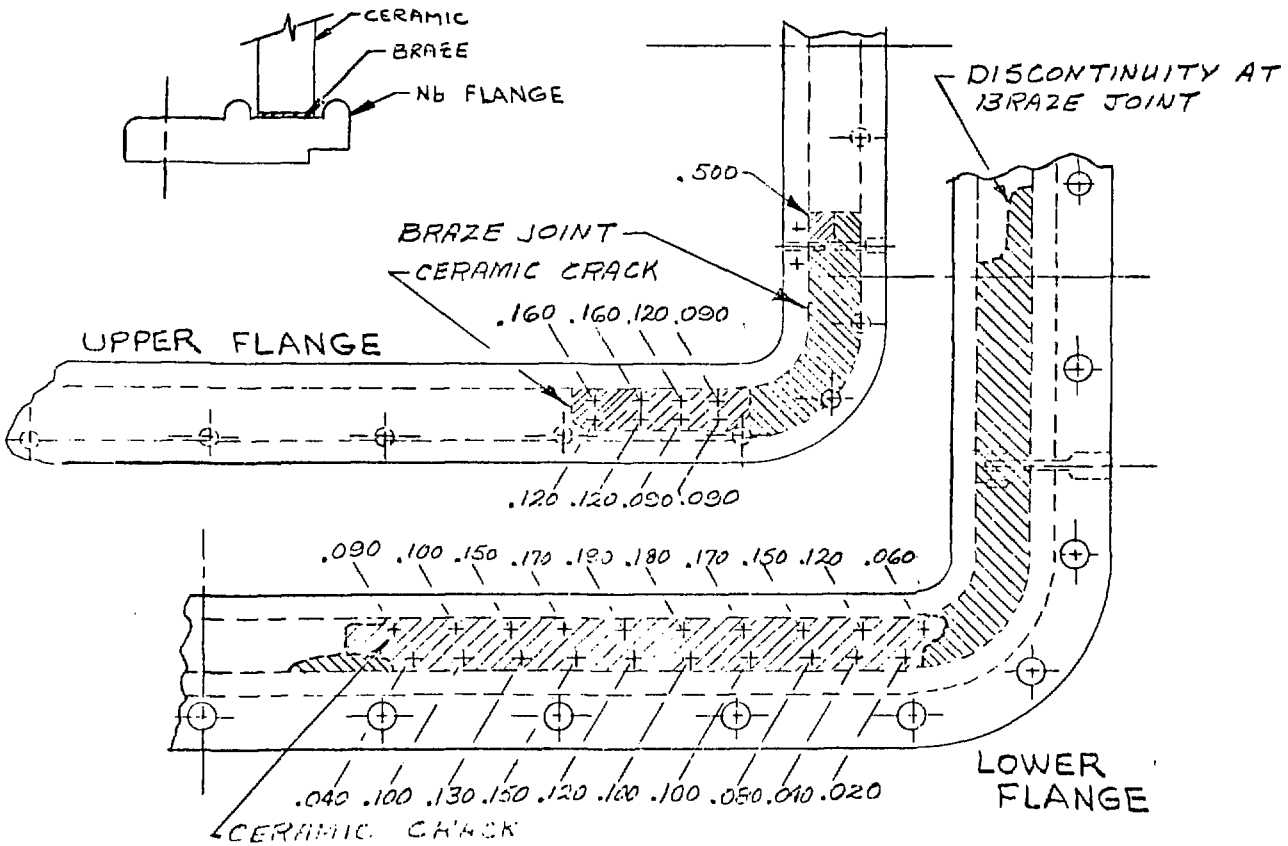

FIGURE 2.2.6-1

by a rebrazing of the insulator. The development of the repair technique resulted in a cost savings to the program in that the machined niobium rings were re-used for the second insulator. The ceramic rings were not re-usable.

The second ceramic insulator was successfully brazed and was helium leak tight. Ultrasonic scans of the assembly showed good solid braze joints with no voids. The brazed assembly was again helium leak tested following installation and alignment of the accelerator grids which occurred approximately six (6) months after the initial brazing and was helium leak tight.